INL/EXT-20-59775
Revision 0

Light Water Reactor Sustainability Program

Techno-Economic Analysis of Synthetic Fuels Pathways Integrated with Light Water Reactors

September 2020
U.S. Department of Energy
Office of Nuclear Energy

INL/EXT-20-59775
Revision 0

Techno-Economic Analysis of Synthetic Fuels Pathways Integrated with Light Water Reactors

L. Todd Knighton, Daniel S. Wendt (INL)

Lesley Snowden-Swan, Jeromy Jenks, Shuyun Li, Steven Phillips, and Jalal Askander (PNNL)

September 2020

Prepared for the
U.S. Department of Energy
Office of Nuclear Energy

Page intentionally left blank

EXECUTIVE SUMMARY

Synthetic fuels (synfuels) and chemicals (synchems) are produced by synthesis from chemical building blocks rather than by conventional petroleum refining. Synthesis gas or syngas (carbon monoxide and hydrogen) is a common intermediate building block in the production of synfuels and synchems. Syngas can be produced by many processes, including biomass or fossil fuel gasification and by co-electrolysis. In co-electrolysis, CO_2 is reacted with water to produce syngas. The CO_2 can be sourced from processes that would otherwise eject the CO_2 to the atmosphere, such as ethanol plants, including dozens of large plants in the United States that convert corn into ethanol that is being blended with the national gasoline, or fossil fuel processes, such as steam methane reforming or natural gas combined cycle (NGCC) power plants. CO_2 is also emitted from biofuels gasification plants. Conversion of CO_2, which would have otherwise been released to the atmosphere, to synfuels using nuclear energy is a potential avenue for adding value to existing light water reactor (LWR) facilities, while producing transportation fuels that are compatible with conventional fuels produced via petroleum refining. The cost of CO_2 separation depends on the purity of the source. Valorization of CO_2 is a critical complementary component of carbon capture and utilization (CCU) and an alternative to carbon capture and sequestration (CCS).

The purpose of this work is to identify, model, perform techno-economic analysis, and compare two possible synfuel production routes utilizing CO_2 as the feedstock. Heat from an LWR nuclear plant is integrated wherever possible to positively affect the economics of the LWR by converting power to fuels during times of low grid electricity demand. Process and economic modeling for a conceptual synfuel production plant co-located (or in near proximity) with an LWR is presented, including the cost of CO_2 captured from an ethanol plant, compressed, and transported to the LWR hybrid plant, co-electrolysis of the CO_2 with water in a solid oxide electrolyzing cell (SOEC) system to produce syngas, and thermo-catalytic conversion of the syngas to transportation fuel. The hybrid LWR/synfuels plant is assumed to be located within 50–150 miles of an ethanol plant (e.g., located in the midwest region of the United States). Performance and n^{th}-plant economics for the co-electrolysis-based processes are evaluated and compared with biomass-gasification-based technology for the synfuel routes considered. Sensitivity analysis around the price of CO_2 and electricity, two of the major cost drivers, is presented for each case. Consideration of a carbon credit is also included in the sensitivity analysis. The primary results and conclusions of the analysis are the following:

- For a plant producing 3,195 barrels per day (BPD) hydrocarbon synfuels via a methanol intermediate with LWR electricity and steam usage of 326 MWe and 133 MWt respectively:
  - The modeled minimum fuel selling price (MFSP) of diesel (91%) and gasoline (9%) blendstock with conservative assumptions is \$4.45/gallon for the base case using a \$33.3/tonne CO_2 cost and \$30/MWh electricity price. That is compared with the biomass gasification route to syngas with an MFSP of \$3.28/gallon. Note that co-electrolysis has a much larger maximum scale of production that can be reached compared to the availability of land competing with food production as in the case of biomass gasification. Also, the scale of the analysis is only about 1/3 of the available energy from a typical LWR but was chosen so that a direct comparison with a biorefinery could be made.
  - There are innovative cryogenic carbon capture (CCC) processes that claim to produce CO_2 for a cost as low as \$20 to \$60/tonne CO_2 (SES 2020), which could also have significant impact on the viability of an LWR/synfuels plant using methanol as intermediate. Further, the refrigerant used in the CCC process could be produced using LWR energy. The synergies of the LWR with the CCC process and techno-economic modeling of the CCC process will be explored in detail in future studies.
  - Sensitivity analysis (Figure ES-1) shows that with optimal CO_2 and electricity prices and inclusion of carbon credits through incentives or mandates this process could be more cost

competitive with petroleum fuels, especially post Covid-19 when oil prices recover somewhat from the current historic lows. With a hypothetical carbon tax of $100/tonne CO_2, the MFSP is reduced to ~$3.75/gallon. A renewable fuel standard (RFS) credit would further aid in competitiveness of fuels produced via this route. Some states already offer credits for clean fuels, including California and New York. These credits are qualified under the U.S. Environmental Policy Act and are applied to select fuels with the assignment of Renewable Identification Numbers (RINs). Clean fuels credits in California have ranged upwards from $0.5 to $2.5 per gallon of gas equivalent.

- Sensitivity analysis varying plant scale for the co-electrolysis with methanol-to-olefins (MTO) fuel process was conducted (Figure ES-2). At a scale of half the base case (326 MWe; 133 MWt), production cost increases by 9%. At a scale 10 times larger than the base case, production cost is reduced to about $3.8/gal. Scaleup of the plant up to the entire electrical output of a general 1-GWe LWR of fuel production would result in about 40 cents/gal cost savings. Note that a scaling factor of 1 is assumed for the SOEC stack; therefore, no benefit is gained for this portion of the capital cost.

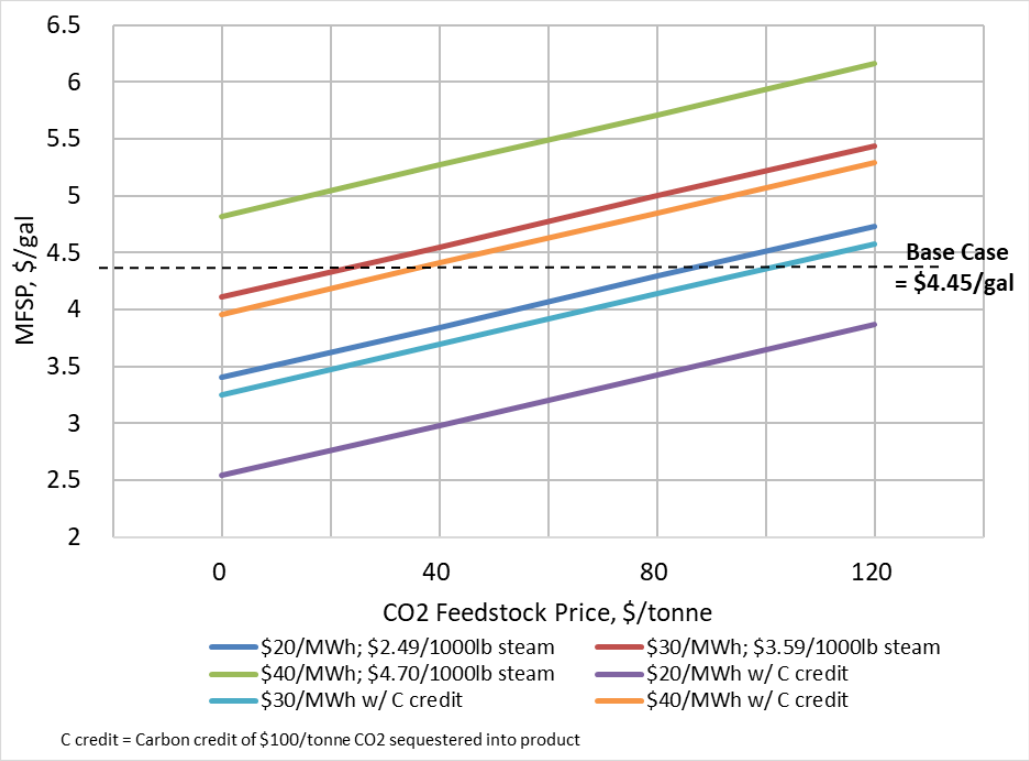

Figure ES-1. Minimum fuel selling price sensitivity for fuels via a co-electrolysis derived syngas to methanol to fuels route.

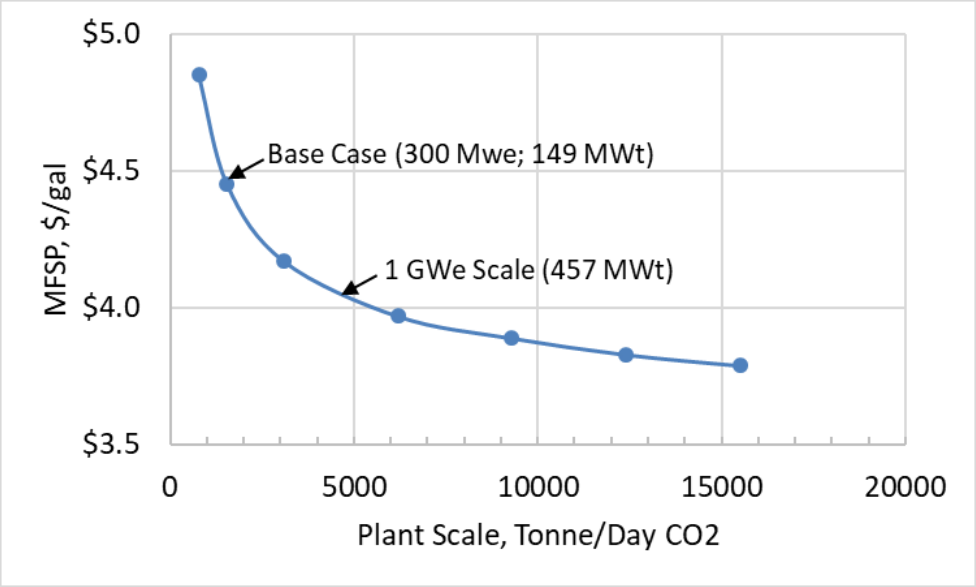

Figure ES-2. Sensitivity of MFSP to plant scale for the co-electrolysis and MTO fuel process.

- The ethanol (EtOH) pathway is considered to be a low-to-mid technology readiness level (TRL) level technology, as the mixed alcohol conversion process to produce ethanol has only been tested at pilot scale. For a plant producing 2,870 BPD hydrocarbon synfuels via an ethanol intermediate with LWR electricity and steam usage of 468 MWe and 66 MWt, respectively:
  - The modeled MFSP is $6.13/gallon using a $33.3/tonne CO_2 cost (including compression and transportation from an ethanol plant to the LWR/synfuels plant) and $30/MWh electricity price. This option has a higher cost compared to the methanol intermediate route primarily because the thermochemical syngas conversion to mixed alcohols process is only about half as carbon efficient at making ethanol as the syngas-to-methanol process.
  - Compared with biomass gasification route, the MFSP of the co-electrolysis case with ethanol intermediate is about 52% higher.
  - Sensitivity analysis (Figure ES-3) indicates it will be somewhat more challenging to make this pathway cost competitive with petroleum fuels even considering optimal feedstock cost and carbon credits.
  - By using a syngas to ethanol process with a higher carbon efficiency (e.g., fermentation) economics for this pathway could potentially be improved.

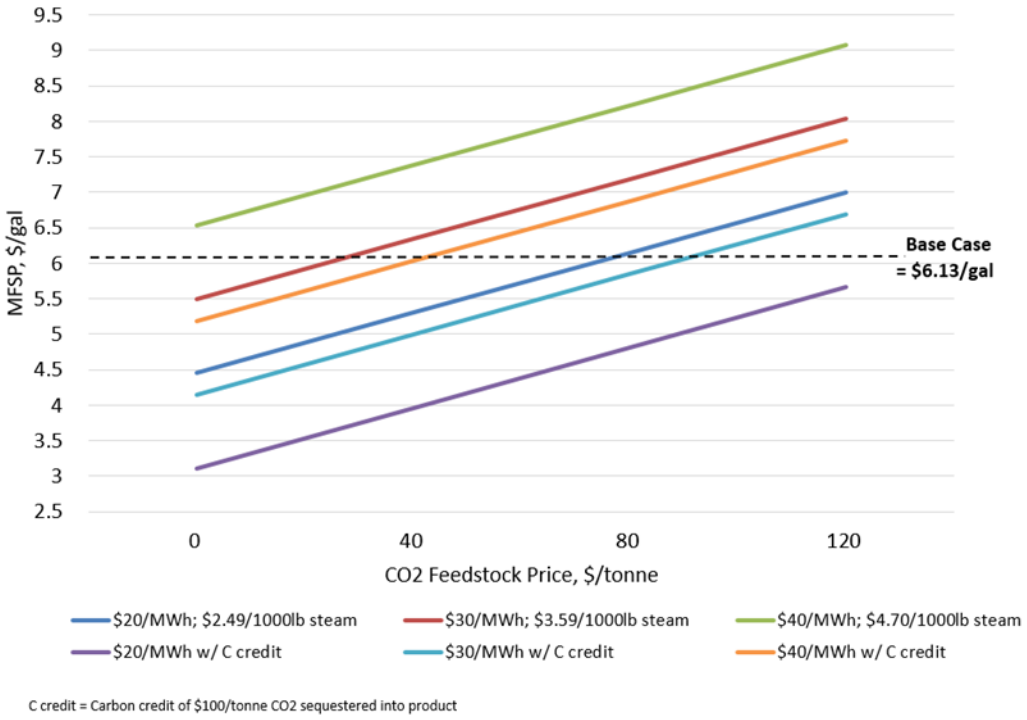

Figure ES-3. Minimum fuel selling price sensitivity for fuels via a co-electrolysis derived syngas to ethanol-to-fuels route.

The results of this study justify further pursuit of synfuels via the methanol-to-fuels as an alternative market for LWR energy use. Co-electrolysis could take all of the energy provided by a single reactor or two reactors to produce the syngas that is converted to methanol. The synfuels could be competitive in price with petroleum fuels if credits for CO_2 emissions reductions reach about \$100/tonne CO_2 or if the price of petroleum fuels rises above the current historic lows. The combination of plant scale-up matching the energy produced by an average nuclear power plant, plus clean energy credits could make synthetic fuels produced by co-electrolysis using LWR energy competitive with petroleum-derived fuels. Together, biomass gasification and nuclear-derived synfuel could feasibly replace a significant volume of U.S. transportation fuels. The nation currently burns 12 million barrels of gasoline and diesel each day. Biomass gasification and co-electrolysis together can feasibly replace over 25% of the petroleum fuels.

Future studies should take into account opportunity sources of CO_2, their purity, and location, financial investment terms and options, and clean energy credits. In addition, synergies between nuclear power plants and the biomass gasification synfuels route should be considered, including biomass feedstock drying and torrefaction, and CO_2 by-product from biomass gasification.

Page intentionally left blank

CONTENTS

FIGURES

TABLES

Page intentionally left blank

ACRONYMS

ACCE	Aspen Capital Cost Estimator
ASR	area-specific resistance
BEA	Battelle Energy Alliance
BETO	Bioenergy Technology Office
BMI	Battelle Memorial Institute
BPD	barrels per day
CAPEX	capital expenses
CCC	Cryogenic carbon capture
CCS	carbon capture and sequestration
CCU	carbon capture utilization
CE	chemical engineering
DME	dimethyl ether
DOE	Department of Energy
EPA	Environmental Protection Agency
ER	electrochemical reduction
EtOH	ethanol
FA	formic acid
FCI	fixed capital investment
FT	Fischer-Tropsch
GHG	greenhouse gas
GREET	Greenhouse Gases, Regulated Emissions, and Energy Use in Transportation model
INL	Idaho National Laboratory
LCFS	low-carbon fuel standard
LWR	light water reactor
LWRS	Light Water Reactor Sustainability program
MAS	mix alcohol synthesis
MeOH	methanol
MFSP	minimum fuel selling price
MTG	methanol can also be converted to hydrocarbons via the methanol-to-gasoline
MTO	methanol-to-olefins
MTP	methanol to propylene
NG	Natural gas
NGCC	Natural gas combined cycle

NPP	Nuclear power plants
OPEX	operating expenses
PNNL	Pacific Northwest National Laboratory
REC	Renewable energy credits
RFS	renewable fuel standard
RIN	renewable identification number
RSTOIC	stoichiometric reactor in AspenTech software
RWGS	reverse water-gas-shift
SES	Sustainabile Energy Solutions
SOEC	solid oxide electrolyzer cell
SOFC	solid oxide fuel cell
TEA	techno-economic analysis
TRL	technology readiness level
UOP	Honeywell UOP, formally known as Universal Oil Products
YSZ	yttria stabilized zirconium
ZEC	Zero emissions credits

1. INTRODUCTION

Nuclear energy is increasingly being recognized as a valuable low-carbon, low-emissions energy source that can help achieve clean energy targets being set by states, commissions, and utilities in the United States. Currently, nuclear power provides about one-fifth of the country's electricity. Nuclear power plants (NPPs) further provide the grid with all-weather season-long baseload capacity that is important to grid reliability and resiliency. Light water reactor (LWR) NPPs in the United States, like other sources of electricity generation, are facing increasing cost pressure on the electricity grid due to historically low-priced natural gas (NG) and the rapid expansion of solar and wind energy. Solar and wind energy provide spikes on the grid during periods of high production, but there will be a continued opportunity for baseload generators, such as NPPs, to provide electricity to the grid when solar and wind energy installations are producing little output. During times of grid overgeneration the NPP energy can be diverted to create other value-added chemical and fuels. Therefore, the U.S. Department of Energy (DOE) Light Water Reactor Sustainability (LWRS) Program is addressing flexible plant operations that can diversify the revenue of NPPs.

Previous reports have evaluated opportunities to couple LWRs with hydrogen production (Knighton 2020a, Knighton 2020b, Hu 2019, Frick 2019). This report analyzes several synthetic fuel (synfuel) production pathways that could be coupled with LWRs to provide alternative options to utility companies for using nuclear energy to create value added products during periods of overgeneration of electricity to the grid. A conceptual integrated plant would consist of a hybrid LWR delivering power and heat to a synthetic fuel and/or chemical facility. The synfuels plant would employ co-electrolysis to convert CO_2 and water into syngas (synthesis gas, a mixture of H_2 and CO). The CO_2 ideally would come from a source that is in close proximity to the LWR and one in which the CO_2 is currently being released to the atmosphere, to take advantage of possible clean energy credits. Sources such as an ethanol plant release CO_2 in high concentration which makes the CO_2 separation and utilization more cost effective. In this report an ethanol plant located between 50 and 100 miles from the LWR is assumed to be the CO_2 source. CO_2 sources in close proximity to LWRs, such as a natural gas combined cycle (NGCC) plant, and state-of-the-art carbon capture technology will be evaluated in future work. The syngas would then be converted to synthetic fuels via the most economical processes. Choices for the conversion of syngas to synfuels include Fischer-Tropsch (FT), methanol-to-gas (MTO), ethanol-to-fuels, as well as other possible options. This report focuses on the evaluation of two possible syngas to fuels pathways: (1) methanol-to-olefins (MTO) and (2) ethanol-to-fuels. It is recognized that there are other possible pathways to fuels as well as pathways to valuable synthetic chemicals from syngas that could be analyzed in future work.

Co-electrolysis is assumed to take place with a solid oxide electrolyzing cell (SOEC) to take advantage of its high efficiency as compared with a standard polymer electrolyte membrane (PEM) electrolyzer. Although higher value synchems offer compelling investment potential, the focus of the techno-economic analysis (TEA) detailed herein is on production of synfuel blendstocks compatible with existing liquid transportation fuels. The methanol (MeOH) and ethanol (EtOH) routes were selected because methanol and ethanol are common intermediates that can either serve as base chemicals or be converted to hydrocarbon fuels; therefore, the analysis is flexible to be used for future synchems analyses. In addition, Pacific Northwest National Laboratory (PNNL) has extensive experience in syngas-based fuels modeling and TEA so existing biomass-based PNNL models for the methanol and ethanol-based conversion routes could be leveraged for this work.

The plant scale chosen is commensurate with the typical scale used for a cellulosic biorefinery (2000 dry ton/day biomass feed) to provide a consistent comparison with renewable fuel from biomass. This is equivalent to a syngas flow of 141 ton/day H_2 and 973 ton/day CO for the methanol-to-fuels-based pathway and 162 ton/day H_2 and 1,909 ton/day CO for the ethanol-to-fuels-based pathway (see Sections 5 and 6). Detailed process models and TEA were developed for synfuel pathways incorporating the use of the LWR heat and electricity as an energy source for the conversion process. Equipment CAPEX and

OPEX are detailed in the economic modeling, including reactor and other unit operation costs, and feedstock and product valuations. Sensitivity analysis around key process and economic assumptions is also presented.

This report begins with a high-level overview of the various possible routes from CO_2 to synfuels and chemicals in Section 2 and a description of the two pathways selected for detailed modeling and analysis. Section 3 outlines the general approach and underlying assumptions for the TEA. Section 4 details the models generated for predicting syngas generation from an SOEC plant and the costing of the SOEC stack. Section 5 and 6 presents the process design and TEA results of the fuel pathways via the syngas-to-methanol and syngas-to-mixed alcohols (primarily ethanol) routes, respectively. Section 7 discusses the current and possible future structure of national and state level carbon credit systems and how these systems may improve the economics of synthetic fuels produced integrated with clean nuclear energy. Section 8 summarizes the results and conclusions for the two fuel routes evaluated.

2. ROUTES FOR CO_2 TO FUELS OR CHEMICALS

There is a myriad of possible ways to make fuels or chemicals from CO_2. This section is intended to give a high-level overview of the some of the possible technology options and selection of the two pathways that were analyzed in detail. Figure 1 provides a flowchart of possible pathways for producing CO_2-derived fuels integrated with an LWR. Steam and power from the LWR are provided for CO/H_2 (syngas) production in addition to any demand required by the chemical plant. Syngas can be produced from CO_2 via co-electrolysis and the reverse water-gas-shift (RWGS) reaction. Co-electrolysis is preferred over having separate electrolyzers for CO_2 and water as it has found to be more efficient (Fu et al. 2010). Syngas is used to produce a wide range of fuels and chemicals, including but not limited to synthetic NG, dimethyl ether, methanol, ethanol, and hydrocarbon fuel blendstocks. Ethanol and methanol can also be produced directly with co-electrolysis. However, it is thermodynamically unfavorable compared to making syngas, as the number of electrons needing fixed is 6 for methanol and 12 for ethanol, versus 2 for CO (Verma et al. 2019). Table 1 lists the numbers of electrons required for CO and other chemicals.

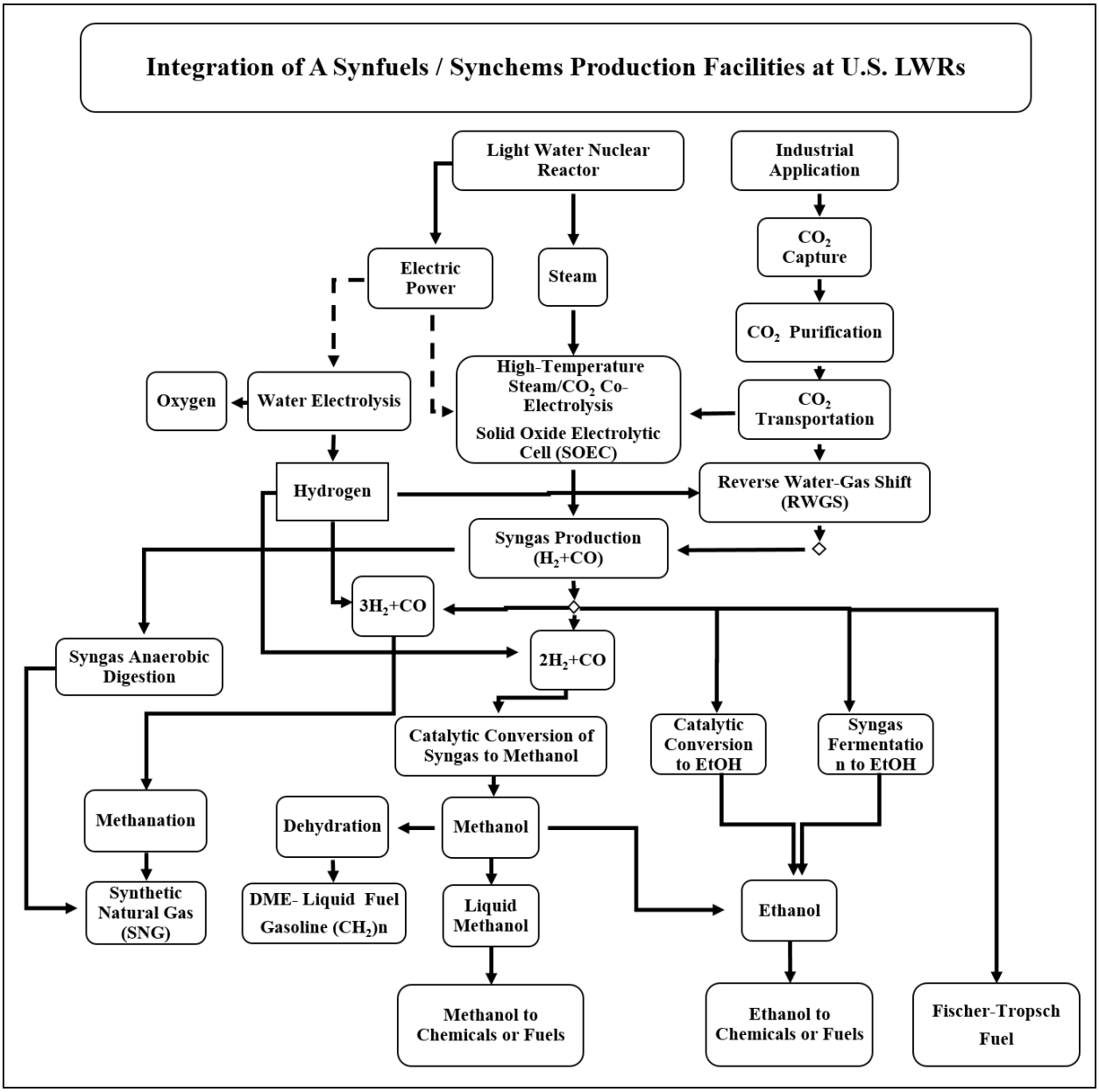

Figure 1. Overview of various synfuel/synchem pathways integrated with an LWR.

Table 1. Number of electrons transferred for converting CO_2 to syngas and chemicals.

Compound	Electrons Transferred
Syngas	2 e-
Formate	2 e-
Methanol	6 e-
Methane	8 e-
Ethanol	12 e-
Octanol	48 e-

2.1.1 Fuels

Syngas can be converted to oxygenate fuel, such as ethanol or methanol, or converted further into hydrocarbon fuels. Ethanol can be produced from syngas through biological or thermochemical means, as shown in Figure 2. Fermentation has been indicated by many researchers as an efficient and cost-effective method for conversion of syngas and several companies have now made the process commercial. LanzaTech now commercially produces ethanol via syngas fermentation using its proprietary Clostridial biocatalyst. Direct thermo-catalytic conversion of syngas to ethanol is also possible using several different catalysts, as shown in Figure 3.

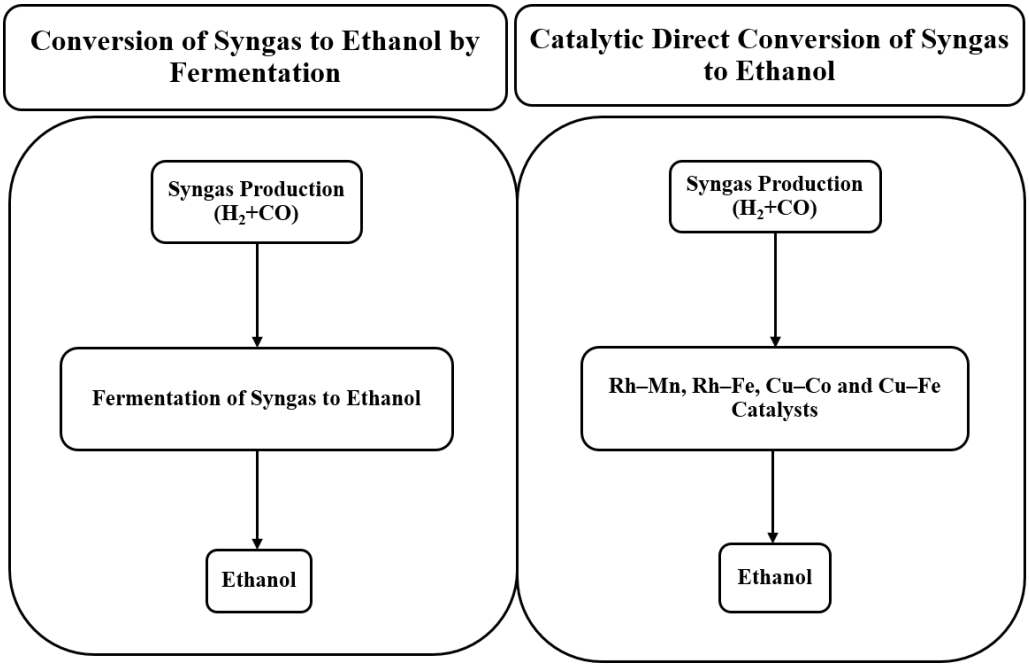

Figure 2. Fermentation and catalysis of syngas to ethanol.

Figure 3 details three alternative pathways for syngas conversion to ethanol that are in earlier stages of development than direct conversion shown in Figure 2. Figure 3a shows a direct conversion of syngas to ethanol through dimethyl ether (DME) as a key intermediate, the catalyst ZnAl2O4 / H-MOR ZnAl2O4 produces ethanol with a selectivity of 52% (Zhou et al. 2018). There are some other fuel alternatives, such as DME, which is a clean-burning, non-toxic, potentially renewable fuel that can be produced from methanol. The path of methanol-to-ethanol production is not necessarily the cheapest. Some other tracks with inexpensive catalysts may be worth evaluating like methyl acetate. The two-step conversion of methanol to ethanol via the methyl-acetate process is at the stage of pre-commercialization. Figure 3b details industrial methanol carbonylation to produce acetic acid that is performed either over the Ir-based (Cativa process) or Rh-based (Monsanto process) catalysts (Lu et al. 2016). Figure 3c shows the methanol conversion process through dimethyl oxalate. In this process ethylene glycol and ethanol can be produced, making it a versatile method for producing essential chemicals (Yue, Ma, & Gong, 2014).

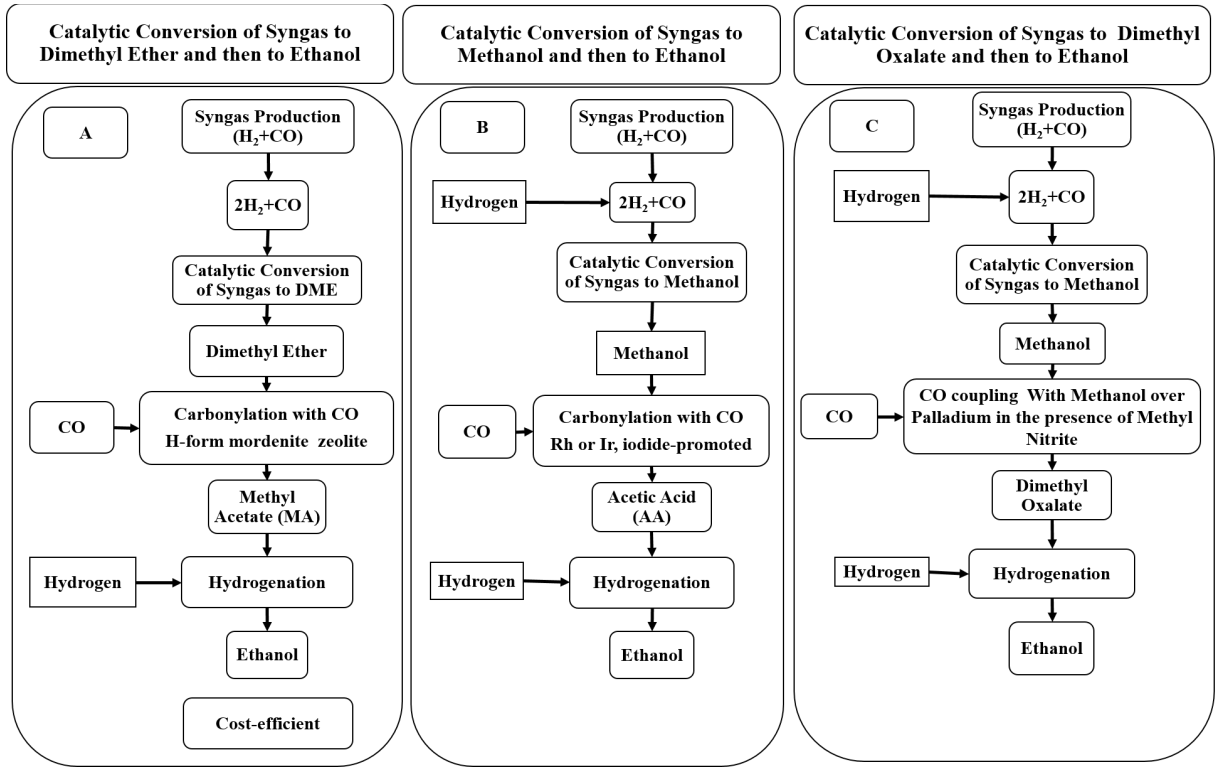

Figure 3. Syngas conversion to ethanol via catalysis.

Methanol can also be converted to hydrocarbons via the methanol-to-gasoline (MTG) process or the MTO process, both of which were originally introduced by the Mobil Oil Corporation. MTG is carried out over a HZSM-5 catalyst with high selectivity and little side-products, producing a hydrocarbon mixture of narrow compositional range (Gogate 2019). The MTO process was developed by essentially controlling process conditions to interrupt the MTG methanol to hydrocarbons reaction and has been commercialized by Honeywell UOP (UOP) and others.

Syngas can also be converted directly into hydrocarbon fuel using the established FT process, as shown in Figure 4. The FT process is the oldest coal-to-liquids technology, invented in the 1920s and used by the Germans during World War II to provide needed liquid hydrocarbon fuels (NETL 2020). Several FT-based commercial plants are operating today, including Sasol's Sasolburg coal-to-liquids plant (South Africa). Sasol started developing designs for a gas-to-liquids plant in Lake Charles, Louisiana, but the project was cancelled in 2017 due to the collapse of oil prices which decreased the differential between the NG feedstock and the value of the fuel products (Griggs 2017).

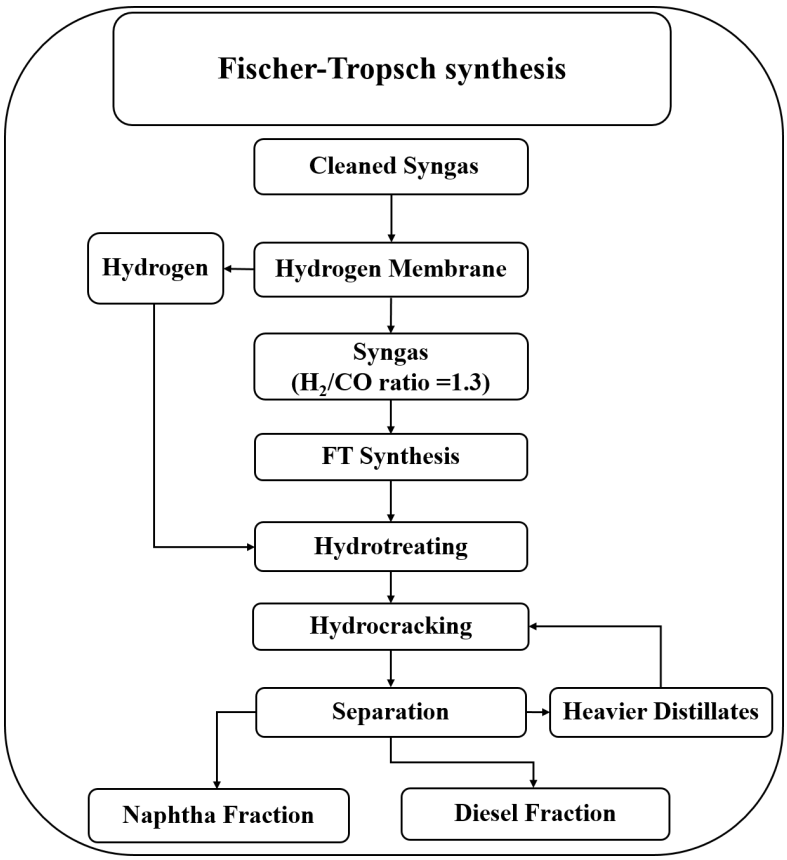

Figure 4. Syngas to hydrocarbon fuel via Fischer-Tropsch synthesis.

2.1.2 Chemicals

Many pathways exist for converting CO_2 to chemicals via thermochemical or electrochemical processes followed by catalysis. CO_2 reduction reactions can yield various valuable multi-carbon compounds including ethylene, acrylic acid, propylene, and C1 chemicals and polymers (Alper & Yuksel Orhan, 2017). As of 2017, 130 Mt of CO_2 is used annually to generate urea, salicylic acid, polycarbonates, and cyclic carbonates (Plasseraud 2010). Figure 5 shows two pathways for converting methanol to propylene or ethylene. The MTO reaction detailed in Figure 5b is one of the most critical reactions in C1 chemistry, which provides a chance for producing basic petrochemicals such as ethylene and propylene (Eng 1998). The methanol-to-propylene (MTP) process shown in Figure 5a produces propylene from methanol (Koempel & Liebner, 2007). Significant differences exist between the MTO and MTP processes in regard to reactor design and productivity (Barger 2002). MTO uses a fluidized-bed reactor, where heat can be removed quickly, and catalysts can be easily regenerated. MTP uses a fixed bed reactor where heat removal is problematic but overcome by using multiple catalyst beds. Fixed bed reactors are easier to scale up compared to fluidized beds, are cheaper and have better product selectivity. However, MTO can use crude methanol whereas MTP must use pure methanol, thus adding to the overall cost for MTP (Jasper & El-Halwagi, 2016). As is evident, the chemical derivatives of ethylene and propylene are numerous and have a variety of industrial applications. Polymerization processes are not detailed here.

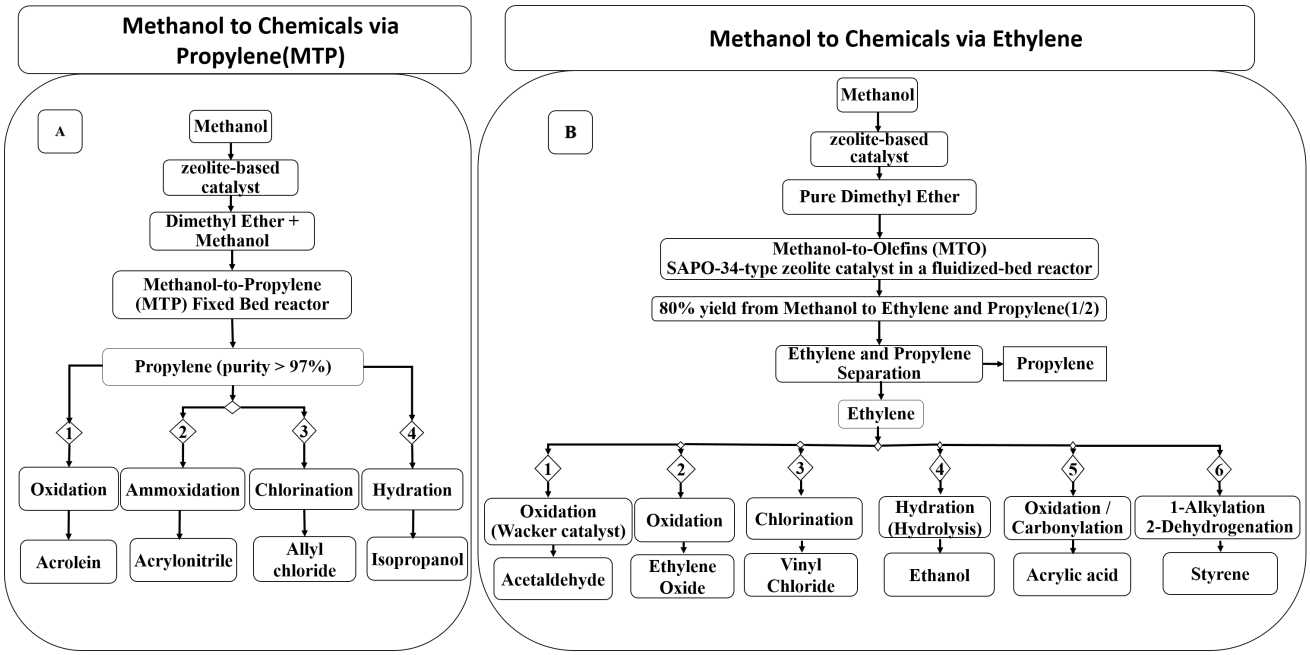

Figure 5. Methanol conversion to chemicals

Ethanol is an essential source of many chemical compounds, including para-xylene. Ethylene is the intermediate compound in the process of producing para-xylene, either directly (Figure 5b), or indirectly (Figure 6a). In a direct path, ethylene is used in more than one step of a complex process to produce para-xylene (Zhang, Qian, Kong, & Wei, 2015). In the indirect method, DMF is the primary compound for the production of para-xylene, and ethylene plays a role in forming double bonds (Lyons, Guironnet, Findlater, & Brookhart, 2012).

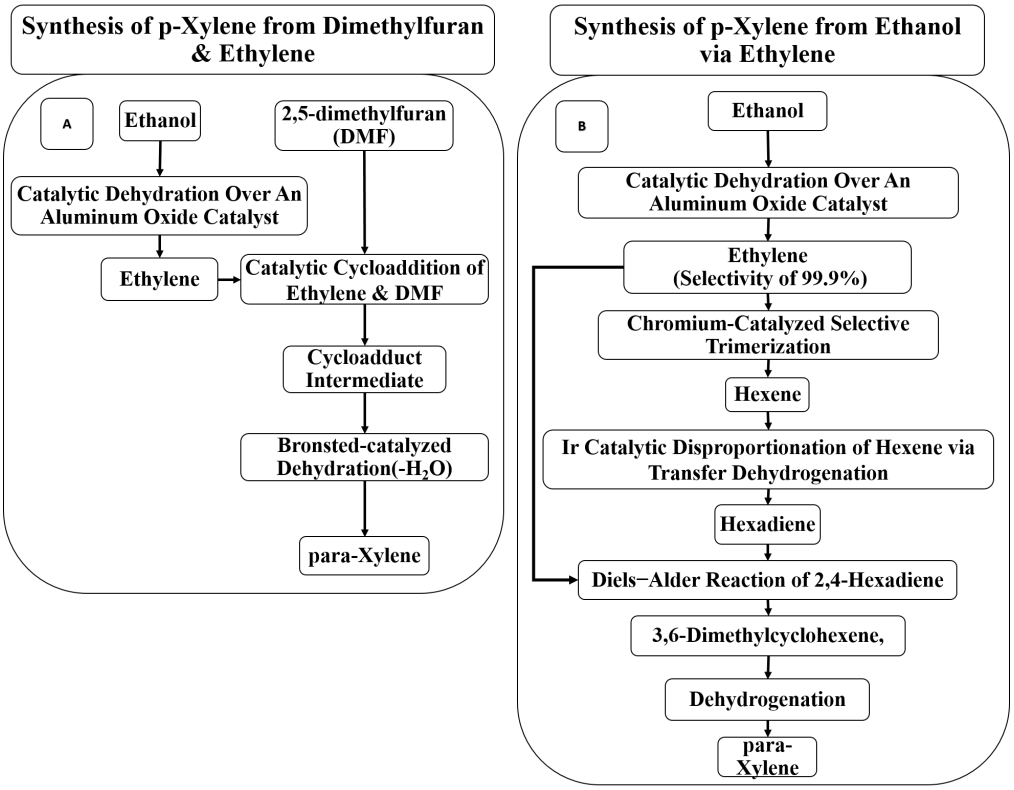

Figure 6. Ethanol conversion to para-xylene.

As a final note on chemical conversion, formic acid (FA) is a critical commodity used in agricultural, pharmaceutical, food, textile, and other chemical markets. The global demand for FA is expected to be 820,000 metric tons in 2021 (Sesto 2016). FA can be produced via electrochemical reduction (ER) or homogenous catalysis of CO_2 and H_2. Processing requirements range from 25 to 400 MJ/kg of FA produced (Rumayor, Dominguez-Ramos, & Irabien, 2018). This would require less than one and up to three LWRs dedicated solely to the production of FA to meet global demand.

2.1.3 Selected Hydrocarbon Fuel Routes for TEA

As the focus of this study is transportation fuels, conversion pathways converting CO_2 to fungible hydrocarbon fuel were selected for detailed modeling and TEA. Production of syngas via co-electrolysis or RWGS result in the same overall chemical equation (Eq. 1); therefore, similar energy consumption. Co-electrolysis via SOEC was selected as Idaho National Laboratory (INL) and PNNL have ongoing R&D in this area. As discussed, the possible range of syngas-to-fuel pathways is very extensive. From this extensive list, the possible range of technologies was down-selected to an ethanol- and methanol-based pathway, as both are versatile chemicals that can be further converted into fuels, and a wide range of chemicals and products (Dagle et al. 2020). As such, future studies building on this work may enable evaluation of chemical products or co-products, which can significantly improve the process economics (Dagle et al. 2020). In addition, existing process models previously developed by PNNL for biomass gasification and conversion to synfuels via the methanol and ethanol-based pathways could be leveraged and adapted.

$$4\ H_2O + 2\ CO_2 + 12\ e^- \rightarrow 4\ H_2 + CO + 3\ O_2 \quad (1)$$

The pathways selected for detailed analysis are shown in Figure 7. The methanol pathway is based on established technology for methanol generation from syngas and production of olefins from methanol using the UOP's commercialized MTO process (Bipin V. Vora, D. et al. 1998). Olefin oligomerization

and hydrogenation technology are based on a PNNL-patented process (Lilga et al. 2016). The methanol pathway is considered to be at a high technology readiness level (TRL), as the syngas-to-methanol technology (using coal or NG) has been in use for decades and there are several industrial installations of the MTO process based on coal gasification, one being in China and one in Belgium (Gogate 2019). The ethanol-based model is based on thermochemical syngas-to-mixed alcohol conversion technology (Stevens et al 1989; Dutta et al 2011) and the ethanol-to-butene process is currently being developed by PNNL (Dagle et al. 2020a). Olefin oligomerization and hydrogenation steps are based on the PNNL patented process, consistent with the methanol process model. The ethanol pathway is considered to be a low-to-mid TRL level technology, as the mixed alcohol conversion process to produce ethanol has only been tested at pilot scale (Summers et al 2019), and the ethanol-to-butene process is still in research stages.

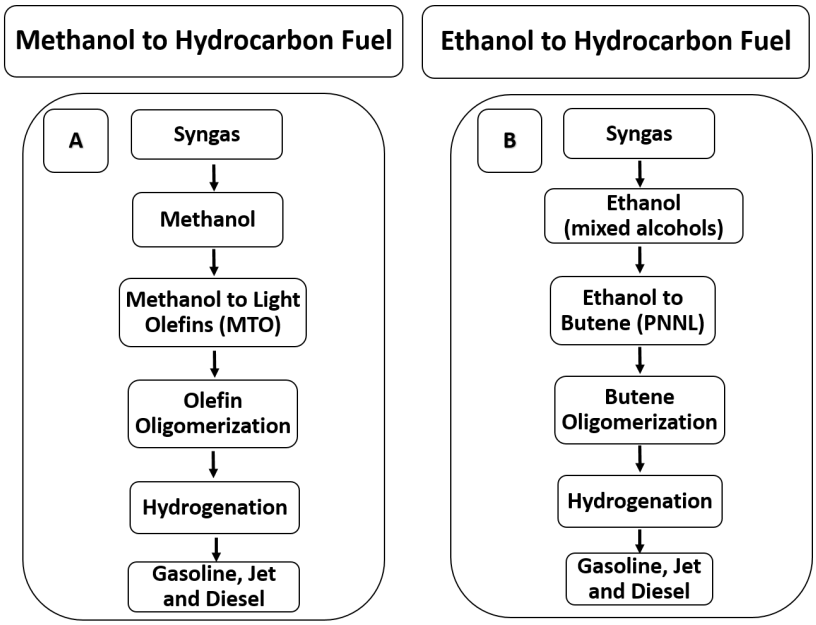

Figure 7. Selected syngas intermediate chemicals and pathways for fuel production through (a) methanol and (b) ethanol.

3. TECHNO-ECONOMIC ANALYSIS METHODOLOGY

The approach to developing conversion process techno-economics is similar to that employed in previous analyses conducted for the DOE's Bioenergy Technologies Office (BETO) (Dutta et al. 2015; Jones et al. 2013, 2014; Tan et al. 2015). Process flow diagrams and models are developed based on experimental research by PNNL, INL, and others, along with information from the literature and commercial vendors for mature and similar technologies. To assure consistency across all conversion pathways, BETO developed a set of economic assumptions that are used for all bioenergy TEAs (DOE 2016), which are also adapted for this work. An important aspect of these assumptions is that they reflect an "n^{th}-plant" design, as described below.

3.1 Definition of N^{th} Plant

A standard reference basis common to the conceptual design reports, known as the "n^{th}" plant design, is used. These assumptions do not account for additional costs that would normally be incurred for a first-of-a-kind plant, including special financing, equipment redundancies, large contingencies, and longer startup times necessary for the first few plants. For n^{th}-plant designs, it is assumed that the costs reflect a future time when the technology is mature, and several plants have already been built and are operating.

The specific assumptions are shown in Table 2. Note that tax incentives and other credits that may be applicable (e.g., credits under the Renewable Fuel Standard or cellulosic biofuels bonus depreciation) but are excluded from the analysis to represent plant economics independent of any government subsidies.

Table 2. Nth-plant assumptions.

Assumption Description	Assumed Value
Internal rate of return (IRR)	10%
Plant financing debt/equity	60%/40% of total capital investment (TCI)
Plant life	30 years
Income tax rate	21%
Interest rate for debt financing	8.0% annually
Term for debt financing	10 years
Working capital cost	5.0% of fixed capital investment (excluding land)
Depreciation schedule	7-years MACRS[(a)] schedule
Construction period	3 years (8% 1st yr, 60% 2nd yr, 32% 3rd yr)
Plant salvage value	No value
Startup time	6 months
Revenue and costs during startup	Revenue = 50% of normal Variable costs = 75% of normal Fixed costs = 100% of normal
On-stream factor	90% (7,920 operating hours per year)

(a) Modified accelerated cost recovery system

3.2 General Cost Estimation Basis

All costs in this report are on a 2019 constant dollar basis. This is the current reference year that BETO uses to facilitate comparison of various conversion technologies (DOE 2016). Capital costs are estimated from a variety of resources. The heat and material balances generated by the simulation software (AspenTech ASPEN-Plus; CHEMCAD v.7) are used to size the major pieces of equipment. Aspen Capital Cost Estimator (ACCE), information from published literature and vendors quotes are used to cost individual pieces of equipment. The original cost reflects the year of the cost quote or estimate, and the scale of the equipment. All capital costs are adjusted to an annualized 2019 basis using the Chemical Engineering magazine's published indices:

$$\text{Cost in 2019 \$} = \text{equipment cost in quote year} \times \left(\frac{\text{2019 index} = 541.7}{\text{quote cost year index}}\right) \quad (2)$$

The scale is adjusted to match the appropriate scaling term (heat exchanger area for example) by using the following expression:

$$\text{Scaled equipment cost} = \text{cost at original scale} \times \left(\frac{\text{scale up capacity}}{\text{original capacity}}\right)^{n} \quad (3)$$

where n is the scale factor, typically, 0.6 to 0.7.

After equipment is scaled and adjusted to the common cost year, factors are applied to calculate the total capital investment. Individual installation factors calculated by ACCE are multiplied by equipment costs, unless installed costs are already available from vendors. The total direct cost is the sum of all the installed equipment costs, plus the costs for buildings, additional piping, and site development. Indirect costs are estimated as 60% of the total installed costs. Factors for the calculation of these additional direct and indirect costs are listed in Table 3. The sum of the direct and indirect costs is the fixed capital investment (FCI). The total capital investment is the fixed capital plus working capital and land costs.

Table 3. Cost factors for direct and indirect costs.

Direct Costs	
	% of Total Installed Cost (TIC)
Buildings	4.0%
Site development	10.0%
Additional piping	4.5%
Total Direct Costs (TDC)	18.5%
Indirect Costs	
	% of TDC
Prorated expenses	10%
Home office and construction fees	20%
Field expenses	10%
Project contingency	10%
Startup and permits	10%
Total Indirect Costs	60%
Working Capital	5% of FCI
Land	HTL: 6 acres @ $15,000/acre Upgrading: 6% of Total Purchased Equipment Cost

Operating costs are estimated by using the results from the ASPEN-Plus heat and material balances and applying raw material and utility prices (given in individual pathway TEAs in following sections). Labor requirements and rates for the modeled synfuels plant are consistent with past TEAs performed for biomass-gasification-based fuel plants and are listed in Table 4. Note that labor needs associated with running the front-end SOEC portion of the plant as compared to a gasifier may be lower; therefore, these costs are likely conservative.

Table 4. Labor costs for modeled synfuels plants.

Fixed Operating Costs	**$/Year**	**No. workers**	**Base yr $/hr**	**$/y Total in 2011$**	**$/y per Worker in 2019$**	**$/y Total in 2019$**	**$/hr in 2019$**
Plant Manager	161,362	1	70.67	161,362	170,761	170,761	82.10
Plant Engineer	76,839	1	33.65	76,839	81,315	81,315	39.09
Maintenance Supr	62,569	1	27.40	62,569	66,214	66,214	31.83
Lab Manager	61,471	1	26.92	61,471	65,052	65,052	31.27
Shift Supervisor	52,690	5	23.08	263,450	55,759	278,795	26.81
Lab Technician	43,908	3	19.23	131,724	46,466	139,397	22.34

Maintenance Tech	43,908	16	19.23	702,528	46,466	743,449	22.34
Shift Operators	**43,908**	**27**	**23.08**	**1,185,516**	**46,466**	**1,254,570**	**22.34**
Yard Employees	30,736	12	13.46	368,832	32,526	390,316	15.64
Clerks & Secretaries	39,517	3	17.31	118,551	41,819	125,456	20.11

With the capital and operating costs, the MFSP is determined using a discounted cash flow rate of return analysis. The MFSP is the plant gate selling price of the fuel product that makes the net present value of the project equal to zero given the financial factors assumed (see Table 2).

4. CO-ELECTROLYSIS OF CO_2 AND WATER TO SYNGAS

SOECs offer a unique method for converting CO_2 and steam into syngas. Co-electrolysis is preferred over separately electrolyzing steam and CO_2 because of reduced cell resistance (area-specific resistance) and lower conversion of CO to C (Stoots 2010). Figure 8 details the process inclusive of the SOEC stack, heat exchangers, compressor, pump, and separators. In this process CO_2 and water enter the stack in vapor phase. Power supplied to the stack yield syngas and oxygen. Oxygen flows from the cathode to the anode and is removed by a sweep gas, typically air. Excess CO_2 and steam are separated from the stack output and reintroduced to the stack inlet.

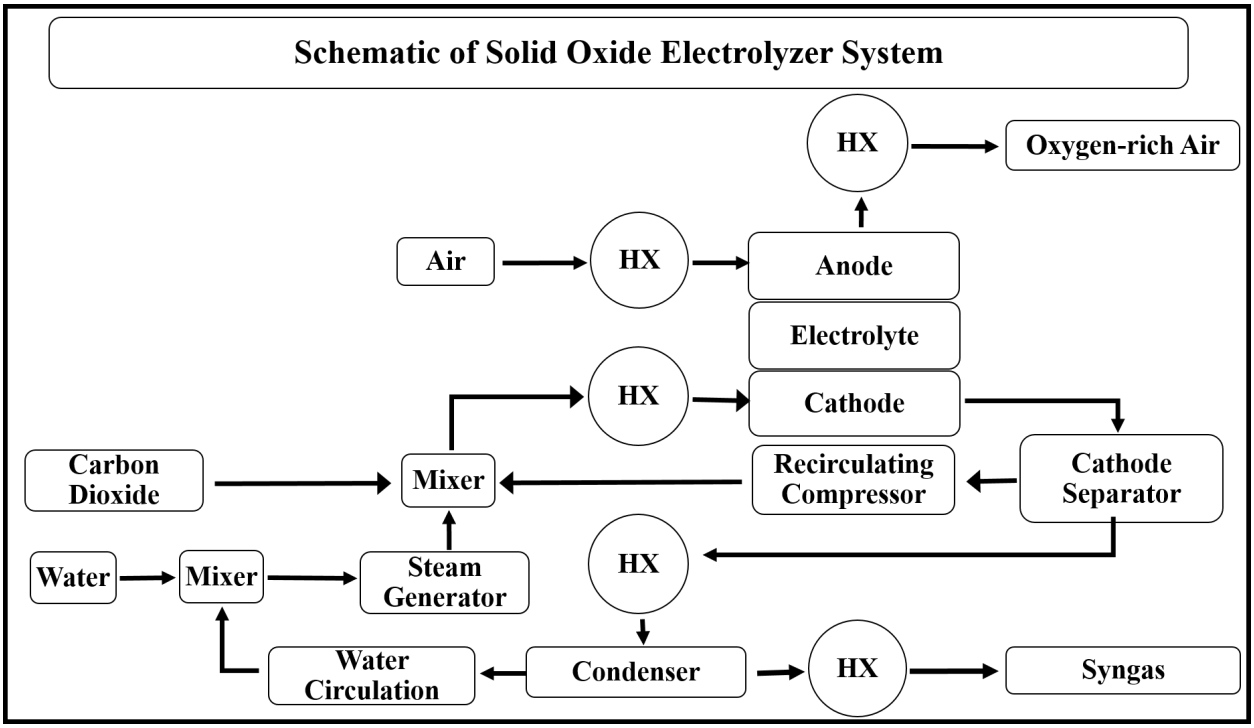

Figure 8. Schematic of SOEC.

4.1 SOEC Design

Co-electrolysis of CO_2 and H_2O have been studied for the better part of a decade as method of producing syngas using the same technology as has been used over several decades for solid oxide fuel cell (SOFC)s. Rather than producing power, SOECs consume electrical energy (and sometimes heat) to convert CO_2 and H_2O in syngas.

Solid oxide electrolysis makes use of the same material and technology as solid oxide fuel cells. A single cell in an SOEC stack is comprised of an anode, cathode, and solid electrolyte. The cathode is typically constructed of nickel and yttria stabilized zirconium and the anode is a mixture of lanthanum, strontium, and manganese oxide. When power is supplied to the SOEC, steam, and CO_2 are converted to H_2, CO, and O_2. This occurs via three reactions, namely the reverse water-gas shift and the co-electrolysis reactions:

$CO_2 + H_2 \leftrightarrow CO + H_2O$ (RWGS) (2)

$CO_2 + 4e^- \rightarrow CO + \frac{1}{2}O_2$ (Electrolysis of CO_2) (3)

$H_2O + 4e^- \rightarrow H_2 + \frac{1}{2}O_2$ (Electrolysis of H_2O) (4)

A model was developed in ASPEN-Plus V10 to represent product stream compositions, and heat and power requirements for an SOEC stack. Inlet mole and conversion fractions were specified to produce the required ratio of H_2/CO in the syngas for the downstream fuel production processes evaluated (~2 for methanol and ~1.2 for mixed alcohol reactors). The model was developed to simply match results from experimentally validated SOEC models from the literature (O'Brien et al. 2009; Redissi 2013) for approximately the same syngas ratios investigated. Initially, a single-pass model, shown in Figure 9, was generated using the same methodology as described by Redissi & Bouallou, 2013. The model introduces $CO_2/H_2O/H_2$ at a molar ratio of 45:45:10 and a temperature of 300°C to the stack. The mixture enters the stack whereupon RWGS occurs modeled as an equilibrium reactor labeled as LRWGS. A topping heater brings the mixture to the adiabatic stack operating temperature, in this case 800°C. Electrolysis occurs at thermo-neutral voltage in the stack modeled by a stoichiometric reactor (RSTOIC) using a fractional conversion from electrolysis reactions at 0.95 and 0.05 for H_2O and CO_2, respectively. RWGS again occurs at 800°C. A comparison between PNNL's model and the one created by Redissi et. al. is given in Table 5.

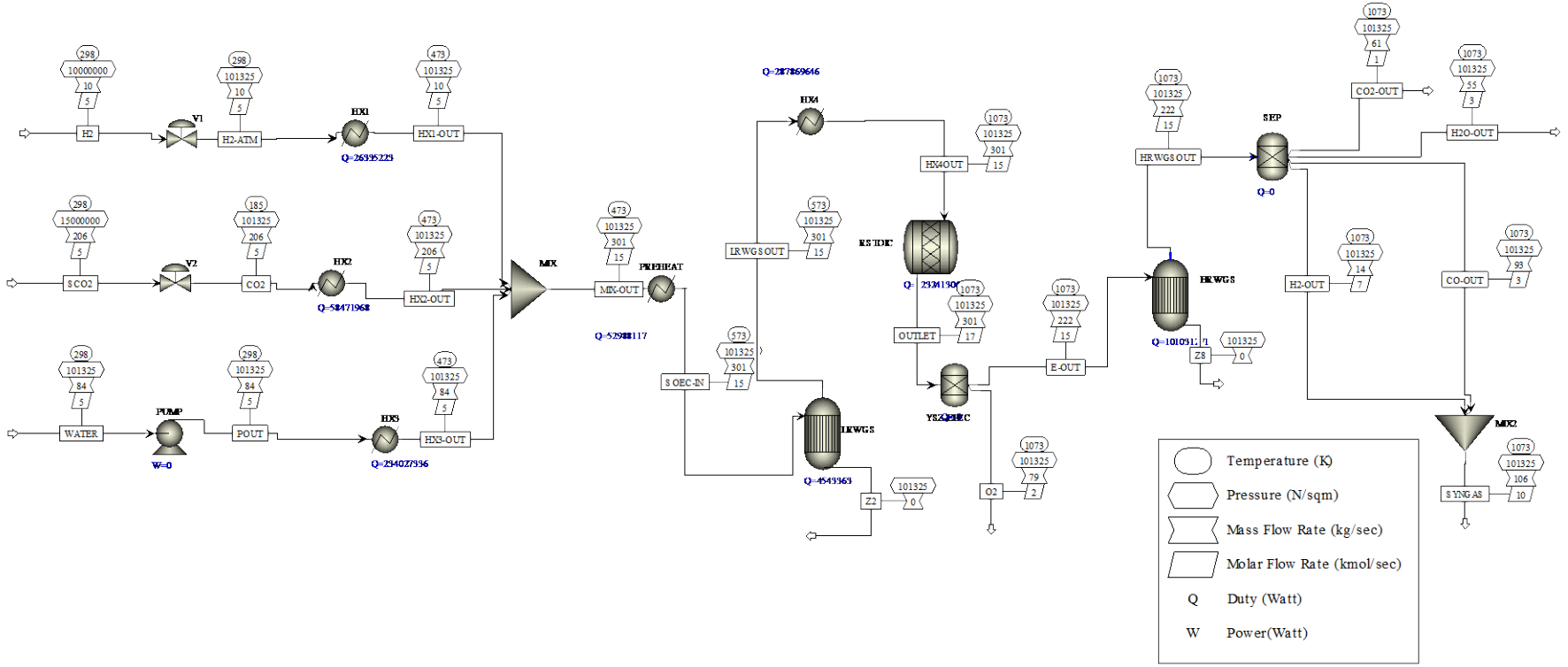

Figure 9. Single-pass model.

Table 5. Comparison of Redissi and PNNL SOEC models.

Outlet Gas	**Redissi Model (2013)**	**PNNL Model for the EtOH-to-Fuels Model (Section 6)**	**Units**
Molar Ratio	1.19	1.18	
CO	7276	7262	kg/hr
H_2	617	618	kg/hr
HX4	6061	6057	kW_t
ELECTRO (RSTOIC)	35000	32300	kW_e
HRWGS	2194	2222	kW_t

Although the Redissi model was validated experimentally, it is not representative of how a typical SOEC plant would operate. Nevertheless, the Redissi model served as a valuable first step in validating a working model for this study. Missing from the Redissi model was heat recuperation and recirculation of steam and CO_2 streams. Additionally, hydrogen is not a primary input to the stack as it is in the aforementioned model. As shown in Figure 10, the model was updated to include heat recuperation (RHX1 and RHX2), greatly reducing the power input to the topping heater. The remaining electrical heaters were replaced with steam heat exchangers available from the LWR at 260–300°C to superheat the incoming gas streams (WX1 and WX2). Approximately 30% of the hydrogen was consumed in the RWGS; this was modeled by recirculating a portion of the hydrogen product to the inlet of the stack. The final syngas ratio was 2:1.

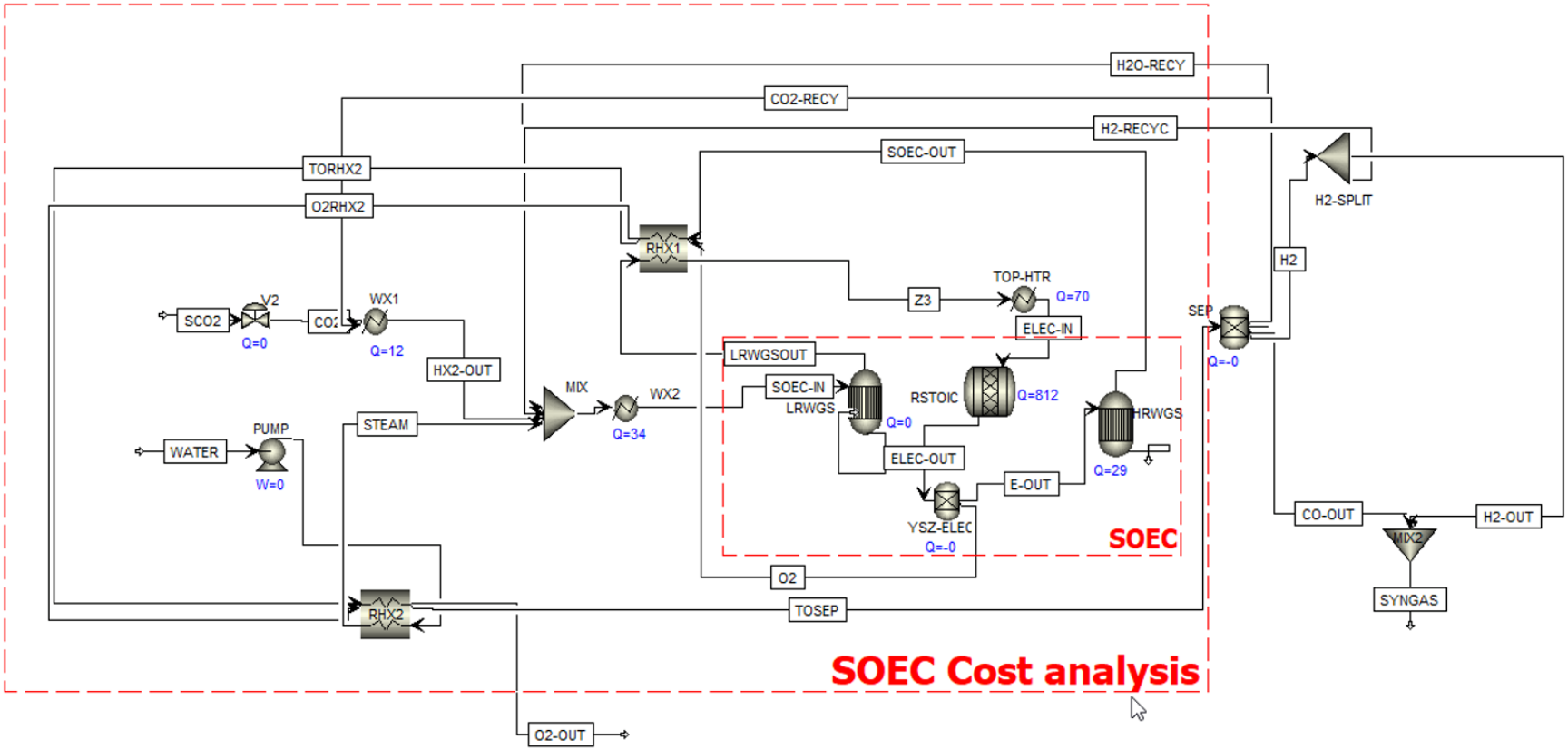

Figure 10. ASPEN-Plus model with recirculation and heat recuperation.

A comparison of a UniSim model developed by INL (O'Brien et al. 2009) and the PNNL model is given in Table 6. Note that the optimal current density and area-specific resistance (ASR) from the O'Brien study were assumed for this analysis. The input and output mole fractions of the PNNL model match fairly closely with the O'Brien study. Potential reasons for the slight discrepancies are slight differences in syngas molar ratio, different modeling platforms, and the data from the O'Brien paper was read visually from a plot; therefore, the data are not stoichiometrically precise. Different SOEC operating pressures have been assumed in the literature. Redissi and Bouallou (2013) and Zhan et al. (2009) used 0.1 Pa. O'Brien et al. (Table 5), as well as Er-rbib et al. (2018) and Stoots et al. (2009) used 3.5 MPa. However, a definitive relationship between pressure and process efficiency is entirely evident from the literature. A slight efficiency gain of 2.6% was reported for operating pressure of low pressure (1.6 bar) versus high pressure (5 bar) (Becker 2012).

Table 6. Comparison of O'Brien, et al. model and PNNL Model

Parameter	O'Brien, et. al. (2009)	Model for the EtOH Process (Section 6)
Inlet Composition	H_2: 24.45% CO_2: 30.23% H_2O: 45.32%	H_2: 22.2% CO_2: 26% H_2O: 51.8%
Outlet Composition	H_2: 34.57% CO:16.05% CO_2: 14.81% H_2O: 34.57%	H_2: 38% CO:13.3% CO_2: 13.2% H_2O:35.4%
Power	300 MWe	812 MWe
Operating Temperature	800°C	800°C
Operating Pressure	3.5 MPa	0.1 Mpa
Current Density[1]	0.4 A/cm^2	0.4 A/cm^2
ASR[1]	1.5 Ohm cm^2	1.5 Ohm cm^2
V_{op} (adiabatic)	1.34	1.34 (thermal neutral)

1 Optimal density and ASR selected from O'Brien

4.2 SOEC Cost Estimation

Two different methods were used to estimate the cost of an SOEC system. One method is based on an extensive cost analysis of SOFCs, and the other is based on an area-specific cost analysis of SOECs. The SOFC method only required the total electrical power required for the stack, whereas the other method required the number of cells required as calculated from Faradays Law.

A detailed cost analysis was conducted for manufacturing, installation and operation of an SOFC for a nominal power output of 270-kW sized for ground-based distribution generation (Weimar et al. 2013). It was found that electricity costs for a mass manufactured SOFC could be $0.07/kWh based on a standard approach to manufacturing cells. A detailed study was conducted to understand the various steps required for manufacturing the units that included materials, equipment, and labor. Volumes were projected at 10,000 units/year. In addition, a sputtering approach for processing the units was considered and found to increase the performance of the stack and reduce capital costs by 33%. The cost study was based on 400-cm^2 cell area; however, the result was specific to power generation.

Given the mole flow of monatomic oxygen from the cathode to the anode as given by the model, the number of cells can be determined from Faradays Law:

$$\Delta\dot{N}_O = \frac{I_e}{2F}; \quad \text{where} \quad I_e = iA_{cell}N_{cells}$$

Where the cell area is 250 cm^2 and the current density is 0.4 A/cm^2.

Using the sputtering method, the power-specific manufacturing and installation costs were found to be $65/kW and $182/kW, respectively. These costs are specific to the stack and housing costs only and does not include ancillary equipment such as heat recuperators and topping heaters. These costs were used for the economic analysis of the SOEC stack for the two pathways evaluated in this study. For the MTO-based fuel pathway (278 MWe, see Section 5), total installed cost of the stack is $68.8M and for the ethanol-based fuel pathway (425 MWe), total installed cost is $105M.

Table 7 shows a comparison of other SOEC cost estimates from the literature compared to Weimer's method for the MTO-based model (Section 5). Giglio, et al. 2015 estimated the area-specific costs for a stack and its enclosure to be $1500/m^2 of SOEC active area (i.e., the cell area). Using an assumed a cell size of around 225 cm^2 (O'Brien 2009) to be acceptable given the available manufacturing techniques in 2009, and along with the current density of 0.4 amp/cm^2 and monatomic oxygen flow across the cell from the model, the total cell area required is found to be 52,986 m^2. The total cost from this approach comes to $79.5M, for a difference of roughly 15% between the two approaches. Estimates from Buttler (2015) and Anghilante (2018) are $93M and $61M. The costs selected for this study (Weimar 2013) is within the range of other literature values shown.

Table 7. SOEC stack cost estimates from literature.

Source	**Basis**	**Installed Cost (Stacks & Enclosure)**	**MTO Model (Section 5) SOEC Plant Cost (2019$; Scale 278 MWe)**
Weimar 2013	Fuel Cell Power	$247/kW	$68.8M
Giglio 2015	SOEC Area	$1500/m^2	$86.7M
Buttler 2015	SOEC Area	$1755/m^2	$101.5MM
Anghilante 2018	SOEC Power	$219.5/kW	$61.5M

5. SYNGAS TO FUELS VIA METHANOL-TO-OLEFINS PROCESS

5.1 Design and Modeling

The overall block flow diagram for the modeled distillate fuel production process through the MTO route is shown in Figure 11. Syngas is first generated via co-electrolysis, as described in Section 4.1. Raw syngas from the SOEC section is compressed to 420 psia. Entrained water is separated in knock-out pots prior to and between stages of compression and recycled back to the SOEC. Amine-based acid gas removal is then used to separate CO_2 from the syngas for recycle back to the SOEC. Removal of CO_2 also serves to reduce its concentration in the syngas feed to the downstream processes, thereby reducing equipment size and capital. Saturated steam at 374°F is used to regenerate the amine solvent in a mass ratio of 2:1 for steam-to-CO_2 removed (Tan et al. 2016). Single-pass conversion of CO_2 is 29% and overall carbon efficiency to CO including recycle is 98.7%.

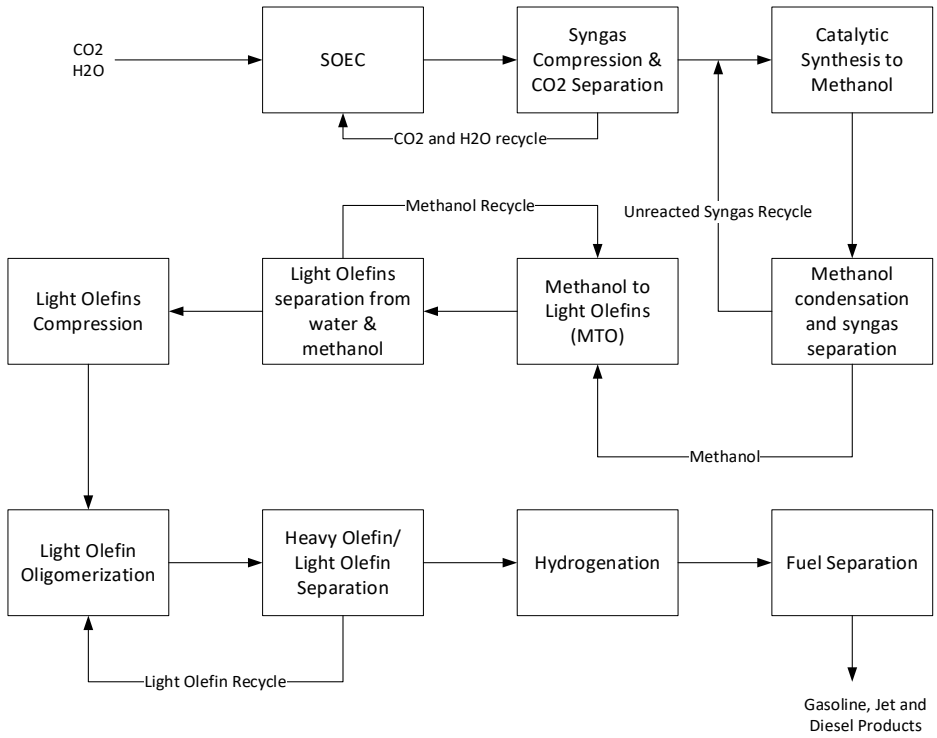

Figure 11. MTO process diagram.

Syngas is then compressed to 925 psia, mixed with unreacted syngas, heated to 440°F, and fed to the methanol reactor. Methanol synthesis occurs over a copper/zinc oxide/alumina catalyst. Process conditions for the methanol reactor are given in Table 8. Heat from the exothermic synthesis reaction is removed from the reactor via steam generation (Tan et al. 2016). Steam is used for downstream reboiler duties and for a portion of the steam needed in the CO_2 removal process. Single-pass conversion of CO is 34% and overall conversion with syngas recycle is 94%. Overall carbon efficiency of CO (and the low levels of CO_2 in syngas) to methanol is 93.2%.

Table 8. Process conditions for methanol synthesis reactor (exothermic).

Assumption	**Jones, et al. (2009) Phillips, et al (2011)**
Temperature, F	440
Pressure, psia	920
H_2: CO ratio	2.0
CO_2 concentration (mol%)	4%
Single-pass CO conversion	34%
Overall CO conversion	94%

Methanol is then preheated and fed to the MTO fluidized-bed reactor where ethylene, propylene, 1-butene, and 1-pentene are produced (Vora and Marker 1998). Table 9 lists the assumed process conditions and conversion efficiencies. Some lights gases and coke are formed by side reactions; the coke is burned off periodically. The effluent mixture from the MTO reactor is cross exchanged to pre-heat the inlet gas and then quenched in a direct-contact, circulating-water spray tower to separate the non-condensable gases from water generated by methanol dehydration. Residual methanol is stripped from the

quench column wastewater and recycled to the MTO reactor. The overall conversion of methanol is 99.98% with an MTO carbon efficiency of 93.4%.

Table 9. Process conditions for methanol-to-olefins (exothermic).

Temperature, F	814
Pressure, psia	19.7
WHSV	1
Single-pass Methanol conversion	99%
Overall methanol carbon efficiency to olefins	93.4%

The olefin-rich gas mixture goes through various separation steps and catalytic reactors to produce longer-chained hydrocarbons in the diesel-boiling range in an oligomerization step (Lilga et al. 2017). Oligomerization reactor conditions and conversions are listed in Table 10. The separation steps include a lean-oil scrubber used to recover olefins and remove methane and other paraffin by-products to prevent their accumulation in recycle streams used to increase the product yield.

Lighter olefins are recycled to increase their carbon number to the desired range of 9 to 16. Two catalysts are used to produce dimers and trimers of the reactive olefins to increase the carbon number. In the first oligomerization reactor, operated at 570°F and 302 psia, an H-Beta Zeolite catalyst is used to produce dimers and trimers of smaller (C2 to C4) olefins to C6+ olefins. The overall oligomerization reaction is exothermic; therefore, no heat is needed to drive the reaction. The assumed net conversions of ethylene, propylene and butene are 75%, 82%, and 27%, respectively. The second reactor, operated at 326°F and 140 psia, uses an Amberlyst catalyst to increase the yield of C9 to C18 compounds. The net conversion assumed for C4, C5, C6, C7, C8, and C9 olefins to their dimers are 40%, 36%, 100%, 26%, 23%, and 3%, respectively.

Table 10. Process conditions for oligomerization of olefins (exothermic).

Assumption	**Reference: Dutta et al 2015; Tan et al 2016b**
Temperature, F (first stage)	320
Pressure, psia (First stage)	302
Temperature, F (second stage)	288
Pressure, psia (second stage)	140
Stage 1 C2-C5 olefins C eff. to C6+ olefins	48%
Stage 2 C2-C5 olefins C eff. to C6+ olefins	49%
Overall C2-C5 olefins C eff. to C6+ olefins	98.6%

Lighter olefins (in the C4 to C9 range) are recovered and recycled as part of the lean-oil scrubber feed, and the heavier olefins are hydrogenated using separately purchased hydrogen over a Pd-on-alumina hydrogenation catalyst operating at 750°F and 130 psia. The H_2 partial pressure is maintained at about 70% of total pressure to minimize coking and to completely hydrogenate all double bonds in the feed. The excess hydrogen is separated from the diesel product after condensation and knock-out pots. It is recycled to the reactor operating pressure using a pressure booster. The hydrogenated product is distilled into gasoline (61%) and diesel (39%) blend stocks in a final distillation column. Overall carbon efficiency of olefins to fuel product is 98.5%.

5.2 Performance and Economic Results

Figure 12 shows the resulting power and heat inputs and outputs for the modeled MTO process. About 92% of the power demand is for the co-electrolysis unit, with the remainder consumed for gas compressors and pumps throughout the plant. Steam is used for heating of the feed CO_2 and water to the SOEC system, for recovery of the amine solvent in the CO_2 recovery process, and for column reboilers and heating of various process streams. About 84% of the steam requirement for the integrated plant is for amine solvent recovery (shown as CO_2 Sep block below). Heat from the methanol reactor (syngas to MeOH block below) is used to produce a portion of the steam requirement, with the balance supplied by saturated steam (536°F) from the LWR. The net power and heat requirements for the fuel plant are 326 MW_e and 136 MW_t. Electrical and thermal energy usage for syngas production for the modeled SOEC portion of the plant is 3.2 MWe/lb syngas and 19.4 MWt/lb syngas, respectively, for a H_2:CO ratio of 2.1. Note that this is only the energy usage for producing raw syngas and does not include steam used to recover amine solvent for separation of CO_2. All reactors downstream of syngas production and CO_2 separation are exothermic; therefore, no steam/heat is needed to drive these steps. However, extra steam is needed for distillation column. For the syngas-to-methanol step, steam is generated on the shell side of the methanol reactor, capturing 31 MW of thermal energy. For the methanol-to-olefins step, 8.5 MWt of steam is generated from heat contained in the flue gas from the MTO reactor catalyst regenerator and 3.3-MWt steam is used to heat the feed stream and for the methanol recycle recovery column reboiler. For the oligomerization step, the heat generated is relatively low quality (<450°F) and is not included in the overall thermal heat generation; however, (it can be used for boiler water preheating. Distillation towers for separation of oligomers use 5.3 MWt of steam in reboilers. For the hydrotreating step, 6.3 MWt of steam is generated from the hot reactor effluent and 2.9 MWt of steam is used for reboiler heat in the diesel/naphtha fractionation column.

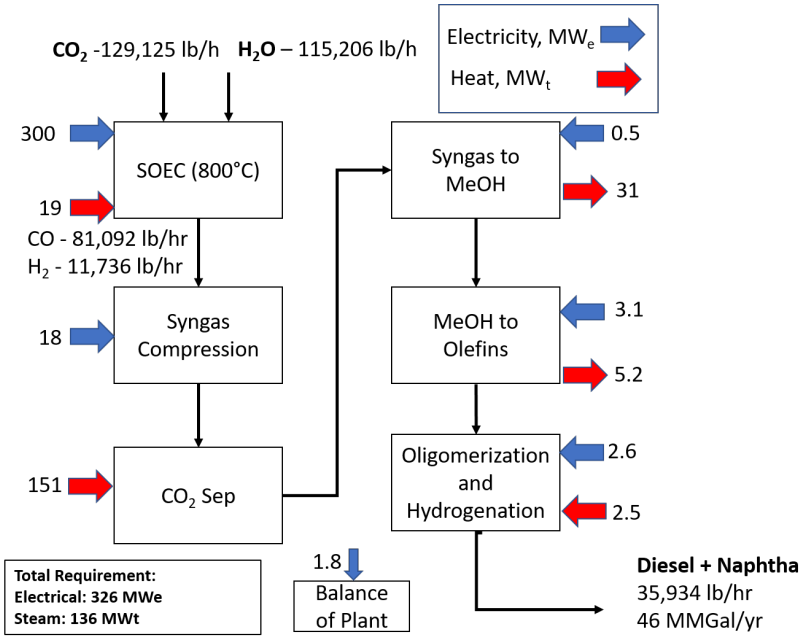

Figure 12. Electrical and thermal inputs/outputs for the synfuels via MTO process using nuclear heat.

Table 11 lists the raw material, waste disposal and utility costs assumed for estimating variable operating costs for the fuel production plant. Boardman et al. (2019) estimated the levelized cost (including capital and operating expenses) of CO_2 delivered to a hybrid LWR-methanol plant scenario including capture from an ethanol plant, compression, storage, and transportation via pipeline to the nuclear power plant. They determined a range of $14.6 to 38.3/tonne for a 530 tonne/day capacity

methanol plant. The mean of this range ($33.3/tonne) was used in this study and sensitivity analysis was conducted around this assumption. For comparison, the breakeven CO_2 sales price estimated for capture from fossil energy plants ranges from $44/tonne to $119/tonne (James et al. 2019). A range of $0 to 120/tonne CO_2 cost was investigated in the sensitivity analysis. Although clean O_2 could potentially be a co-product of the process, to be conservative, no O_2 credit is included in the analysis.

Table 11 Variable operating costs for the MTO to fuels model TEA.

Variable Operating Costs	**2019 Price**	**Unit**	**Reference**
Raw Materials			
CO_2	33.3	$/tonne	Boardman et al. 2019
Methanol Synthesis Catalyst	12.03	$/lb	SRI PEP 2007 Yearbook
MTO Catalyst	37.14	$/lb	Gelbein 2003
1st Stage Oligomerization Catalyst	11.30	$/lb	Dutta et al. 2015
2nd Stage Oligomerization Catalyst	18.10	$/lb	Tan et al. 2016b
Hydrogenation Catalyst	59.0	$/lb	Gerber 1999.
Amine Makeup	1.70	$/lb	Phillips et al. 2007
Boiler Chemicals	3.26	$/lb	Phillips et al. 2007
Cooling Tower Chemicals	1.95	$/lb	Phillips et al. 2007
Hydrogen gas (for hydrotreating of oligomers)	0.95	$/lb	2020 PEP Yearbook
Waste Disposal			
Wastewater treatment	3.20	$/100 ft3	Phillips et al. 2007
Utilities			
Cooling Tower makeup	236.5	¢/1000 gal	Phillips et al. 2007
Process Water to SOEC	327.0	¢/1000 gal	Redissi et al. 2013
Boiler Feed Water makeup	236.5	¢/1000 gal	Phillips et al. 2007
Process Steam	359	¢/1000 lb steam	Boardman et al. 2019, Knighton et al. 2020c
Electricity	3.0	¢/kwh	Boardman et al. 2019, Knighton et al. 2020c

Table 12 gives the major performance and economic results for the synfuel plant. Also presented for comparison is the biomass case, where gasification of woody feedstock is used on the front end instead of co-electrolysis. Woody feedstock cost is assumed to be $63.23/dry ton (Hartley et al. 2019). Feedstock CO_2 and water for the SOEC are 1,549 ton/day and 331,369 gal/day, respectively. For perspective, this is about 1.75 times the daily CO_2 produced from a typical corn ethanol plant (100 million gallon/year) and about half the capacity of an Olympic-sized swimming pool, respectively. Fuel generation is about 1,184 barrel/day (BPD) of diesel and 2,012 BPD of naphtha (motor gasoline blendstock). The U.S. demand for diesel and gasoline in 2019 was 3.3 million BPD and 9.3 million BPD, respectively (EIA 2020b). Energy efficiency for the co-electrolysis process is similar to the gasification case, but overall carbon efficiency is much higher due to the high selectivity of the electrolysis reactions. Feedstock cost is

higher for the biomass case due to the lower carbon efficiency as compared to the co-electrolysis case. Capital costs for the syngas generation are higher for the co-electrolysis case due to the assumed cost of the SOEC stacks. However, syngas cleanup and methanol production costs are lower due to a cleaner and lower total flow of gas (fewer light ends and CO_2 than from gasification) through the compression system and reactor than results from biomass gasification. The fuel production cost breakdown is given on the bottom half of Table 12 and illustrated in Figure 13. The MFSP for the SOEC case is $4.44/gal, with electricity and steam cost making up about half of the total production cost. Optimistic and conservative cases using the lower and upper bounds respectively for estimated electricity and steam price from an LWR (2c/kWh with $2.49/1000 lb1000lb and 4c/kWh with $4.70/1000 lb1000lb steam, respectively) are included for comparison. Most of the steam requirement is for removal of CO_2 from the syngas (recovery of amine solvent). In the biomass gasification case, extra steam is generated from heat recovered from the char combustor, which supplies all heat needs for the plant as well as onsite generation of power. In the SOEC case, steam must be supplied from the LWR.

Table 12. Economic results for syngas to fuels process (all costs in 2019 $).

Flowrates	**Co-electrolysis**		**Biomass Gasification**	
CO_2 Feed, lb/hr (ton/day)	129,125 (1,549)		Biomass: 183,718 (2205)	
H_2O Feed, lb/hr (ton/day)	115,206 (1,381)		N/A	
Diesel Blendstock, lb/hr (BPD)	13,841 (1,184)		14,026 (1,185)	
Gasoline Blendstock, lb/hr (BPD)	22,107 (2,102)		21,938 (2,103)	
Diesel Blendstock, mmBtu/hr (MW)	262.0 (76.8)		262.2 (76.8)	
Gasoline Blendstock, mmBtu/hr (MW)	421.4 (123.5)		421.6 (123.6)	
Carbon efficiency (C in synfuel/C in feed)	86.1%		32.4%	
Energy efficiency (fuel)/(power+steam+H_2)	41.5%		43.0% (including input biomass)	
Capital Costs, $ million				
Installed costs				
Syngas Generation		87.4		51.3
Syngas Compression and Cleanup		53.0		71.8
Methanol Production		30.6		49.0
Hydrocarbon Fuel Production		60.1		58.8
Steam Cycle / Power Gen		5.4		34.1
Balance of plant		4.8		7.7
Total installed capital cost		241.3		272.7
Indirect costs		125.2		140.9
Fixed capital investment		400.7		451.900
Total capital investment (TCI)		**422.3**		**475.2**
Operating Costs and Production Cost Breakdown				
	$ million/yr	**$/gal fuel blendstock**	**$ million/yr**	**$/gal fuel blendstock**
Variable operating cost				
Feedstock	15.5	0.33	45.8	0.99
Hydrogen (for hydrotreating oligomers)	4.0	0.09	3.6	0.08
Catalyst and Chemicals	3.9	0.08	4.8	0.10
Waste Disposal	0.3	0.01	6.0	0.13
Electricity	77.1	1.67	0.8	0.02
Steam	22.3	0.48		
Fixed costs	21.9	0.47	23.7	0.51

Flowrates	Co-electrolysis		Biomass Gasification	
Capital depreciation	20.0	0.43	22.6	0.49
Average income tax	5.0	0.11	5.6	0.12
Average return on investment	35.4	0.77	38.6	0.83
MFSP, $/gal fuel (39% diesel, 61% gasoline)		4.44		3.28
MFSP, $/GGE fuel (39% diesel, 61% gasoline)		4.42		3.26
MFSP, $/gal diesel blendstock		4.25		3.14
MFSP, $/gal gasoline blendstock		4.35		3.21

Economic studies from the literature for synthetic fuels production yield a wide price range. This is to be expected with the highly variable processes and technical and economic assumptions that are possible. One of the most established technologies for converting syngas to hydrocarbon fuel is via the FT route. Several pilot and demonstration tests using co-electrolysis-based syngas with FT synthesis from syngas to fuels were conducted between 2014 and 2022 in Europe (Dieterich 2020). Several groups have conducted TEAs for FT fuels via electrolysis of CO_2. Li et al. (2016) reported a range of $3.80 to 9.20/gal with a range of well-to-gate energy efficiency of 41 to 65%. Becker et al. (2012) found a range of $4.4 to 15/GGE (gasoline-gallon equivalent) for electricity price range of $0.02 to 0.14/kWh and plant capacity range of 90% to 40% and reported an overall efficiency of 51% (LHV). In a study by Fu et al. (2010), production cost ranged from $2.50 to 6.79/gal with an electricity price of $22-88MWh. Cost results from this analysis lie within the general cost range of FT fuels found in the literature.

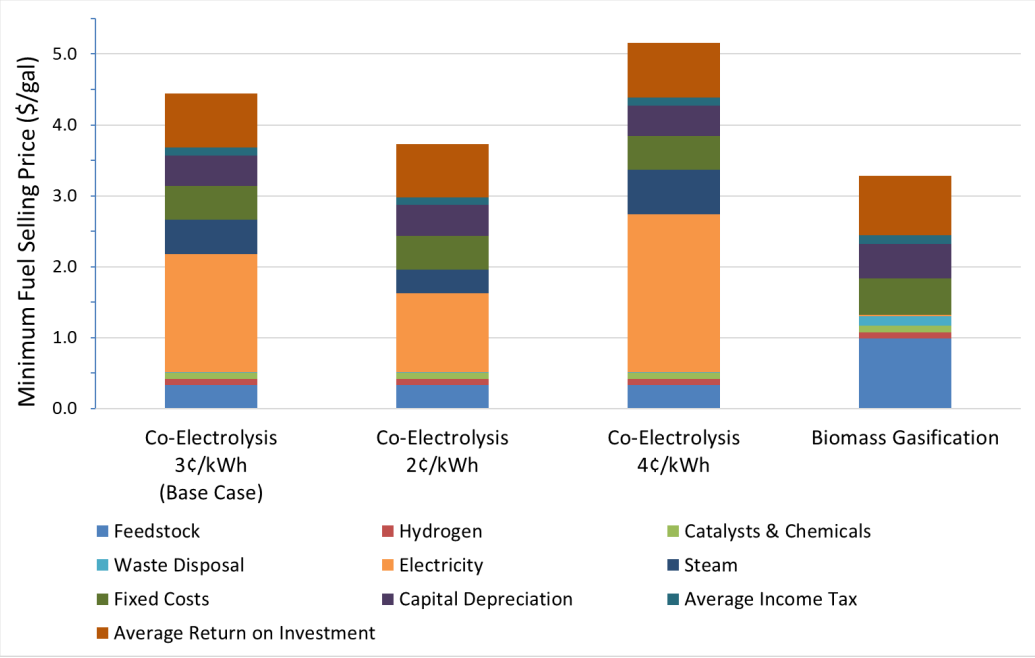

Figure 13. Fuel production cost breakdown for renewable fuel blendstock via co-electrolysis and biomass gasification and the MTO route for the conversion of the syngas to synfuels.

It is evident that the MFSP for the low-carbon fuel from this pathway fuel is higher than current market petroleum fuel prices (Figure 14). However, possible carbon credits through government incentives or mandates are not considered in these results and could be substantial if put into place in the

future. For example, credits like those granted under the Environmental Protection Agency (EPA) Renewable Fuel Standard (RFS) for biofuels may be a good first approximation for future incentives associated with CO_2-based fuels. State programs such as California's low-carbon fuel standard (LCFS) could bring additional value incentives. Renewable identification number (RIN) credits for advanced biofuel, defined as fuel with associated lifecycle greenhouse gas (GHG) emissions that is 60% lower than the petroleum baseline (e.g., gasoline and diesel), was valued in the range of $1.01 to 2.74 per gallon over the 2018–2019 time period (Figure 15, EPA 2020). Lifecycle GHG emissions for the MTO-based fuel from co-electrolysis are estimated at 13.8 g CO_2-e/MJ as shown in Table 13. This represents an 85% reduction in GHGs compared to petroleum diesel (91.8 g CO_2-e/MJ, GREET 2019). Note that this is a relatively high-level estimate that includes emissions associated with feedstock production/preparation (compression of CO_2 feed at the ethanol plant for CO_2 and woody biomass collection and preparation for the gasification case), electricity (nuclear power for the co-electrolysis case and grid power for the biomass case) and hydrogen used for hydrotreating olefins into final fuel blendstock.

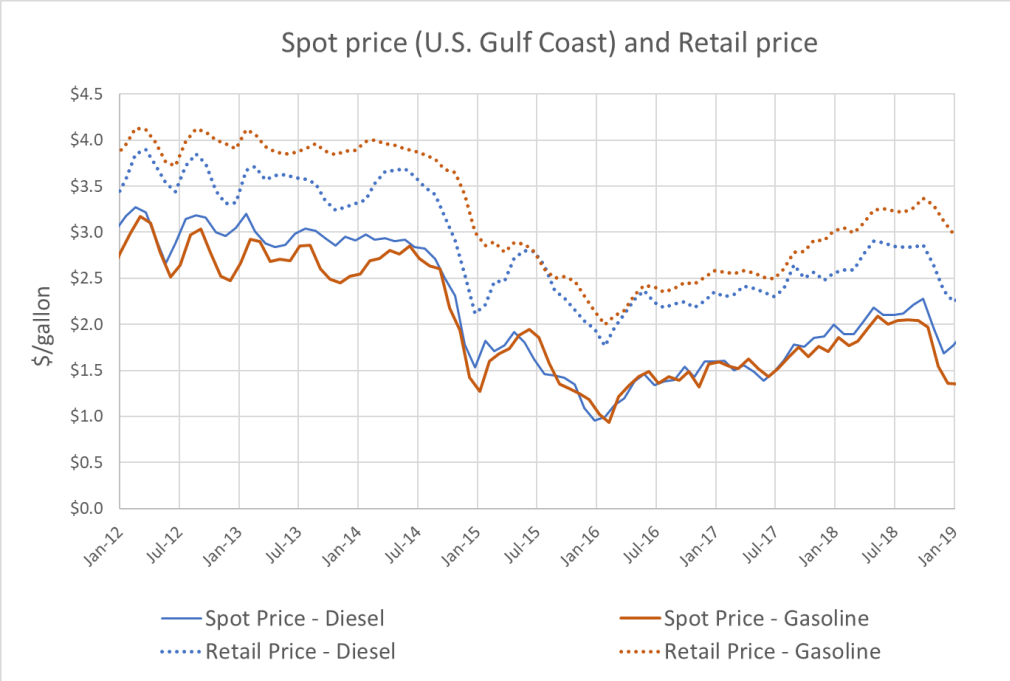

Figure 14. Petroleum fuel price history (EIA 2020b).

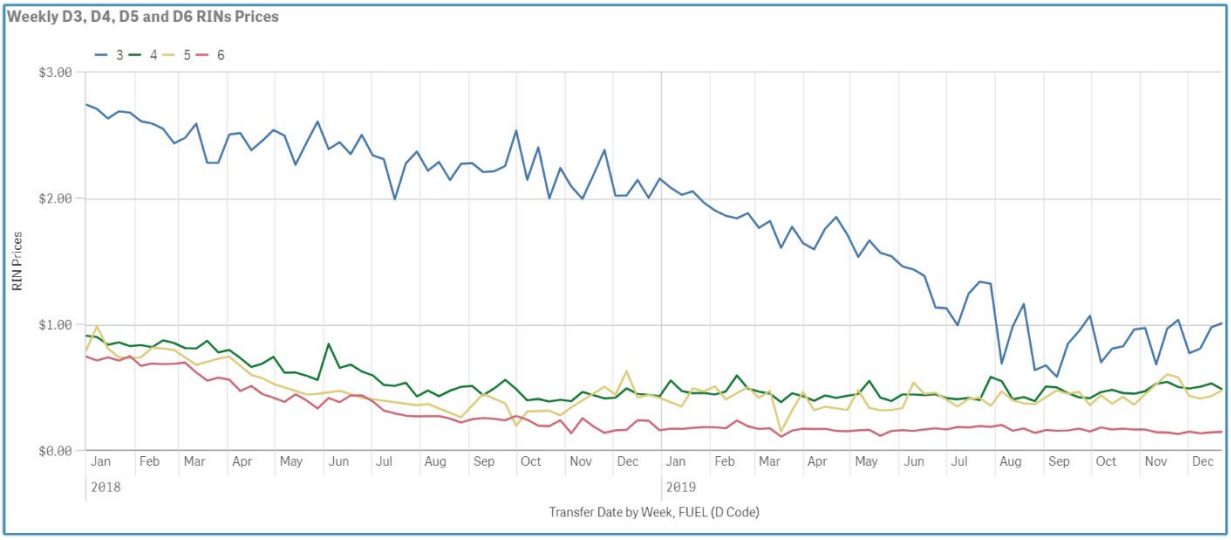

Figure 15. Price for renewable fuel credits during 2018–2019 (EPA 2020?)

Table 13. Greenhouse gas emissions calculation for fuel from the MTO-based pathway.

	Co-Electrolysis	**GHG Factor and Ref**	**Biomass Gasification**	**Ref for GHG Emission Factor**
Feedstock	6.2 (CO_2 compression)	157.1 kWh/tonne feed, Boardman et al. 2019; 142 kg CO_2-e/mmBtu grid mix, GREET 2019	13.9 (50/50 forest residue/clean pine)	109 kg CO_2-e/dry ton, Hartley et al. 2019
Electricity	3.6 (nuclear)	2.4 kg CO_2-e/mmBtu, GREET 2019	0.7 (grid mix)	142 kg CO_2-e/mmBtu, GREET 2019
Hydrogen for Hydrotreating	3.9	105 kg CO_2-e/mmBtu, GREET 2019	3.9	105 kg CO_2-e/mmBtu, GREET 2019
Total*	13.8		18.5	
Reduction from Petroleum Diesel	85%		80%	

*Does not include contribution of chemicals and catalysts consumption.

Sensitivity analysis (Figure 16) investigating variable CO_2 cost, CO_2 credits, and electricity price shows that with optimal CO_2 and electricity prices and inclusion of carbon credits through incentives or mandates could make this process more cost competitive with petroleum fuels. With a hypothetical carbon tax of $100/tonne CO_2 the MFSP is reduced to ~$3.75/gallon. An RFS credit would further aid in competitiveness of fuels produced via this route. Carbon sequestered into fuel minus CO_2 emitted in process off gas combustion and embodied GHGs for H_2 requirement for hydrotreating of the final fuel was estimated. The carbon credit reduces MFSP by approximately $0.86/gal, somewhat less than the average 2018/2019 D3 advanced biofuel RIN price of $1.88. This analysis indicates that fuel from this pathway could be more competitive with petroleum prices with a combination of lower electricity price, lower CO_2 price, and qualifying carbon credits. If a D3 RIN-type price could be applied, competitiveness could be further improved.

Also, there are innovative cryogenic carbon capture (CCC) processes that could have significant impact on the viability of an LWR/synfuels plant using methanol as intermediate. Further, the refrigerant used in the CCC process could be produced using LWR energy. The synergies of the LWR with the CCC process and techno-economic modeling of the CCC process will be explored in detail in future studies.

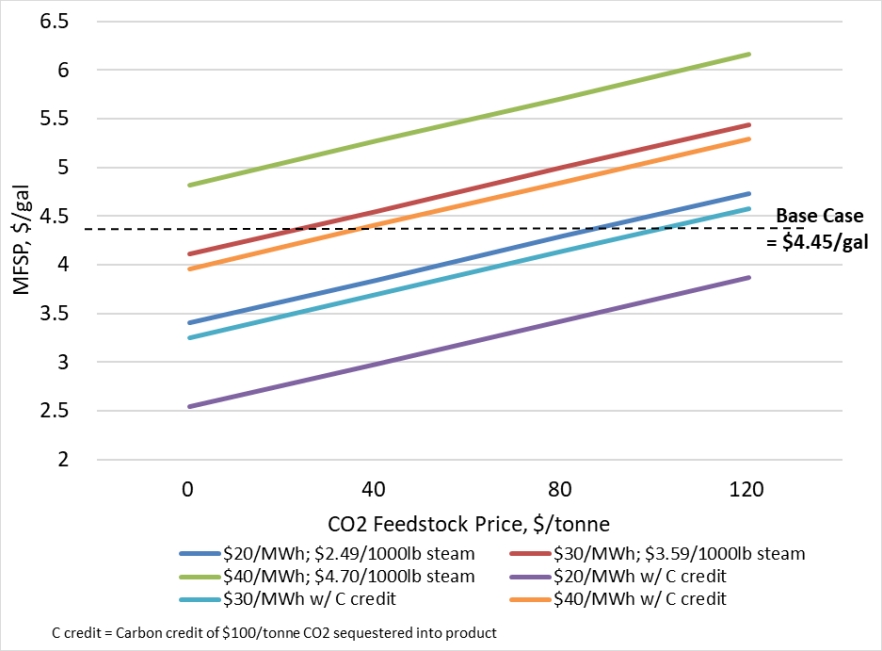

Figure 16. Sensitivity of MFSP for MTO fuel to CO_2 and electricity price and considering the potential impact of a carbon credit.

The scale of the processing plant is also an important cost driver for any chemical process due to manufacturing economies of scale. Economies of scale are realized for most equipment, stemming from the fact that the surface area to volume ratio for cylinders and spheres decreases as capacity (volume) is increased. Sensitivity analysis varying plant scale for the co-electrolysis with MTO fuel process was conducted, the results of which are shown in Figure 17. At a scale of half the base case (326 MWe; 133 MWt), production cost increases by 9%. At a scale 10 times larger than the base case, production cost is reduced to about $3.8/gal. Scaleup of the plant up to the entire electrical output of a general 1-GWe LWR of fuel production would result in about 40 cents/gal cost savings. Note that a scaling factor of 1 is assumed for the SOEC stack; therefore, no benefit is gained for this portion of the capital cost. This is because SOEC stacks are built up in modules. To increase the scale of an electrolysis system, more modules of the same size are added to the system.

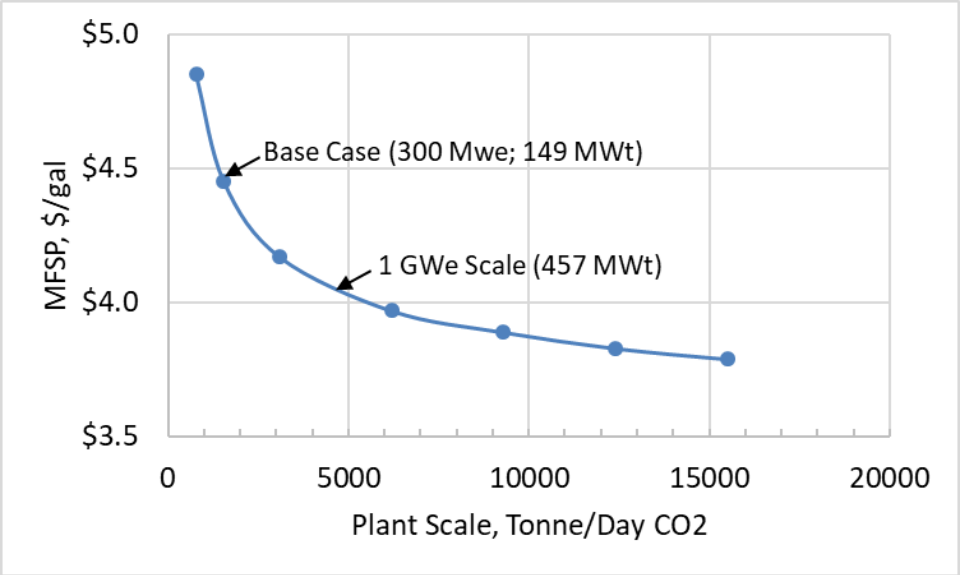

Figure 17. Sensitivity of MFSP to plant scale for the co-electrolysis and MTO fuel process.

6. SYNGAS TO FUELS VIA MIXED ALCOHOLS PROCESS

6.1 Design and Modeling

The overall block flow diagram for the modeled fuel production process through the ethanol route is shown in Figure 18. Similar to MTO pathway, unreacted CO_2 is captured using an amine-based solvent while water is separated in a knock-out tank prior to recycling back to the SOEC. The syngas from the amine absorption column is compressed to 3,000 psi (207 bar) using a five-stage centrifugal compressor with inter-stage cooling. Single-pass conversion of CO_2 is 34% and overall carbon efficiency to CO including recycle is 98.5%.

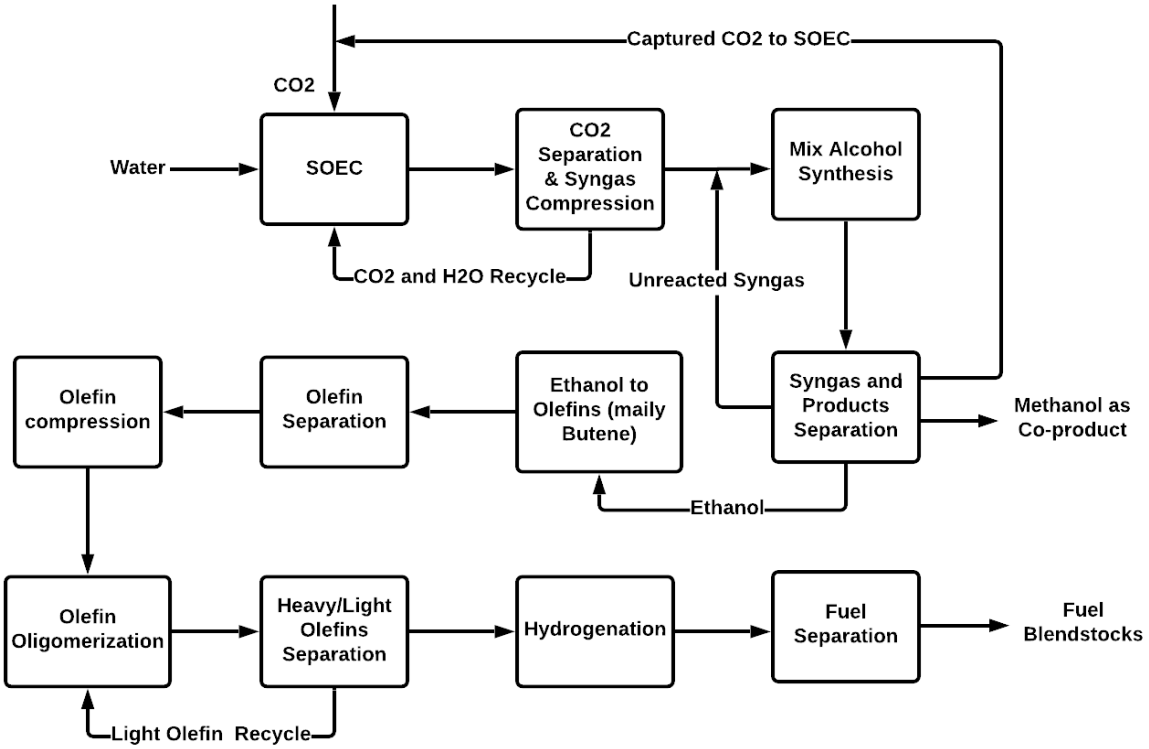

Figure 18. Syngas to fuel via EtOH pathway.

The compressed syngas is then mixed with recycled syngas and methanol and preheated to 595°F (313°C) before entering the alcohol synthesis reactor. Within the alcohol reactor, the syngas contacts a metal-sulfide catalyst to product methanol and ethanol with a small number of light hydrocarbons (e.g., methane, ethane, and propane). The main reaction for producing ethanol is showing as below:

$$2CO + 4H_2 \rightarrow C_2H_5OH + H_2O$$

The reaction's stoichiometry suggests the desired H_2/CO ratio of 2. However, the employed metal-sulfide catalysts can prompt waste gas shift reaction and generate H_2 from CO. Thus, a lower H_2:CO ratio of 1.5 is used in this work (Dutta et al. 2011). Heat must be removed from the reactors because the synthesis reaction is exothermic. Reactor temperature is controlled at 611°F by generating saturated steam at 681 psia. Table 14 lists process conditions and performance for the mixed alcohol reactor. The reactor effluent is cooled in a series of exchangers to condense the alcohols, which are then separated from unreacted syngas in a flash vessel. The gas stream goes through a set of acid gas removal units to separate the unreacted syngas from undesired gases before recycling back to the mixed alcohol reactor. Also acid gas removal unit here is to capture CO_2 to be used as carbon source for SOEC (Samavati et al. 2018; Becker et al. 2012). About 10% gas is purged to prevent excessive buildup of inert gases (e.g., light hydrocarbons) for heat generation. The methanol/ethanol mixture is separated in a distillation column, where the ethanol and some propanol is recovered from the bottoms containing 99% of the ethanol fed to the column, and the top stream is further processed to produce 99.85 wt% industrial-grade methanol. Single-pass conversion of CO is 29% and overall conversion with syngas recycle is 79%. Overall carbon efficiencies of CO to ethanol and methanol are 45%, and 5%, respectively.

Table 14. Process conditions for mixed alcohol synthesis

Assumptions	Values	Reference
Temperature, F	611	Dutta et al. 2011
Pressure, psia	3000	
H_2: CO ratio	1.5	
CO_2 concentration (mol%)	15%	
Sulfur (ppm)	70	
Single-pass CO conversion	29%	
Overall CO conversion	79%	
CO selectivity to ethanol	63%	

Ethanol is then preheated and co-fed with hydrogen (5 mol% H_2 in the feeding) to multiple reactors in parallel for producing 1-butene with a small amount of ethylene, propylene, acetaldehyde, diethyl ether and alkane. Some coke is formed by side reactions; the coke is burned off by taking each reactor into regeneration mode on a continuous cycle. The total olefin selectivity over Ag/ZrO2/SiO2 catalyst is 88% with 1-butene selectivity of 65% based on the PNNL experimental data. The effluent mixture from the olefin reactor (mainly butene) is cross exchanged to pre-heat the inlet ethanol feed and then quenched in a direct-contact, circulating-water spray tower to separate the non-condensable gases from water generated by ethanol dehydration. Conversion of ethanol is 100% and carbon efficiency of ethanol to olefins is 95.5%.

The butene-rich gas mixture is compressed to 340 psi (23 bar) and heated to 437°F (225°C) before entering the first oligomerization reactor to produce C4, C6 and C8 oligomerization products. Ni on a silicoaluminate catalyst can be used in the first oligomerization stage. The product from the first oligomerization stage is introduced to the second oligomerization reactor to increase the yield of C9 to C16 compounds. The net conversion assumed for C2, C3, C4, C6, and C8 olefins to their dimers are 88%, 77%, 88%, 20%, and 50%, respectively (Lilga et al. 2016).

Lighter olefins (in the C4 to C9 range) are separated from the heavier olefins via flash evaporation and distillation. The light olefin is recycled back to the first oligomerization reactor while the heavier olefins are hydrogenated using purchased hydrogen over a Pd-on-alumina hydrogenation catalyst operating at 700°F (371°C) and 300 psi (20 bar). The H_2 partial pressure in the hydrotreater is maintained at about 70% of total pressure to minimize coking and to completely hydrogenate all double bonds in the feed. The excess hydrogen is separated from the diesel product after condensation and knock-out pots. It is recycled to the reactor operating pressure using a pressure booster. The hydrogenated product is distilled into diesel blendstocks in a final distillation column. Overall carbon efficiency of olefins to fuel product is 97.3%.

6.2 Performance and Economic Results

However, extra heat is needed for light/heavy oligomer and diesel distillation columns.

Figure 19 shows the resulting power and heat inputs and outputs for the modeled EtOH pathway. The net power requirement for the plant is 468 MWe and the steam requirement is 66 MWt. The co-electrolysis unit consume about 91% of the electricity demand and the rest 9% is mainly for gas compressors and pumps throughout the plant. Steam is needed for heating of the feed CO_2 and water to the SOEC system, amine solvent regeneration in the CO_2 separation (shown as CO_2 Sep block below) and heating demand for downstream. As shown in Figure 19, the most significant steam requirement for the integrated plant is for amine recovery in the CO_2 separation. When comparing to MTO pathway, the steam requirement from LWR for the integrated plant is only 44% of steam demand for the MTO pathway. This is because the heat recovered from the mixed alcohol reactor and from the offgas gas

combustor is substantial. Electrical and thermal energy usage for syngas production for the modeled SOEC system is 2.5 kWe/lb syngas and 0.2 kWt/lb syngas, respectively for a H_2:CO ratio of 1.2. All reactors downstream of syngas production and CO_2 separation are exothermic; therefore, no steam/heat is needed to drive these steps. However, extra heat is needed for light/heavy oligomer and diesel distillation columns.

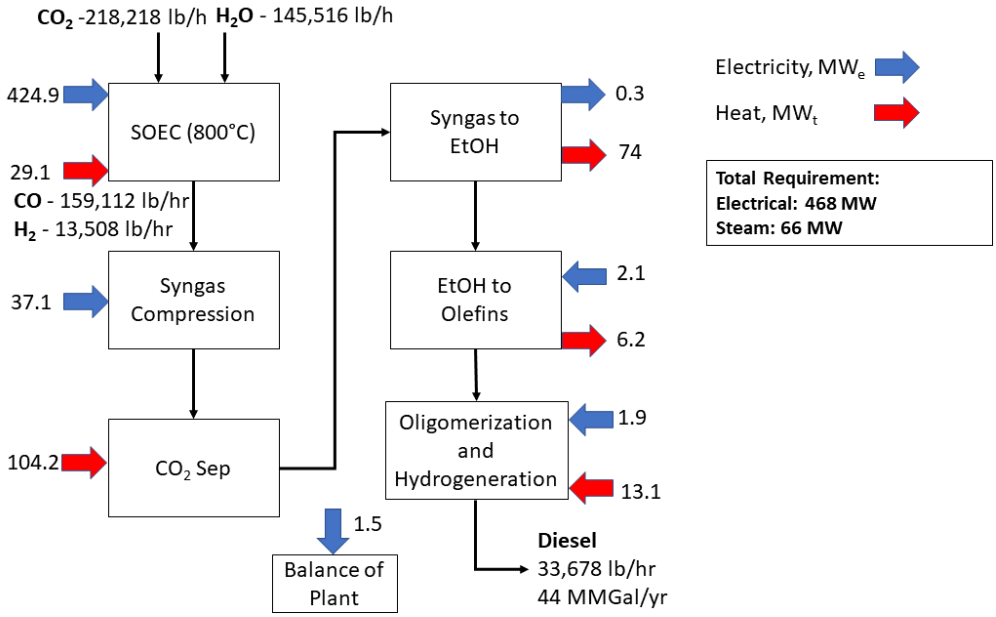

Figure 19. Heat and power inputs/outputs for the syngas-to-fuel process using SOEC.

Figure 20 shows the carbon distribution for EtOH pathway. As mentioned, the off-gases of MAS is purged to control the inert gases concentration in the mixed alcohol synthesis (MAS) reactor feeding so that lower the MAS reactor cost. The off-gas from MAS comprises unconverted syngas (6.5% feeding carbon), produced alkane (14.6% feeding carbon), and CO2 (13.8% feeding carbon). The off-gases are currently used as fuel to produce heat for this process. Such considerable carbon loss can be partly attributed to the low CO conversion and low selectivity in the MAS reactor. In the Co-electrolysis case, this purge stream is used as fuel to produce heat for this process. But for biomass case, this stream can be recycled back to tar reformer to recover the carbon in the syngas and light alkane. This is the main reason that biomass case shows better carbon efficiency, as shown in Table 16. To improve the carbon efficiency, 70% CO_2 is captured in the acid removal unit to be recycled back to SOEC subsystem. The overall carbon efficiency for fuel product is 41.4%, nearly 50% of the carbon efficiency of MTO pathway. A higher selectivity catalyst can further increase the carbon efficiency and decrease the cost for this pathway.

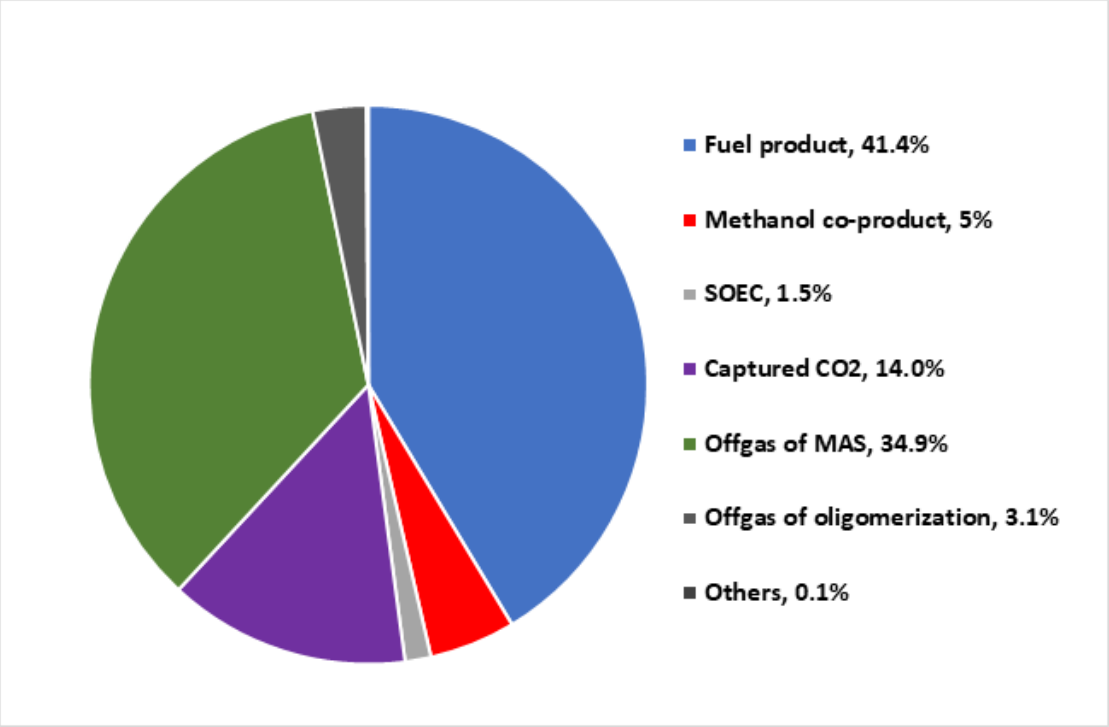

Figure 20. Carbon distribution for SOEC syngas to fuel via EtOH pathway.

Table 15 lists the catalyst cost for estimating variable operating costs for this pathway and please refer to Table 8 for CO_2, waste disposal, and utility costs.

Table 15. Variable operating costs for the MTO to fuels model TEA.

Catalyst and Chemicals	**2019 Price**	**Unit**	**Reference**
Mixed Alcohol Catalyst	42.67	$/lb	Dutta et al. 2011
Butene (C4) Catalyst	1.15	$/lb	2014 PEP Yearbook for Acetic Acid using a silver gauze catalyst
Oligomerization Catalyst	18.10	$/lb	Tan et al. 2016b
Hydrogenation Catalyst	59.03	$/lb	Gerber 1999
DEPG makeup	95.59	$/million lb acid gas removed	Dutta et al. 2011
Selective amine makeup	21.17	$/million lb acid gas removed	Dutta et al. 2011
Hydrogen (for hydrotreating oligomers)	0.95	$/lb	2020 PEP Yearbook
Methanol	0.38	¢/gal	2020 PEP Yearbook

Table 16 gives the major economic results for fuel plant via EtOH pathway. Also presented for comparison is the biomass case, where gasification of woody feedstock is used on the front end instead of co-electrolysis. The fuel production cost breakdown for each case is given in Figure 21. The fuel MFSP for the pathway is $6.13/gal. The electricity and utility (mainly steam) and CO_2 feeding for the SOEC are the major cost drivers. Electricity and steam cost contribute 45% of the MFSP while CO_2 feeding contributes 10% of the MFSP. Compared to MFSP of the MTO pathway, the MFSP for EtOH pathway increased by $1.68/gal due to the lower carbon efficiency as explained earlier thus higher capital cost associated with large SOEC and expensive equipment cost for acid gas removal system.

Table 16. Economic results for syngas to fuels process (all costs in 2019 $).

Flowrates	**Co-electrolysis**		**Biomass Gasification**	
CO_2 Feed, lb/hr (ton/day)	218,218 (2,619)		Biomass: 183,718 (2,205)	
H_2O Feed, lb/hr (ton/day)	145,165 (1,742)		N/A	
Fuel, lb/hr (BPD)	33678 (2,873)		33,672 (2,869)	
Fuel, mmBtu/hr (MW)	637.2 (186.7)		636.2 (186.4)	
Carbon efficiency (C in synfuel/C in feed)	41.4%		30.4%	
Energy efficiency (fuel)/(power+steam+H_2+natural gas)	32.7%		41.5% (including input biomass)	
Capital Costs, $ million				
Installed costs				
Syngas Generation		115.6		49.9
Syngas Compression and Cleanup		57.5		110.8
Methanol Production		80.0		84.5
Hydrocarbon Fuel Production		27.0		25.6
Steam Cycle / Power Gen		3.3		33.5
Balance of plant		7.4		9.2
Total installed capital cost		290.8		312.5
Indirect costs		147.7		159.0
Fixed capital investment		472.7		508.7
Total capital investment (TCI)		497.9		535.7
Operating Costs				
	$ million/yr	**$/gal**	**$ million/yr**	**$/gal**
Variable operating cost				
Feedstock	27.9	0.64	45.8	1.10
Hydrogen (for hydrotreating oligomers)	1.9	0.04	1.5	0.04
Catalyst and Chemicals	19.8	0.45	5.2	0.13
Waste Disposal	0.0	0.00	2.5	0.06
Electricity	119.1	2.73	10.4	0.25
Steam	15.8	0.36		
Co-product credits	-13.9	-0.32	0.00	0.00
Fixed costs	24.6	0.56	25.9	0.62
Capital depreciation	23.6	0.54	25.4	0.61
Average income tax	5.9	0.14	6.3	0.15
Average return on investment	42.7	0.98	44.1	1.06
MFSP, $/gal biocrude		6.13		4.03
MFSP, $/GGE biocrude		5.79		3.87

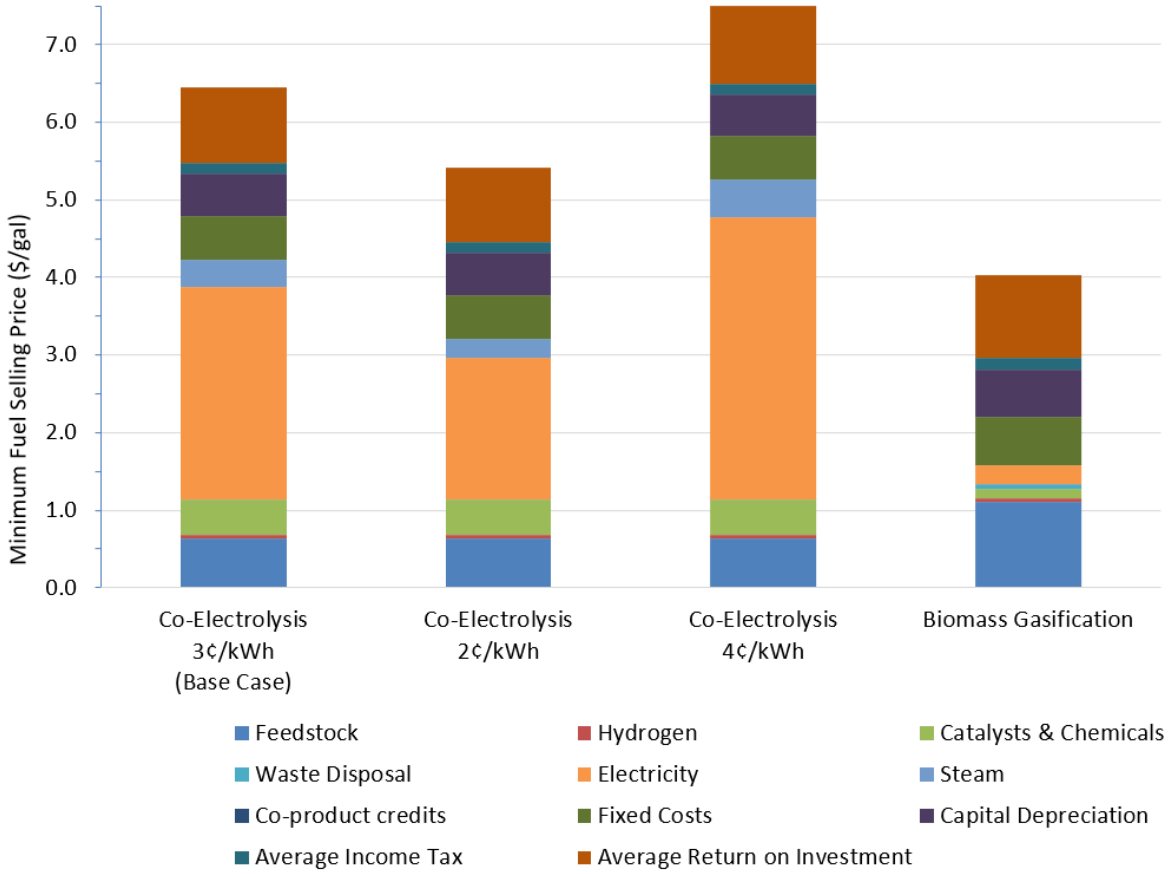

Figure 21. Fuel production cost breakdown for renewable fuel blendstock via the EtOH route.

A similar sensitivity study investigating variable CO_2 cost and electricity price is presented in Figure 22. Cases with and without a $100/ton carbon credit are included to investigate the possible impact of government mandates or incentives. The carbon credit reduces MFSP by $1.35/gal for cases with the same electricity and steam price, which is higher than MFSP reduction of MTO pathway. This is because more CO_2 is captured/installed for per mass fuel product via EtOH pathway. Table 17 shows GHG emissions for co-electrolysis and biomass via EtOH pathway. It is found that lifecycle GHG emissions (18.7 g CO_2-e/MJ for fuel from EtOH pathway) are reduced by 80% compared to the petroleum diesel (91.8 g CO_2-e/MJ, GREET 2019), which shows higher GHG emission reduction than biomass case. Note that the calculated GHG emissions including emissions for CO_2 compression, nuclear power and hydrogen inputs (GREET 2019).

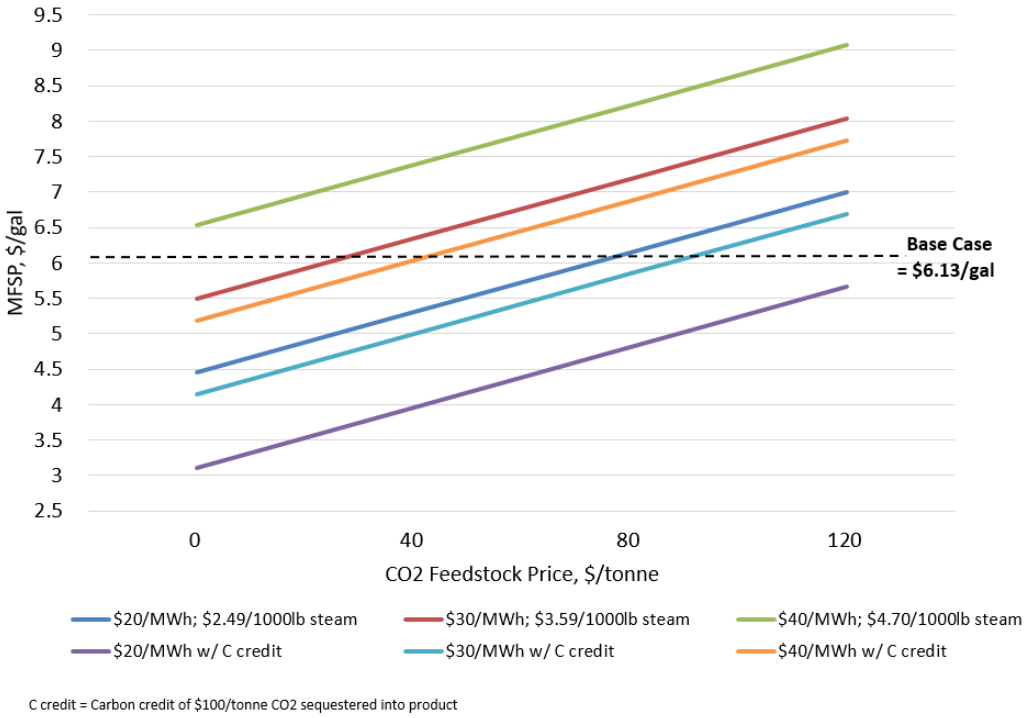

Figure 22. Sensitivity of MFSP for EtOH fuel to CO_2 and electricity price and considering the potential impact of a carbon credit.

Table 17. Greenhouse gas emissions calculation for synfuel via EtOH pathway.

	Co-Electrolysis	**GHG Factor and Ref**	**Biomass Gasification**	**Ref for GHG Emission Factor**
Feedstock	11.2 (CO_2 compression)	157.1 kWh/tonne feed, Boardman et al. 2019; 142 kg CO_2-e/mmBtu grid mix, GREET 2019	15.0 (50/50 forest residue/clean pine)	109 kg CO_2-e/dry ton, Hartley et al. 2019
Electricity	5.6 (nuclear)	2.4 kg CO_2-e/mmBtu, GREET 2019	12.6 (grid mix)	142 kg CO_2-e/mmBtu, GREET 2019
Hydrogen for Hydrotreating	1.9	105 kg CO_2-e/mmBtu, GREET 2019	1.9	105 kg CO_2-e/mmBtu, GREET 2019
Total*	18.7		29.5	
Reduction from Petroleum Diesel	80%		68%	

*Does not include contribution of chemicals and catalysts consumption.

7. LOW-CARBON FUEL CREDITS APPLICABLE TO SYNTHETIC FUELS PRODUCTION

A recent report (Knighton 2020b) studied the framework of options that can incentivize nuclear power plant operations by providing credits for the low-carbon grid power and non-electric products that may be produced from nuclear power, similar to renewable energy credits (REC). Some conclusions from this report are highlighted below as they apply to synthetic fuel produced by coupling with low-carbon nuclear energy. The report highlighted the status quo of the EPA RFS, carbon tax/credit systems, LCFS of California, the new green hydrogen standard in New York as well as other possible future frameworks that may incentivize nuclear energy operators and downstream industry employing low-carbon electricity and non-electric products. More generally these credits can be termed zero emissions credits (ZEC), including renewables and nuclear energy.

For example, electricity, hydrogen, and products produced from hydrogen such as steel and ammonia could create ZECs or "low-carbon" green energy credits that can be used by obligated industry entities needing to reduce their carbon footprint. Green steel produced from hydrogen using nuclear energy could qualify for very large (~$150/tonne) carbon credits in the European export markets. It is conceivable that synthetic fuel produced using low-carbon nuclear energy and feedstock CO_2 that would otherwise be exhausted to the atmosphere from natural gas combined cycle or ethanol plants, could be included in these existing and future national and state "ZEC" programs.

Other reports completed by the DOE LWRS program have highlighted the vast and diverse markets for non-electric products that can be produced using nuclear energy (Knighton 2020a, Hu 2019, Frick 2019). The current report has supplemented these studies by providing a first look into two possible pathways for producing synthetic transportation fuels by coupling with low-carbon nuclear energy.

Nuclear energy is a large portion of the low-carbon generation mix in the U.S. There is precedent for nuclear energy being included in existing and proposed clean energy frameworks and legislation (New York and Illinois Clean Energy Standards for electricity generated from nuclear energy, California LCFS for transportation fuels, and New York curtailed hydrogen credits). Electricity, hydrogen, and synthetic fuels produced from nuclear energy can be considered low carbon and comparable to renewable energy such as solar and wind even after the entire life cycle is considered (including uranium mining, fuel manufacture, plant construction, etc.).

Retiring nuclear plants and not valuing this low-carbon energy with the commensurate credits given to renewable energy may lead to drastic increases in carbon emissions (from substitute baseload plants such as NGCC) at a time when decreases in carbon emissions are being sought, which would be contrary to the goals of decarbonization.

Important points to consider related to possible future low-carbon / zero emissions credit legislation:

- The retention of nuclear power generation is critical to achieving federal and states' decarbonization goals across multiple energy sectors
- Producing hydrogen and other products such as synthetic fuels from nuclear power, especially at low demand periods, increases the capacity utilization factor of NPPs, which can improve the economics of their operation
- The contribution of nuclear power to zero-carbon power markets can be extended further to serve other energy sectors such as transportation, as well as building and industrial heat demand, thus contributing to the goals of decarbonization across multiple energy sectors.

8. CONCLUSIONS

Detailed process modeling and techno-economic analyses have been conducted for two potential power-to-fuels processing routes for integration with steam and electricity from an LWR, namely using

co-electrolysis to produce syngas and then either using a methanol to synfuels pathway or an ethanol to synfuels pathway. The methanol to synfuels pathway appears to be more economical than the ethanol pathway. The models reflect a conceptual fuel production plant nearby or co-located with an LWR that uses CO_2 offgas from an ethanol production plant in the region as feedstock to a co-electrolysis SOEC system for syngas production followed by conversion of syngas to oxygenate intermediate (methanol or ethanol), and final diesel and naphtha blendstock finishing. It is important to note that these results reflect a low-level cost estimate (e.g., "study estimate") due to uncertainties around the costs and performance of the SOEC and other downstream steps that are still in development. It should also be emphasized that these costs reflect n^{th}-plant economics (see Section 3.1), which takes advantage of assumed technology improvements at a future time after which several plants have been built and are operating. As such, they do not include additional expenses that can be expected with building a first-of-a-kind plant, such as longer startup times and large project contingencies.

Using the base case assumptions of \$33.3/tonne CO_2 cost and \$30/MWh electricity cost, the modeled MFSP for the methanol-based route to fuel is estimated to be \$4.45/gal for a fuel production plant of 3,194 BPD capacity (91% diesel and 9% motor gasoline blendstock). Electricity and steam consumption from the LWR for fuel production are 326 MWe and 133 MWt, respectively. Production costs for the co-electrolysis routes using these above assumptions leads to a cost about 40% higher than using wood gasification for syngas production, primarily due to electricity usage and steam usage for co-electrolysis and CO_2 separation (heat from gasification supplies all the steam and almost all of the power needs for the gasification plant). The assumptions used in the base case are conservative and do not account for improving technologies in the areas of CCC.

This analysis highlights the opportunities available to improve the economics of synfuel production through co-electrolysis routes to be competitive with biomass gasification and petroleum refining:

1. Potential reduction in cost of CO_2 feedstock from the \$33.3/tonne CO_2 using innovative CCC processes to capture carbon from ethanol plants and investigation into the cost and synergies of other sources such as NGCC plants.
2. Potential CO_2 credits and/or LCFS program credits (California as a first example) or RFS credits under the EPA.
3. There is considerable opportunity in producing various high-value synthetic chemicals, which could be the subject of future techno-economic studies. This report investigated only two possible synthetic fuels routes.

Overall carbon efficiency of CO_2 to fuel is about 2.75 times higher than the biomass gasification case due to the high efficiency of the co-electrolysis process. Thermal efficiencies of the co-electrolysis and biomass cases are similar. Sensitivity analysis shows that a combination of lower electricity and steam price (\$20/MWh and \$2.49/1000 lb1000lb steam), low CO_2 price (\$15-50/ton), and inclusion of carbon credit of a \$100/tonne can make the process more competitive with petroleum fuels. GHG analysis indicates that the fuels have 85% less GHG emissions than petroleum fuels (diesel) and could conceivably qualify for the highest RIN credit if approved by the EPA. This, along with additional state incentives could bring an even higher potential credit for the fuel.

Economic studies from the literature for synthetic fuels production yield a wide price range. This is to be expected with the highly variable processes and technical and economic assumptions that are possible. One of the most established technologies for converting syngas to hydrocarbon fuel is via the FT route. Several pilot and demonstration tests using co-electrolysis-based syngas with FT synthesis from syngas to fuels were conducted between 2014 and 2022 in Europe (Dieterich 2020). Several groups have conducted TEAs for FT fuels via electrolysis of CO_2. Li et al. (2016) reported a range of \$3.80 to 9.20/gal with a range of well-to-gate energy efficiency of 41 to 65%. Becker et al. (2012) found a range of \$4.4 to 15/GGE (gasoline-gallon equivalent) for electricity price range of \$0.02 to 0.14/kWh and plant capacity

range of 90% to 40% and reported an overall efficiency of 51% (LHV). In a study by Fu et al. (2010), production cost ranged from $2.50 to 6.79/gal with an electricity price of $22 to 88MWh. Cost results from this analysis lie within the general cost range of FT fuels found in the literature. The variability of these study results presents a future opportunity for fine tuning modeling and results to determine the most viable routes for producing synthetic fuels when coupled with an LWR.

The base case modeled MFSP for the ethanol-based fuel route is $6.13/gal. This option has a higher production cost than the methanol route primarily because the syngas to ethanol process is only half as carbon efficient as the syngas-to-methanol process. This leads to about twice the demand for CO_2 feedstock and electricity in the SOEC. Compared to the biomass gasification case, production cost is about 52% higher. Overall carbon efficiency to fuel is 41.4% (46.4% including methanol co-product), about 40% higher than the biomass gasification case. Thermal efficiency is 34.7%, about 21% lower than the gasification case. Lifecycle GHG emissions for the fuel are 80% reduced from the petroleum baseline. Sensitivity analysis shows that reducing MFSP to levels that are competitive with petroleum ($2–3/gal) is challenging, even when considering optimal electricity and CO_2 costs, and carbon credits for this fuel pathway. Utilization of a more efficient route from syngas to ethanol, such as syngas fermentation, which can be in the 90% range, or use of a more selective catalyst for ethanol production, could potentially help reduce costs. Finally, production of high-value synchems could provide more economic impetus than synfuels for integration with LWR operations.

A recent report (Knighton 2020b) studied the framework of options that can incentivize nuclear power plant operations by providing credits for the low-carbon grid power and non-electric products that may be produced from nuclear power, similar to REC. Some conclusions from this report are highlighted below as they apply to synthetic fuel produced by coupling with low-carbon nuclear energy.

Other reports completed by the DOE LWRS program have highlighted the vast and diverse markets for non-electric products that can be produced using nuclear energy (Knighton 2020a, Hu 2019, Frick 2019). The current report has supplemented these studies by providing a first look into two possible pathways for producing synthetic transportation fuels by coupling with low-carbon nuclear energy.

Retiring nuclear plants and not valuing this low-carbon energy with the commensurate credits given to renewable energy may lead to drastic increases in carbon emissions (from substitute baseload plants such as NGCC) at a time when decreases in carbon emissions are being sought, which would be contrary to the goals of decarbonization.

Important points to consider related to possible future low-carbon/zero emissions credit legislation:

- The retention of nuclear power generation is critical to achieving federal and states' decarbonization goals across multiple energy sectors
- Producing hydrogen and other products such as synthetic fuels from nuclear power, especially at low demand periods, increases the capacity utilization factor of NPPs, which can improve the economics of their operation
- The contribution of nuclear power to zero-carbon power markets can be extended further to serve other energy sectors such as transportation, as well as building and industrial heat demand, thus contributing to the goals of decarbonization across multiple energy sectors.

9. REFERENCES

Alper, E., and Yuksel Orhan, O., 2017, "CO_2 utilization: Developments in conversion processes," *Petroleum,* Vol. 3, No. 1, pp. 109–126. doi:https://doi.org/10.1016/j.petlm.2016.11.003

Anghilante, R., Colomar, D., Brisse, A., and Marrony, M., 2018, "Bottom-up cost evaluation of SOEC systems in the range of 10-100 MW," *International Journal of Hydrogen Energy,* Vol. 43, No. 45, pp. 20309–20322, doi:10.1016/j.ijhydene.2018.08.161.

Barger, P., 2002, "Methanol to Olefins (Mto) and Beyond," In *Zeolites for Cleaner Technologies,* Vol. 3, pp. 239–260, Published By Imperial College Press And Distributed By World Scientific Publishing Co.

Becker, W.L., R.J. Braun, M. Penev, and M. Melaina, 2012, ". Production of Fischer-Tropsch liquid fuels from high temperature solid oxide co-electrolysis units," Energy, Vol. 47, pp.: 99–115.

Bipin V. Vorq, E., T.L. Marker, H.R. Nilsen, 1998, "Process for Producing Light Olefins from Crude Methanol," US Patent 5,714,662.

Boardman R.D. et al. 2019. Evaluation of Non-electric Market Options for a Light-water Reactor in the Midwest. INL/EXT-19-55090. Idaho National Laboratory. Idaho Falls, ID

Buttler, A., Koltun, R., Wolf, R., and Spliethoff, H., 2015, "A detailed techno-economic analysis of heat integration in high temperature electrolysis for efficient hydrogen production," *International Journal of Hydrogen Energy,* Vol. 40, No. 1, pp. 38–50. doi:10.1016/j.ijhydene.2014.10.048

Dagle, R.A. and V.M. Dagle. 2020a, "Single-reactor conversion of ethanol to 1-/2-butenes," US Patent 10,647,622.

Dagle, R.A., A.D. Winkelman, K.K. Ramasamy V.L. Dagle, and R.S. Weber, 2020, ". Ethanol as a Renewable Building Block for Fuels and Chemicals," I&EC research, https://dx.doi.org/10.1021/acs.iecr.9b05729.

Dieterich, V., et al. 2020, ". Power-to-liquid via synthesis of methanol, DME or Fischer–Tropsch-fuels: a review," Energy Environ. Sci., DOI: 10.1039/d0ee01187h.

Dutta A., A.H. Sahir, E. Tan, D. Humbird, L.J. Snowden-Swan, P.A. Meyer, and J. Ross, et al. 2015, ". Process Design and Economics for the Conversion of Lignocellulosic Biomass to Hydrocarbon Fuels: Thermochemical Research Pathways with In Situ and Ex Situ Upgrading of Fast Pyrolysis Vapors," PNNL-23823, Richland, Washington,WA Pacific Northwest National Laboratory.

Dutta, A., M. Talmadge, J. Hensley, M. Worley, D. Dudgeon, D. Barton, P. Groenendijk, D. Ferrari, B. Stears, E.M. Searcy, C.T. Wright, and J.R. Hess, 2011, "Process Design and Economics for Conversion of Lignocellulosic Biomass to Ethanol: Thermochemical Pathway by Indirect Gasification and Mixed Alcohol Synthesis,"". NREL/TP-5100-51400.

Energy Information Agency, 2020a, "Diesel Usage,". diesel usage https://www.eia.gov/energyexplained/diesel-fuel/use-of-diesel.php.

Energy Information Agency. 2020b. Spot prices: https://www.eia.gov/dnav/pet/pet_pri_spt_s1_d.htm; Retail prices: https://www.eia.gov/petroleum/gasdiesel/. Accessed 9/8/2020.

Eng, C. N. A., E.C.; Vora, B.V.. (1998). *Integration of the UOP/HYDRO MTO process into ethylene plants*. Paper presented at the AIChE Spring National Meeting, New Orleans, LA, USA.

Environmental Protection Agency (EPA). 2020, ". RIN Trades and Price Information," https://www.epa.gov/fuels-registration-reporting-and-compliance-help/rin-trades-and-price-information,. Accessed September 8, /2020.

Frick, K. et al., “Evaluation of Hydrogen Production Feasibility for a Light Water Reactor in the Gasoline Uusage,” https://www.eia.gov/tools/faqs/faq.php?id=23&t=10.

Gelbein, A. 2003, PEP Review 2001-11 UOP Methanol to Olefins, SRI Consulting, Menlo Park, California.CA

Giglio, E., Lanzini, A., Santarelli, M., and Leone, P. (2015), “Synthetic natural gas via integrated high-temperature electrolysis and methanation: Part II—Economic analysis,” *Journal of Energy Storage,* Vol. 2, pp. 64–79. doi:https://doi.org/10.1016/j.est.2015.06.004

Gogate, M. RMR. 2019, “. Methanol-to-olefins process technology: current status and future prospects,” Petroleum Science and Technology. Vol. 37, No. 5, pp. 559–565.

GREET, The Greenhouse Gases, Regulated Emissions, and Energy Use in Transportation, Model 2019.

Griggs, T. (2017), “Low oil prices claim Sasol’s proposed $15 billion gas-to-liquids plant near Lake Charles,” The Advocate. https://www.theadvocate.com/baton_rouge/news/business/article_3c940178-d051-11e7-8493-07a7ef24d003.html, accessed September 28, 2020.

Hartley, D.S., D.N. Thompson, and H. Cai. 2020, “. Woody Feedstocks 2019 State of Technology Report,” INL/EXT-20-57181, Idaho National Laboratory, Idaho Falls, Idaho.ID

Hu, Hongqiang et al., “Technoeconomic Analysis on an Electrochemical Nonoxidative Deprotonation Process for Ethylene Production from Ethane,” (December 2019), Idaho National Laboratory, INL/EXT-19-56936, https://lwrs.inl.gov/Flexible%20Plant%20Operation%20and%20Generation/Technoeconomic_Analysis_on_an_Electrochemical_Nonoxidative_Deprotonation_Process.pdf.

James, R., A. Zoelle, D. Keairns, M. Turner, M. Woods, and N. Kuehn, 2019, “Cost and Performance Baseline for Fossil Energy Plants Volume 1: Bituminous coal and Natural Gas to Electricity,” NETL-PUB-22638, National Energy Technology Laboratory, Pittsburg, PittsburghPA.

Jasper, S., and El-Halwagi, M. M., 2016, “A Techno-Economic Comparison between Two Methanol-to-Propylene Processes,” Vol. 3, No. 684, 2015, *Processes,* Vol. 4, No. 2, doi:ARTN 11 10.3390/pr4020011.

Jones, S. and Y. Zhu, 2009, Techno-economic Analysis for the Conversion of Lignocellulosic Biomass to Gasoline via the Methanol-to-Gasoline (MTG) Process, PNNL-18481, Pacific Northwest National Laboratory, Richland, Washington.

Jones, S., P. Meyer, L. Snowden-Swan, A. Padmaperum, E. Tan, A. Dutta, J. Jacobson, and K. Cafferty. 2013. Process Design and Economics for the Conversion of Lignocellulosic Biomass to Hydrocarbon Fuels Fast Pyrolysis and Hydrotreating Bio-oil Pathway, PNNL-23053, Pacific Northwest National Laboratory, Richland, WashingtonWA.

Knighton L.T. et al. 2020a. *Scale and Regionality of Nonelectric Markets for U.S. Nuclear Light Water Reactors*. INL/EXT-20-57885. Idaho National Laboratory Idaho Falls, ID

Knighton L.T. et al. 2020b. *Clean Energy Credits for the Production of Low Carbon Hydrogen, Steel and Ammonia using Nuclear Energy*,. INL/EXT-20-58508. Idaho National Laboratory. Idaho Falls, Idaho.ID

Koempel, H., and Liebner, W. (2007). Lurgi's Methanol to Propylene (MTP®) Report on a successful commercialisation. In F. Bellot Noronha, M. Schmal, and E. Falabella Sousa-Aguiar (Eds.), *Studies in Surface Science and Catalysis, Elsevier*, Vol. 167, pp. 261–267.

Lilga, M.; Hallen, R.; Albrecht, K.; Cooper, A.; Frye, J.; Ramasamy, K., “ Systems and Processes for Conversion of Ethylene Feedstocks to Hydrocarbon Fuels,” U.S.. US 0194257 A1, July 7, 2016.

Lilga, M.A., et al. 2016,. “Systems and processes for conversion of ethylene feedstocks to hydrocarbon fuels,” U.S..” US Patent US 2016/0194572 A1 Midwest. (September 2019),). Idaho National Laboratory,

INL/EXT-19-55395, OSTI1569271. DOI: 10.2172/1569271, National Energy Technology Laboratory, 2020. 10.2 Fischer-Tropsch Synthesis. Accessed at https://www.netl.doe.gov/research/coal/energy-systems/gasification/gasifipedia/ftsynthesis

Lu, Z., Yin, H., Wang, A., Hu, J., Xue, W., Yin, H., and Liu, S., 2016, Hydrogenation of ethyl acetate to ethanol over Cu/ZnO/MOx (MOx=SiO2, Al_2O_3, and ZrO2) catalysts, *Journal of Industrial and Engineering Chemistry,* Vol. 37, 208–215, doi:https://doi.org/10.1016/j.jiec.2016.03.028.

Lyons, T. W., Guironnet, D., Findlater, M., and Brookhart, M. (2012). Synthesis of p-Xylene from Ethylene. *Journal of the American Chemical Society,* Vol. 134, No. 38, pp. 15708–15711. doi:10.1021/ja307612b

O'Brien, J. E., McKellar, M. G., Stoots, C. M., Herring, J. S., and Hawkes, G. L. (2009), "Parametric study of large-scale production of syngas via high-temperature co-electrolysis," *International Journal of Hydrogen Energy, 34*(9), pp. 4216–4226, doi:10.1016/j.ijhydene.2008.12.021.

Phillips et. al, 2010, Gasoline from Wood via Integrated Gasification, Synthesis, and Methanol-to-Gasoline Technologies, NREL/TP-5100-47594, National Renewable Energy Laboratory, Golden, ColoradoCO.

Phillips, S. et al. 2007, "Thermochemical Ethanol via Indirect Gasification and Mixed Alcohol Synthesis of Lignocellulosic Biomass," NREL/TP-510-41168, National Renewable Energy Laboratory, Golden, Colorado.

Phillips, S. et al. 2007. Thermochemical Ethanol via Indirect Gasification and Mixed Alcohol Synthesis of Lignocellulosic Biomass. NREL/TP-510-41168. National Renewable Energy Laboratory, Golden, CO.

Plasseraud, L., 2010, "Carbon Dioxide as Chemical Feedstock," Edited by Michele Aresta. *ChemSusChem,* Vol. 3, No. 5, pp. 631–632. doi:10.1002/cssc.201000097

Redissi, Y., and Bouallou, C., 2013, "Valorization of Carbon Dioxide by Co-Electrolysis of CO_2/H_2O at High Temperature for Syngas Production," *Energy Procedia,* Vol. 37, pp. 6667–6678. doi:10.1016/j.egypro.2013.06.599.

Rumayor, M., Dominguez-Ramos, A., and Irabien, A., 2018, "Formic Acid Manufacture: Carbon Dioxide Utilization Alternatives," *Applied Sciences*, Vol. 8, No. 6, doi:10.3390/app8060914.

Process for Ethylene Production from Ethane" (December 2019). Idaho National Laboratory, INL/EXT-19-56936, https://lwrs.inl.gov/Flexible%20Plant%20Operation%20and%20Generation/Technoeconomic_Analysis_on_an_Electrochemical_Nonoxidative_Deprotonation_Process.pdf

Qingxi Fu,* Corentin Mabilat, Mohsine Zahid, Annabelle Brisse and Ludmila Gautier, 2010, ". Syngas production via high-temperature steam/CO_2 co-electrolysis: an economic assessment," Energy Environ. Sci., 2010, Vol. 3, pp. 1382–1397. DOI: 10.1039/c0ee00092b.

Samavati, Mahrokh, Andrew Martin, Massimo Santarelli, and Vera Nemanova, 2018, "Synthetic Diesel Production as a Form of Renewable Energy Storage," Energies, Vol. 11, No. 5, https://doi.org/10.3390/en11051223.

Sesto, B., 2016, "Formic Acid," In *Chemical Economics Handbook*: HIS Chemical.

Stevens, R.R., M.M Conway, 1989, "Mixed Alcohols Production from Syngas," US Patent 4,831,060.

Stoots, C., 2010, "Production of Synthesis Gas by High-Temperature Electrolysis of H_2O and CO_2 (Coelectrolysis),")." Presentation given at the Sustainable Fuels from CO_2, H_2O, and Carbon-Free Energy conference, Columbia University, New York, New York,NY Accessed at http://energy.columbia.edu/files/2012/11/Coelectrolysis-Rev-2.pdf 9/9/2020.

Summers, Matthew, Matthew Hoffman, Chang-hsien Liao, Matthew Hart, Richard Seiser, Robert Cattolica, Reinhard Rauch, and Matthias Binder, West Biofuels, 2019, ". West Biofuels Fuel Ethanol and Value-Added Chemicals from Biomass Residues," California Energy Commission. Publication Number: CEC-600-2019-140.

Sustainabile Energy Solutions (SES). https://sesinnovation.com/faq.html, accessed September 9, /2020.Yap and J. Lukas, 2015, "Process Design and Economics for the Conversion of Lignocellulosic Biomass to Hydrocarbons via Indirect Liquefaction Thermochemical Research Pathway to High-Octane Gasoline Blendstock Through Methanol/Dimethyl Ether Intermediates," NREL/TP-5100-62402, National Renewable Energy Laboratory, Golden, Colorado.

Tan,, "Conceptual process design and economics for the production of high-octane gasoline blendstock via indirect liquefaction of biomass through methanol/dimethyl ether intermediates," *Biofuels, Bioproducts and Biorefining,* Vol. 10, No.Tan E., L.J. Snowden-Swan, M. Talmadge, A. Dutta, S.B. Jones, K. Kallupalayam Ramasamy, and M.J. Gray, et al. 2016b, ". Comparative Techno-economic Analysis and Process Design for Indirect Liquefaction Pathways to Distillate-range Fuels via Biomass-derived Oxygenated Intermediates Upgrading," Biofuels, Bioproducts *and* Biorefining*,* Vol. 11, No. 1, pp. :41–66. doi:10.1002/bbb.1710

Tan E., M. Talmadge, A. Dutta, J. Hensley, L.J. Snowden-Swan, D. Humbird, and J. Schaidle, et al. 2016. "Conceptual process design and economics for the production of high-octane gasoline blendstock via indirect liquefaction of biomass through methanol/dimethyl ether intermediates." Biofuels, Bioproducts & Biorefining 10, no. 1:17-35. PNNL-SA-113776. doi:10.1002/bbb.1611

Tan, E., M. Talmadge, A. Dutta, J. Hensley, J. Schaidle, M. Biddy, D. Humbird, L. Snowden-Swan, J. Ross, D. Sexton, R. Yap, and J. Lukas. 2015. Process Design and Economics for the Conversion of Lignocellulosic Biomass to Hydrocarbons via Indirect Liquefaction Thermochemical Research Pathway to High-Octane Gasoline Blendstock Through Methanol/Dimethyl Ether Intermediates. NREL/TP-5100-62402. National Renewable Energy Laboratory, Golden, CO.

Vora, B. V.BV and T.L.TL Marker, ". Process for Producing Light Olefins from Crude Methanol," US 5714662. February 3, 1998.

Weimar, M. R., Chick, L. A., Gotthold, D. W., and Whyatt, G. A. (2013). *Cost Study for Manufacturing of Solid Oxide Fuel Cell Power Systems,* Retrieved from United States: https://www.osti.gov/biblio/1126362.

Xuping Li,*,†,‖ Paul Anderson,‡ Huei-Ru Molly Jhong,‡ Mark Paster,‖ James F. Stubbins,§,‖ and Paul J. A. Kenis. 2016. "Greenhouse Gas Emissions, Energy Efficiency, and Cost of Synthetic Fuel Production Using Electrochemical CO_2 Conversion and the Fischer−Tropsch Process," *Energy Fuels*, 2016, Vol. 30, pp. 5980−5989. DOI: 10.1021/acs.energyfuels.6b00665

Yue, H. R., Ma, X. B., and Gong, J. L. (2014), "An Alternative Synthetic Approach for Efficient Catalytic Conversion of Syngas to Ethanol," *Accounts of Chemical Research,* Vol. 47, 5, pp. 1483–1492, Retrieved from <Go to ISI>://WOS:000336415700004

Zhang, J., Qian, W., Kong, C., and Wei, F., 2015, "Increasing para-Xylene Selectivity in Making Aromatics from Methanol with a Surface-Modified Zn/P/ZSM-5 Catalyst," *ACS Catalysis,* Vol. 5, No. 5, pp. 2982–2988, doi:10.1021/acscatal.5b00192.

Zhu Y., S.A. Tjokro Rahardjo, C. Valkenburg, L.J. Snowden-Swan, S.B. Jones, and M.A. Machinal. 2011, ". Techno-economic Analysis for the Thermochemical Conversion of Biomass to Liquid Fuels," PNNL-19009, Richland, Washington,WA: Pacific Northwest National Laboratory.

Zhou, W., Kang, J. C., Cheng, K., He, S., Shi, J. Q., Zhou, C.,... Wang, Y. (2018,). "Direct Conversion of Syngas into Methyl Acetate, Ethanol, and Ethylene by Relay Catalysis via the Intermediate Dimethyl

Ether,". *Angewandte Chemie-International Edition,* Vol. 57, No. (37), pp. 12012-–12016. doi:10.1002/anie.201807113.

Alper, E., & Yuksel Orhan, O. (2017). CO_2 utilization: Developments in conversion processes. *Petroleum, 3*(1), 109-126. doi:https://doi.org/10.1016/j.petlm.2016.11.003

Anghilante, R., Colomar, D., Brisse, A., & Marrony, M. (2018). Bottom-up cost evaluation of SOEC systems in the range of 10-100 MW. *International Journal of Hydrogen Energy, 43*(45), 20309-20322. doi:10.1016/j.ijhydene.2018.08.161

Barger, P. (2002). METHANOL TO OLEFINS (MTO) AND BEYOND. In *Zeolites for Cleaner Technologies* (Vol. Volume 3, pp. 239-260): PUBLISHED BY IMPERIAL COLLEGE PRESS AND DISTRIBUTED BY WORLD SCIENTIFIC PUBLISHING CO.

Buttler, A., Koltun, R., Wolf, R., & Spliethoff, H. (2015). A detailed techno-economic analysis of heat integration in high temperature electrolysis for efficient hydrogen production. *International Journal of Hydrogen Energy, 40*(1), 38-50. doi:10.1016/j.ijhydene.2014.10.048

Eng, C. N. A., E.C.; Vora, B.V.. (1998). *Integration of the UOP/HYDRO MTO process into ethylene plants*. Paper presented at the AIChE Spring National Meeting, New Orleans, LA, USA.

Giglio, E., Lanzini, A., Santarelli, M., & Leone, P. (2015). Synthetic natural gas via integrated high-temperature electrolysis and methanation: Part II—Economic analysis. *Journal of Energy Storage, 2*, 64-79. doi:https://doi.org/10.1016/j.est.2015.06.004

Jasper, S., & El-Halwagi, M. M. (2016). A Techno-Economic Comparison between Two Methanol-to-Propylene Processes (vol 3, 684, 2015). *Processes, 4*(2). doi:ARTN 11

10.3390/pr4020011

Koempel, H., & Liebner, W. (2007). Lurgi's Methanol To Propylene (MTP®) Report on a successful commercialisation. In F. Bellot Noronha, M. Schmal, & E. Falabella Sousa-Aguiar (Eds.), *Studies in Surface Science and Catalysis* (Vol. 167, pp. 261-267): Elsevier.

Lu, Z., Yin, H., Wang, A., Hu, J., Xue, W., Yin, H., & Liu, S. (2016). Hydrogenation of ethyl acetate to ethanol over Cu/ZnO/MOx (MOx=SiO2, Al_2O_3, and ZrO2) catalysts. *Journal of Industrial and Engineering Chemistry, 37*, 208-215. doi:https://doi.org/10.1016/j.jiec.2016.03.028

Lyons, T. W., Guironnet, D., Findlater, M., & Brookhart, M. (2012). Synthesis of p-Xylene from Ethylene. *Journal of the American Chemical Society, 134*(38), 15708-15711. doi:10.1021/ja307612b

O'Brien, J. E., McKellar, M. G., Stoots, C. M., Herring, J. S., & Hawkes, G. L. (2009). Parametric study of large-scale production of syngas via high-temperature co-electrolysis. *International Journal of Hydrogen Energy, 34*(9), 4216-4226. doi:10.1016/j.ijhydene.2008.12.021

Plasseraud, L. (2010). Carbon Dioxide as Chemical Feedstock. Edited by Michele Aresta. *ChemSusChem, 3*(5), 631-632. doi:10.1002/cssc.201000097

Redissi, Y., & Bouallou, C. (2013). Valorization of Carbon Dioxide by Co-Electrolysis of CO_2/H_2O at High Temperature for Syngas Production. *Energy Procedia, 37*, 6667-6678. doi:10.1016/j.egypro.2013.06.599

Rumayor, M., Dominguez-Ramos, A., & Irabien, A. (2018). Formic Acid Manufacture: Carbon Dioxide Utilization Alternatives. *Applied Sciences, 8*(6). doi:10.3390/app8060914

Sesto, B. (2016). Formic Acid. In *Chemical Economics Handbook*: HIS Chemical.

Weimar, M. R., Chick, L. A., Gotthold, D. W., & Whyatt, G. A. (2013). *Cost Study for Manufacturing of Solid Oxide Fuel Cell Power Systems*. Retrieved from United States: https://www.osti.gov/biblio/1126362

https://www.osti.gov/servlets/purl/1126362

Yue, H. R., Ma, X. B., & Gong, J. L. (2014). An Alternative Synthetic Approach for Efficient Catalytic Conversion of Syngas to Ethanol. *Accounts of Chemical Research, 47*(5), 1483-1492. Retrieved from <Go to ISI>://WOS:000336415700004

Zhang, J., Qian, W., Kong, C., & Wei, F. (2015). Increasing para-Xylene Selectivity in Making Aromatics from Methanol with a Surface-Modified Zn/P/ZSM-5 Catalyst. *ACS Catalysis, 5*(5), 2982-2988. doi:10.1021/acscatal.5b00192

Zhou, W., Kang, J. C., Cheng, K., He, S., Shi, J. Q., Zhou, C.,... Wang, Y. (2018). Direct Conversion of Syngas into Methyl Acetate, Ethanol, and Ethylene by Relay Catalysis via the Intermediate Dimethyl Ether. *Angewandte Chemie-International Edition, 57*(37), 12012-12016. doi:10.1002/anie.201807113

Appendix A. Process Flow Diagrams (PFDs) and Material and Energy Balances for MTO Pathway

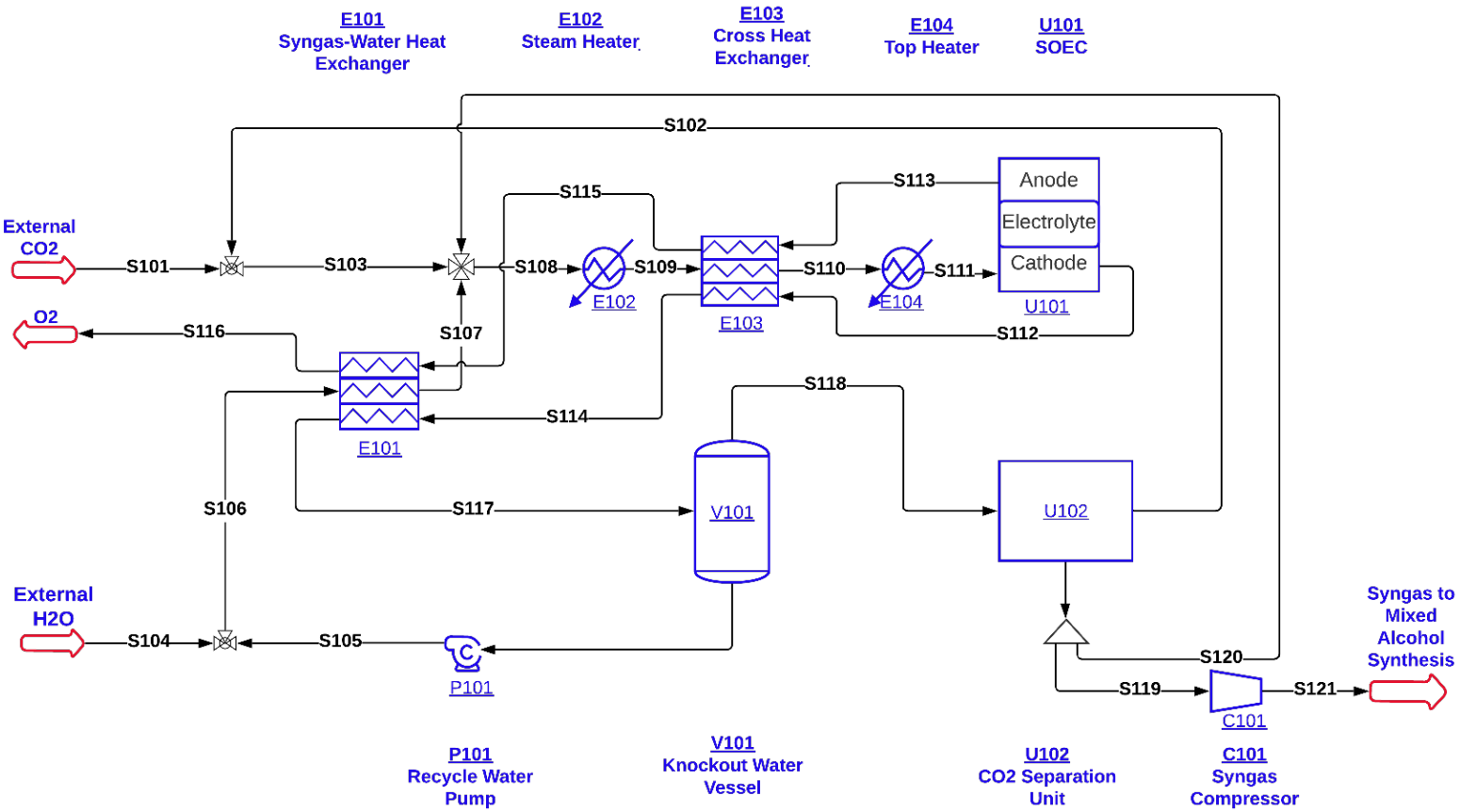

Fig. A1. Area 100: SOEC flowsheet Diagram

Name	S101	S102	S103	S104	S105	S107	S108	S109	S110	S111	S112
- - Overall - -											
Mass flow lb/h	129125.3	323359	452483	115206	121284.2	236490	236490	774753	774754	774754	774753
Temp F	**77**	110	99.4328	**77**	110.0557	93.9734	553.3106	261.6744	624.2324	1250	1472
Pres psia	**15**	14.9	14.9	**15**	35	15	15	14.9	14.9	14.9	14.9
Vapor mass fraction	1	0.9773	0.9842	0	0	0	1	1	1	1	1
Enth MMBtu/h	-496.43	-1284.6	-1781.1	-786.36	-823.75	-1610.1	-1314.3	-3260.3	-3193.7	-2999.3	-2925.7
Flow rates in lb/h											
Oxygen	0	0	0	0	0	0	0	0	0	0	0
Nitrogen	0	0	0	0	0	0	0	0	0	0	0
Argon	0	0	0	0	0	0	0	0	0	0	0
Carbon	0	0	0	0	0	0	0	0	0	0	0
Hydrogen	0	0	0	0	0.001	0.001	0.001	9602.314	13846.53	13846.53	13846.53
Carbon Monoxide	0	0	0	0	0.0033	0.0033	0.0033	66349.85	7375.472	7375.472	7375.456
Carbon Dioxide	129125.3	304597	433721	0	32.7886	32.7885	32.7885	435139	527800	527800	527799
Methane	0	0	0	0	0	0	0	0	0	0	0
Acetylene	0	0	0	0	0	0	0	0	0	0	0
Ethane	0	0	0	0	0	0	0	0	0	0	0
Propane	0	0	0	0	0	0	0	0	0	0	0
Water	0	18761.94	18761.92	115206	121251.4	236457.3	236457.3	263662	225732	225732	225731.8

Table A1 Mainstreams for SOEC part

Name	S113	S114	S115	S116	S117	S118	S119	S120	S121
- - Overall - -									
Mass flow lb/h	139474	635272	139474	139473.3	635267	513980	104841.7	85779.55	95202.76
Temp F	1472	696.4612	700	110	110	110	110	110	120
Pres psia	14.9	14.9	14.9	14.9	14.9	14.9	14.9	14.9	420
Vapor mass fraction	1	1	1	1	0.8091	1	1	1	1
Enth MMBtu/h	47.336	-2190.5	19.992	0.99975	-2467.2	-1643.5	-201.54	-164.89	-145.39
Flow rates in lb/h									
Oxygen	139474	0	139474	139473.3	0	0	0	0	0
Nitrogen	0	0	0	0	0	0	0	0	0
Argon	0	0	0	0	0	0	0	0	0
Carbon	0	0	0	0	0	0	0	0	0
Hydrogen	0	21338.47	0	0	21338.46	21338.46	11736.16	9602.313	11736.15
Carbon Monoxide	0	147446	0	0	147445	147444.4	81094.27	66349.85	81092
Carbon Dioxide	0	307711	0	0	307708	307673.7	1692.198	1384.526	1691.172
Methane	0	0	0	0	0	0	0	0	0
Acetylene	0	0	0	0	0	0	0	0	0
Ethane	0	0	0	0	0	0	0	0	0
Propane	0	0	0	0	0	0	0	0	0
Water	0	158776	0	0	158775.5	37523.88	10319.06	8442.865	683.4388

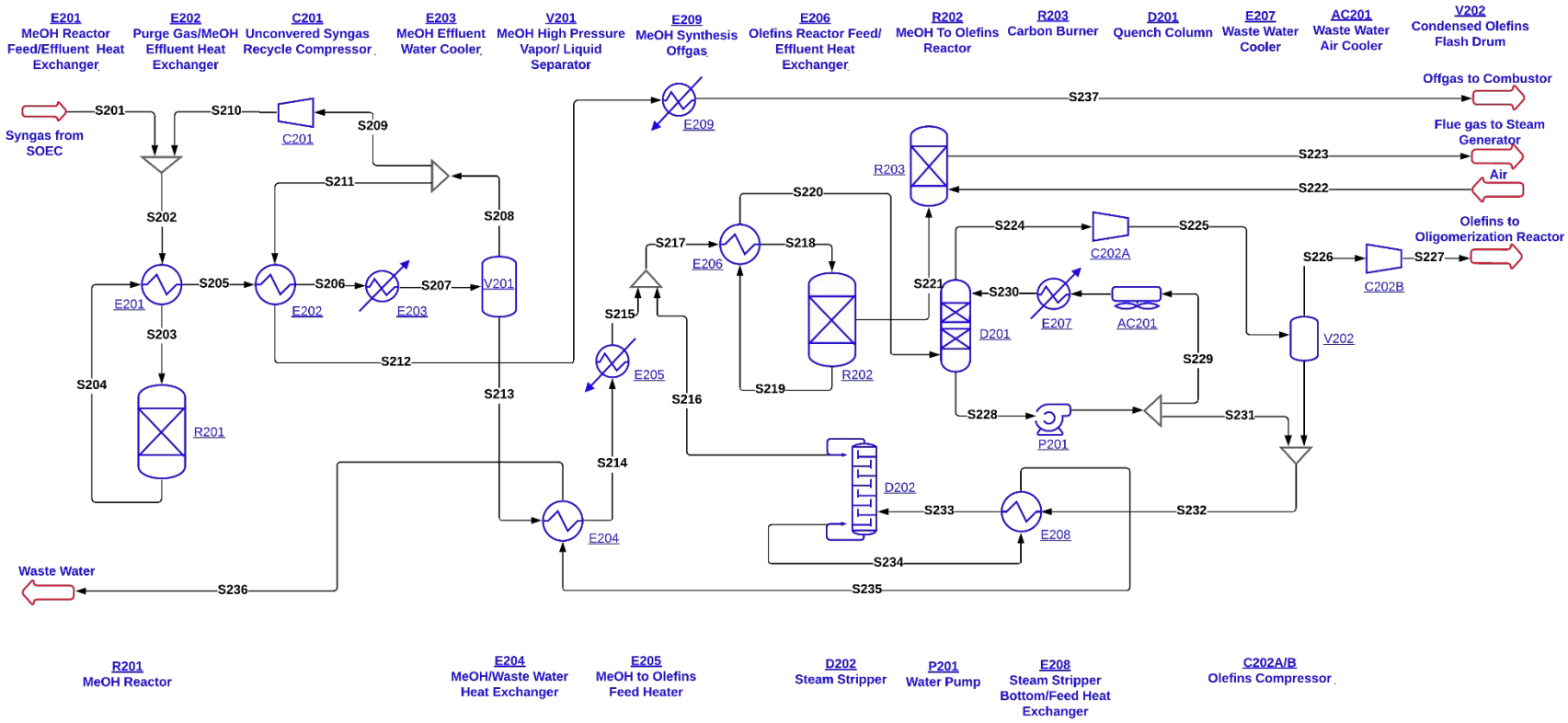

Fig. A2. Area 200: SOEC Syngas to MeOH to Olefins Flowsheet Diagram

Table A2 Mainstreams for SOEC syngas to MeOH to olefins part

Name	S201	S202	S203	S204	S205	206	S207	S208	S209	S210	S211	S212
Mass flow lb/h	95202.78	312046	312046	312047	312047	312034	312034	223549.6	216843	216843	6706.487	6706.487
Temp F	160	136.8361	440	500	232.1108	231.4588	110	111.6981	111.6981	125.5931	111.6981	212.1052
Pres psia	925	925	920	**870**	**870**	870	865	865	865	925	**865**	865
Vapor mass fraction	1	1	1	1	0.9047	0.9023	0.7092	1	1	1	1	1
Enth MMBtu/h	-142.85	-568.73	-511.07	-617.52	-675.18	-675.55	-723.3	-440.87	-427.64	-425.89	-13.226	-12.831
Flow rates in lb/h												
Ethylene	0	0	0	0	0	0	0	0	0	0	0	0
Propylene	0	0	0	0	0	0	0	0	0	0	0	0
1-Butene	0	0	0	0	0	0	0	0	0	0	0	0
1-Pentene	0	0	0	0	0	0	0	0	0	0	0	0
Oxygen	0	0	0	0	0	0	0	0	0	0	0	0
Nitrogen	0	0	0	0	0	0	0	0	0	0	0	0
Argon	0	0	0	0	0	0	0	0	0	0	0	0
Carbon	0	0	0	0	0	0	0	0	0	0	0	0
Hydrogen	11736.15	33758.51	33758.51	22707.27	22707.27	22705.94	22705.94	22703.47	22022.36	22022.36	681.104	681.1041
Carbon Monoxide	81092	225897	225897	149307	149307	149300.2	149300.2	149283.5	144805	144805	4478.506	4478.508
Carbon Dioxide	1691.172	46010	46010	45811.33	45811.34	45812.18	45812.18	45689.55	44318.86	44318.86	1370.686	1370.687
Methane	0	0	0	0	0	0	0	0	0	0	0	0
Acetylene	0	0	0	0	0	0	0	0	0	0	0	0
Ethane	0	0	0	0	0	0	0	0	0	0	0	0
Propane	0	0	0	0	0	0	0	0	0	0	0	0
Water	683.4388	701.027	701.027	782.3618	782.3619	782.3661	782.3661	18.1322	17.5882	17.5882	0.544	0.544
Nitric Oxide	0	0	0	0	0	0	0	0	0	0	0	0
Methanol	0	5679.233	5679.233	93439	93439	93433.33	93433.33	5854.879	5679.233	5679.233	175.6464	175.6446
Ethanol	0	0	0	0	0	0	0	0	0	0	0	0
N-Butane	0	0	0	0	0	0	0	0	0	0	0	0

Name	S213	S214	S215	S216	S217	S218	S219	S220	S221	S222	S223	S224
Mass flow lb/h	88484.47	88484.46	88484.46	2175.076	90659.52	90659.52	89903.73	89903.73	755.6842	75856	76611.74	38514.77
Temp F	111.6981	214.9916	225.5228	311.7697	227.3972	241	955.1583	280.3557	884.3167	**68**	1112	99.9664
Pres psia	865	65	**65**	**80**	65	65	**65**	60	65	**14.7**	55	35
Vapor mass fraction	0	0.004602	0.1003	1	0.1489	1	1	1	0	1	1	1
Enth MMBtu/h	-282.43	-273.9	-269.58	-12.138	-281.72	-248.72	-248.9	-281.89	0.17839	-0.17016	9.4413	7.5536
Flow rates in lb/h												
Ethylene	0	0	0	0.8677	0.8677	0.8677	14854.09	14854.09	0	0	0	14853.23
Propylene	0	0	0	0.7993	0.7993	0.7993	14846.51	14846.51	0	0	0	14845.71
1-Butene	0	0	0	0.0902	0.0902	0.0902	4558.43	4558.43	0	0	0	4558.34
1-Pentene	0	0	0	0.0083	0.0083	0.0083	1726.659	1726.659	0	0	0	1726.651
Oxygen	0	0	0	0	0	0	0	0	0	17675	15661.38	0
Nitrogen	0	0	0	0	0	0	0	0	0	58181	58180.75	0
Argon	0	0	0	0	0	0	0	0	0	0	0	0
Carbon	0	0	0	0	0	0	0	0	755.6842	0	0	0
Hydrogen	2.4736	2.4736	2.4736	0.0002	2.4738	2.4738	18.5691	18.5691	0	0	0	18.5689
Carbon Monoxide	16.6489	16.6489	16.6489	0	16.649	16.649	10.4065	10.4065	0	0	0	10.4065
Carbon Dioxide	122.6372	122.6372	122.6372	0.2133	122.8505	122.8505	427.2035	427.2035	0	0	2769.041	426.9965
Methane	0	0	0	0.0191	0.0191	0.0191	945.8989	945.8989	0	0	0	945.8798
Acetylene	0	0	0	0	0	0	0	0	0	0	0	0
Ethane	0	0	0	0.0178	0.0178	0.0178	324.947	324.947	0	0	0	324.9293
Propane	0	0	0	0.0051	0.0051	0.0051	204.9155	204.9155	0	0	0	204.9103
Water	764.2342	764.2342	764.2342	2101.311	2865.531	2865.531	51850.75	51850.75	0	0	0.0317	543.2985
Nitric Oxide	0	0	0	0	0	0	0	0	0	0	0.5435	0
Methanol	87578.48	87578.47	87578.47	71.7435	87650.21	87650.21	87.6505	87.6505	0	0	0	8.1391
Ethanol	0	0	0	0	0	0	0	0	0	0	0	0
N-Butane	0	0	0	0.0005	0.0005	0.0005	47.6997	47.6997	0	0	0	47.6992

Table A2 Mainstreams for SOEC syngas to MeOH to olefins part

Name	S225	S226	S227	S228	S229	S230	S231	S232	S233	S234	S235	S236	S237
Mass flow lb/h	38514.77	38406	38406	361389	310000	310000	51389	51497.75	51497.75	49323	49323	49322.7	6706.487
Temp F	140	140	140	264.8912	264.9761	100	264.9761	264.7157	291.9037	312.9306	284.7157	113	73
Pres psia	145	145	195	60	90	**85**	90	90	**90**	80	**80**	80	50
Vapor mass fraction	0.9972	1	1	0	0	2.10E-05	0	0	0	0	0	0	1
Enth MMBtu/h	7.8499	8.5847	8.4859	-2396.4	-2055.6	-2107	-340.76	-341.49	-340.06	-324.9	-326.33	-334.85	-13.36
Flow rates in lb/h													
Ethylene	14853.23	14853.23	14853.23	6.0824	5.2175	5.2175	0.8649	0.8677	0.8677	0	0	0	0
Propylene	14845.71	14845.71	14845.71	5.6102	4.8125	4.8125	0.7978	0.7993	0.7993	0	0	0	0
1-Butene	4558.34	4558.34	4558.34	0.6337	0.5436	0.5436	0.0901	0.0902	0.0902	0	0	0	0
1-Pentene	1726.651	1726.651	1726.651	0.0584	0.0501	0.0501	0.0083	0.0083	0.0083	0	0	0	0
Oxygen	0	0	0	0	0	0	0	0	0	0	0	0	0
Nitrogen	0	0	0	0	0	0	0	0	0	0	0	0	0
Argon	0	0	0	0	0	0	0	0	0	0	0	0	0
Carbon	0	0	0	0	0	0	0	0	0	0	0	0	0
Hydrogen	18.5689	18.5689	18.5689	0.0013	0.0011	0.0011	0.0002	0.0002	0.0002	0	0	0	681.1041
Carbon Monoxide	10.4065	10.4065	10.4065	0.0003	0.0003	0.0003	0	0	0	0	0	0	4478.508
Carbon Dioxide	426.9965	426.9902	426.9902	1.4565	1.2494	1.2494	0.2071	0.2133	0.2133	0	0	0	1370.687
Methane	945.8798	945.8797	945.8797	0.1336	0.1146	0.1146	0.019	0.0191	0.0191	0	0	0	0
Acetylene	0	0	0	0	0	0	0	0	0	0	0	0	0
Ethane	324.9293	324.9292	324.9292	0.1249	0.1071	0.1071	0.0178	0.0178	0.0178	0	0	0	0
Propane	204.9103	204.9103	204.9103	0.0362	0.031	0.031	0.0051	0.0051	0.0051	0	0	0	0
Water	543.2985	434.7347	434.7347	360816	309508	309508	51307.45	51416	51416	49315.05	49315.05	49314.72	0.544
Nitric Oxide	0	0	0	0	0	0	0	0	0	0	0	0	0
Methanol	8.1391	7.9344	7.9344	559.1503	479.64	479.64	79.5103	79.715	79.715	7.9719	7.9719	7.9718	175.6446
Ethanol	0	0	0	0	0	0	0	0	0	0	0	0	0
N-Butane	47.6992	47.6992	47.6992	0.0034	0.0029	0.0029	0.0005	0.0005	0.0005	0	0	0	0

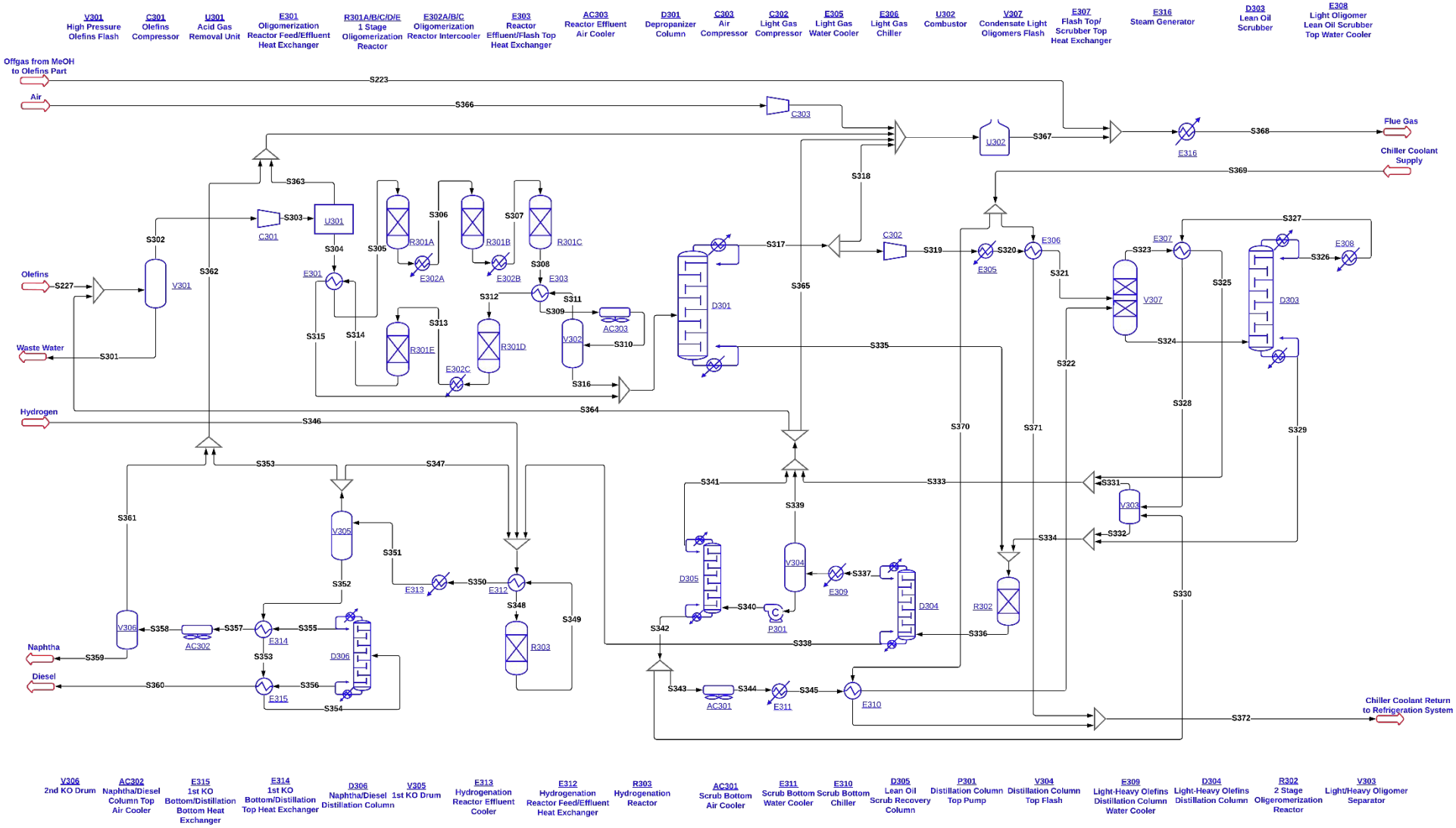

Fig. A3. Area 300: Olefins to Fuel Process Flowsheet Diagram

Table A3 Mainstreams for olefins to fuel part

Name	S301	S302	S303	S304	S305	S306	S307	S308	S309	S310	S311	S312	S313
Mass flow lb/h	35295.18	73663.47	73663.47	72841.2	72841.19	72841.09	72841	72841	72841	72841	47040.06	47040	47040
Temp F	66.7377	97.8243	236.3009	236.3009	320	320	320	439.918	337.4287	140	140	320	300
Pres psia	**125**	125	350	302	302	282	270	260	258	256	**256**	256	241
Vapor mass fraction	1	1	1	1	1	1	0.9988	1	0.9744	0.6458	1	1	1
Enth MMBtu/h	-41.621	-32.809	-28.33	-24.377	-21.045	-28.677	-35.191	-35.191	-39.875	-50.343	-39.118	-34.433	-38.06
Flow rates in lb/h													
Ethylene	3960.914	18818.15	18818.15	18818.15	18818.15	13969	10226.85	7422.232	7422.232	7422.232	7201.271	7201.304	5358.738
Propylene	1296.435	16146.09	16146.09	16146.09	16146.09	11199.5	7467.497	4770.796	4770.796	4770.796	4322.044	4322.055	2759.457
1-Butene	2207.961	6767.495	6767.495	6767.497	6767.495	6767.382	6041.953	5075.368	5075.368	5075.368	3970.505	3970.515	3488.222
1-Pentene	348.4259	2075.551	2075.551	2075.551	2075.551	2700.343	2511.055	2015.722	2015.722	2015.722	1177.311	1177.311	1030.412
1-Hexene	193.7778	193.776	193.776	193.7761	193.776	2686.498	3508.956	3463.363	3463.363	3463.363	1227.471	1227.47	1606.982
1-Heptene	200.7485	200.7624	200.7624	200.7625	200.7624	2152.885	3719.176	4804.262	4804.262	4804.262	873.0463	873.0461	1719.111
1-Octene	0.4364	0.4365	0.4365	0.4365	0.4365	2144.016	4196.579	5806.601	5806.601	5806.601	484.8181	484.8172	1586.574
1-Nonene	0.0005	0.0005	0.0005	0.0005	0.0005	1142.602	2317.547	3265.705	3265.705	3265.705	118.5926	118.5921	673.2315
1-Decene	0	0	0	0	0	843.359	1943.42	3007.6	3007.6	3007.6	45.9536	45.9533	541.4342
1-Undecene	0	0	0	0	0	547.2524	1262.044	1967.548	1967.548	1967.548	12.3228	12.3227	339.6726
1-Dodecene	0	0	0	0	0	25.1906	374.4311	830.59	830.59	830.59	2.0831	2.0831	161.6522
1-Tridecene	0	0	0	0	0	0	0	0	0	0	0	0	0
1-Tetradecene	0	0	0	0	0	24.0915	282.4377	728.7387	728.7387	728.7387	0.3429	0.3429	105.1085
1-Pentadecene	0	0	0	0	0	0	0	0	0	0	0	0	0
1-Hexadecene	0	0	0	0	0	0.048	235.8898	697.5134	697.5134	697.5134	0.0603	0.0603	53.3902
N-Dodecylcyclope	0	0	0	0	0	0	0	0	0	0	0	0	0
1-Octadecene	0	0	0	0	0	0	114.2602	346.015	346.015	346.015	0.006	0.006	11.8652
Oxygen	0	0	0	0	0	0	0	0	0	0	0	0	0
Nitrogen	0	0	0	0	0	0	0	0	0	0	0	0	0
Hydrogen	322.8165	341.3914	341.3914	341.3915	341.3914	341.3914	341.3914	341.3914	341.3914	341.3914	340.5882	340.5848	340.5848
Carbon Monoxide	180.9251	191.3344	191.3344	191.3344	191.3344	191.3344	191.3344	191.3344	191.3344	191.3344	190.594	190.5933	190.5933
Carbon Dioxide	0	426.966	426.966	0	0	0	0	0	0	0	0	0	0
Methane	16444.68	17390.79	17390.79	17390.8	17390.79	17390.79	17390.79	17390.79	17390.79	17390.79	17228.46	17228.39	17228.39
Acetylene	0	0	0	0	0	0	0	0	0	0	0	0	0
Ethane	5648.928	5973.932	5973.932	5973.934	5973.932	5973.932	5973.932	5973.932	5973.932	5973.932	5730.505	5730.484	5730.484
Propane	3615.158	3819.978	3819.978	3819.98	3819.978	3819.978	3819.978	3819.978	3819.978	3819.978	3416.776	3416.804	3416.804
Water	0	387.4694	387.4694	0	0	0	0	0	0	0	0	0	0
Nitric Oxide	0	0	0	0	0	0	0	0	0	0	0	0	0
Methanol	0	7.8408	7.8408	0	0	0	0	0	0	0	0	0	0
Ethanol	0	0	0	0	0	0	0	0	0	0	0	0	0
N-Butane	873.9836	921.4963	921.4963	921.4966	921.4963	921.4963	921.4963	921.4963	921.4963	921.4963	697.3105	697.2637	697.2637
N-Pentane	0	0	0	0	0	0	0	0	0	0	0	0	0
N-Hexane	0	0	0	0	0	0	0	0	0	0	0	0	0
N-Decane	0	0	0	0	0	0	0	0	0	0	0	0	0
N-Nonane	0	0	0	0	0	0	0	0	0	0	0	0	0
N-Hexadecane	0	0	0	0	0	0	0	0	0	0	0	0	0
N-Heptane	0	0	0	0	0	0	0	0	0	0	0	0	0
N-Octane	0	0	0	0	0	0	0	0	0	0	0	0	0
N-Undecane	0	0	0	0	0	0	0	0	0	0	0	0	0
N-Dodecane	0	0	0	0	0	0	0	0	0	0	0	0	0
N-Tridecane	0	0	0	0	0	0	0	0	0	0	0	0	0
N-Tetradecane	0	0	0	0	0	0	0	0	0	0	0	0	0
N-Pentadecane	0	0	0	0	0	0	0	0	0	0	0	0	0
N-Heptadecane	0	0	0	0	0	0	0	0	0	0	0	0	0
N-Octadecane	0	0	0	0	0	0	0	0	0	0	0	0	0
1,2-Propylene Gl	0	0	0	0	0	0	0	0	0	0	0	0	0

Name	S314	S315	S316	S317	S318	S319	S320	S321	S322	S323	S324	S325	S326
Mass flow lb/h	47040	47040	25800.93	39958	599.3695	39358.6	39358.6	39358.6	12946.86	33577.16	18728.3	33577.16	11225
Temp F	386.9899	272.4433	140	39.9998	39.9998	155.8839	110	35	40	50.0388	40.797	77.0238	199.7471
Pres psia	**231**	231	256	130	130	300	300	300	300	300	300	300	200
Vapor mass fraction	1	0.9797	0	1	1	1	1	0.9133	0	1	0	1	1
Enth MMBtu/h	-38.06	-41.392	-11.225	-44.255	-0.66383	-41.49	-42.456	-44.413	-6.4014	-41.617	-9.1935	-41.138	-3.9054
Flow rates in lb/h													
Ethylene	3967.822	3967.822	220.9619	4188.784	62.8318	4125.952	4125.952	4125.952	5.3808	3740.481	390.8523	3740.481	390.8414
Propylene	1646.858	1646.858	448.7531	2053.53	30.803	2022.727	2022.727	2022.727	0	1199.527	823.2	1199.527	822.3773
1-Butene	2926.338	2926.338	1104.864	3367.38	50.5107	3316.87	3316.87	3316.87	1927.545	1801.75	3442.665	1801.75	3383.977
1-Pentene	780.5585	780.5585	838.4112	1141.73	17.1259	1124.604	1124.604	1124.604	946.8618	281.5116	1789.954	281.5116	1450.04
1-Hexene	1588.405	1588.405	2235.892	953.4202	14.3013	939.1189	939.1189	939.1189	1812.17	162.8821	2588.408	162.8821	820.5661
1-Heptene	2301.433	2301.433	3931.216	0.2803	0.0042	0.2761	0.2761	0.2761	6017.5	167.0311	5850.747	167.0311	578.4904
1-Octene	2441.324	2441.324	5321.783	0	0	0	0	0	39.374	0.3507	39.0233	0.3507	1.5194
1-Nonene	1118.27	1118.27	3147.112	0	0	0	0	0	0.1264	0.0004	0.1261	0.0004	0.0022
1-Decene	1012.527	1012.527	2961.647	0	0	0	0	0	0.0013	0	0.0013	0	0
1-Undecene	663.2382	663.2382	1955.225	0	0	0	0	0	0	0	0	0	0
1-Dodecene	370.5573	370.5573	828.507	0	0	0	0	0	0	0	0	0	0
1-Tridecene	0	0	0	0	0	0	0	0	0	0	0	0	0
1-Tetradecene	311.4017	311.4017	728.3959	0	0	0	0	0	0	0	0	0	0
1-Pentadecene	0	0	0	0	0	0	0	0	0	0	0	0	0
1-Hexadecene	227.9133	227.9133	697.4532	0	0	0	0	0	0	0	0	0	0
N-Dodecylcyclope	0	0	0	0	0	0	0	0	0	0	0	0	0
1-Octadecene	79.1884	79.1884	346.009	0	0	0	0	0	0	0	0	0	0
Oxygen	0	0	0	0	0	0	0	0	0	0	0	0	0
Nitrogen	0	0	0	0	0	0	0	0	0	0	0	0	0
Hydrogen	340.5848	340.5848	0.8032	341.3879	5.1208	336.2671	336.2671	336.2671	0	335.2026	1.0646	335.2026	1.0646
Carbon Monoxide	190.5933	190.5933	0.7404	191.3336	2.87	188.4636	188.4636	188.4636	0	187.1028	1.3608	187.1028	1.3608
Carbon Dioxide	0	0	0	0	0	0	0	0	0	0	0	0	0
Methane	17228.39	17228.39	162.3366	17390.73	260.8609	17129.87	17129.87	17129.87	0	16750.91	378.9619	16750.91	378.9616
Acetylene	0	0	0	0	0	0	0	0	0	0	0	0	0
Ethane	5730.484	5730.484	243.4271	5973.91	89.6086	5884.301	5884.301	5884.301	103.8174	5156.637	831.4813	5156.637	831.4214
Propane	3416.804	3416.804	403.2019	3619.639	54.2946	3565.345	3565.345	3565.345	1151.492	3046.817	1670.02	3046.817	1667.567
Water	0	0	0	0	0	0	0	0	0	0	0	0	0
Nitric Oxide	0	0	0	0	0	0	0	0	0	0	0	0	0
Methanol	0	0	0	0	0	0	0	0	0	0	0	0	0
Ethanol	0	0	0	0	0	0	0	0	0	0	0	0	0
N-Butane	697.2637	697.2637	224.1858	735.8415	11.0376	724.8039	724.8039	724.8039	942.5951	746.9574	920.4415	746.9574	896.8092
N-Pentane	0	0	0	0	0	0	0	0	0	0	0	0	0
N-Hexane	0	0	0	0	0	0	0	0	0	0	0	0	0
N-Decane	0	0	0	0	0	0	0	0	0	0	0	0	0
N-Nonane	0	0	0	0	0	0	0	0	0	0	0	0	0
N-Hexadecane	0	0	0	0	0	0	0	0	0	0	0	0	0
N-Heptane	0	0	0	0	0	0	0	0	0	0	0	0	0
N-Octane	0	0	0	0	0	0	0	0	0	0	0	0	0
N-Undecane	0	0	0	0	0	0	0	0	0	0	0	0	0
N-Dodecane	0	0	0	0	0	0	0	0	0	0	0	0	0
N-Tridecane	0	0	0	0	0	0	0	0	0	0	0	0	0
N-Tetradecane	0	0	0	0	0	0	0	0	0	0	0	0	0
N-Pentadecane	0	0	0	0	0	0	0	0	0	0	0	0	0
N-Heptadecane	0	0	0	0	0	0	0	0	0	0	0	0	0
N-Octadecane	0	0	0	0	0	0	0	0	0	0	0	0	0
1,2-Propylene Gl	0	0	0	0	0	0	0	0	0	0	0	0	0

Name	S327	S328	S329	S330	S331	S332	S335	S336	S337	S338	S339	S340	S341
Mass flow lb/h	11225	11225	7503.309	1911.893	1610.758	11526.13	32882.93	51912.38	16436.77	35475.6	806.9302	15629.84	770.971
Temp F	110	70.0387	381.4774	226.5302	80	80	373.7397	374.3492	278.8481	499.4171	110	110.953	125.9993
Pres psia	200	200	200	300	200	200	140	130	130	130	125	200	200
Vapor mass fraction	0.3044	0.136	0	0	1	0	0	0.3199	1	0	1	0	1
Enth MMBtu/h	-5.2632	-5.7421	-1.4343	-0.73381	-1.1804	-5.394	-9.569	-16.397	-4.7242	-9.2559	-0.55937	-7.3534	-0.47736
Flow rates in lb/h													
Ethylene	390.8414	390.8414	0.0109	0.7947	185.0399	206.5962	0	206.6071	206.6071	0	83.0754	123.5316	117.3554
Propylene	822.3773	822.3773	0.8228	0	150.9266	671.4506	42.0808	0	0	0	0	0	0
1-Butene	3383.977	3383.977	58.6876	284.6377	248.2704	3420.344	663.8214	2462.093	2462.093	0.0004	141.474	2320.619	108.4654
1-Pentene	1450.04	1450.04	339.9143	139.8211	38.1533	1551.708	477.2403	1129.973	1129.945	0.0282	24.0792	1105.865	19.1996
1-Hexene	820.5661	820.5661	1767.84	267.6122	8.8923	1079.286	2870.877	2117.697	2109.911	7.7852	16.2026	2093.708	13.8748
1-Heptene	578.4904	578.4904	5272.259	888.636	4.1524	1462.974	6232.371	10470.17	6944.222	3525.928	19.6438	6924.578	18.2856
1-Octene	1.5194	1.5194	37.5039	5.8155	0.0074	7.3276	7763.11	6151.44	45.2949	6106.145	0.048	45.2469	0.0485
1-Nonene	0.0022	0.0022	0.1238	0.0187	0	0.0209	4265.383	3546.801	0.1452	3546.657	0.0001	0.1452	0.0001
1-Decene	0	0	0.0013	0.0002	0	0.0002	3974.175	5143.062	0.0015	5143.06	0	0.0015	0
1-Undecene	0	0	0	0	0	0	2618.464	3447.335	0	3447.336	0	0	0
1-Dodecene	0	0	0	0	0	0	1199.065	1942.397	0	1942.398	0	0	0
1-Tridecene	0	0	0	0	0	0	0	2290.946	0	2290.946	0	0	0
1-Tetradecene	0	0	0	0	0	0	1039.798	4000.606	0	4000.607	0	0	0
1-Pentadecene	0	0	0	0	0	0	0	2084.322	0	2084.322	0	0	0
1-Hexadecene	0	0	0	0	0	0	925.3666	1784.24	0	1784.241	0	0	0
N-Dodecylcyclope	0	0	0	0	0	0	0	744.3994	0	744.3995	0	0	0
1-Octadecene	0	0	0	0	0	0	425.1975	851.7502	0	851.7504	0	0	0
Oxygen	0	0	0	0	0	0	0	0	0	0	0	0	0
Nitrogen	0	0	0	0	0	0	0	0	0	0	0	0	0
Hydrogen	1.0646	1.0646	0	0	1.0072	0.0574	0	0.0574	0.0574	0	0.0527	0.0047	0.0047
Carbon Monoxide	1.3608	1.3608	0	0	1.2249	0.1359	0	0.1359	0.1359	0	0.1171	0.0188	0.0188
Carbon Dioxide	0	0	0	0	0	0	0	0	0	0	0	0	0
Methane	378.9616	378.9616	0.0003	0	291.4415	87.5201	0	87.5204	87.5203	0	61.7069	25.8134	25.8134
Acetylene	0	0	0	0	0	0	0	0	0	0	0	0	0
Ethane	831.4214	831.4214	0.06	15.3308	323.9398	522.8124	0.001	522.8734	522.8735	0	167.7602	355.1132	235.9632
Propane	1667.567	1667.567	2.4523	170.0303	297.8096	1539.788	200.3679	1742.608	1742.608	0	234.2084	1508.4	186.9541
Water	0	0	0	0	0	0	0	0	0	0	0	0	0
Nitric Oxide	0	0	0	0	0	0	0	0	0	0	0	0	0
Methanol	0	0	0	0	0	0	0	0	0	0	0	0	0
Ethanol	0	0	0	0	0	0	0	0	0	0	0	0	0
N-Butane	896.8092	896.8092	23.6324	139.1954	59.8929	976.1118	185.6079	1185.352	1185.352	0.0004	58.5617	1126.79	44.9876
N-Pentane	0	0	0	0	0	0	0	0	0	0	0	0	0
N-Hexane	0	0	0	0	0	0	0	0	0	0	0	0	0
N-Decane	0	0	0	0	0	0	0	0	0	0	0	0	0
N-Nonane	0	0	0	0	0	0	0	0	0	0	0	0	0
N-Hexadecane	0	0	0	0	0	0	0	0	0	0	0	0	0
N-Heptane	0	0	0	0	0	0	0	0	0	0	0	0	0
N-Octane	0	0	0	0	0	0	0	0	0	0	0	0	0
N-Undecane	0	0	0	0	0	0	0	0	0	0	0	0	0
N-Dodecane	0	0	0	0	0	0	0	0	0	0	0	0	0
N-Tridecane	0	0	0	0	0	0	0	0	0	0	0	0	0
N-Tetradecane	0	0	0	0	0	0	0	0	0	0	0	0	0
N-Pentadecane	0	0	0	0	0	0	0	0	0	0	0	0	0
N-Heptadecane	0	0	0	0	0	0	0	0	0	0	0	0	0
N-Octadecane	0	0	0	0	0	0	0	0	0	0	0	0	0
1,2-Propylene Gl	0	0	0	0	0	0	0	0	0	0	0	0	0

Name	S342	S343	S344	S345	S346	S347	S348	S349	S350	S351	S353	S354	S355
Mass flow lb/h	14858.87	12946.81	12946.86	12946.86	525	1012.512	37013.06	37013.2	37013.18	37013.18	0.4949	35968.86	22120.14
Temp F	226.5302	**226.5261**	140	110	475.7908	463.692	700	1133.93	873.2641	110	110.1105	351.3476	364.3641
Pres psia	300	**300**	300	300	450	450	130	125	120	113	100	100	30
Vapor mass fraction	0	0	0	0	1	1	1	1	1	0.0282	1	0	1
Enth MMBtu/h	-5.7031	-4.9693	-5.6971	-5.9204	0.72914	0.96769	0.88321	0.88321	-7.5591	-31.415	-4.13E-05	-26.157	-14.089
Flow rates in lb/h													
Ethylene	6.1762	5.3809	5.3808	5.3808	0	0	0	0	0	0	0	0	0
Propylene	0	0	0	0	0	0	0	0	0	0	0	0	0
1-Butene	2212.153	1927.583	1927.545	1927.545	0	0	0.0004	0	0	0	0	0	0
1-Pentene	1086.666	946.8629	946.8618	946.8618	0	0	0.0282	0	0	0	0	0	0
1-Hexene	2079.834	1812.168	1812.17	1812.17	0	0	7.7852	0	0	0	0	0	0
1-Heptene	6906.294	6017.391	6017.5	6017.5	0	0	3525.928	0	0	0	0	0	0
1-Octene	45.1984	39.3707	39.374	39.374	0	0	6106.145	0	0	0	0	0	0
1-Nonene	0.1451	0.1264	0.1264	0.1264	0	0	3546.657	0	0	0	0	0	0
1-Decene	0.0015	0.0013	0.0013	0.0013	0	0	5143.06	0	0	0	0	0	0
1-Undecene	0	0	0	0	0	0	3447.336	0	0	0	0	0	0
1-Dodecene	0	0	0	0	0	0	1942.398	0	0	0	0	0	0
1-Tridecene	0	0	0	0	0	0	2290.946	0	0	0	0	0	0
1-Tetradecene	0	0	0	0	0	0	4000.607	0	0	0	0	0	0
1-Pentadecene	0	0	0	0	0	0	2084.322	0	0	0	0	0	0
1-Hexadecene	0	0	0	0	0	0	1784.241	0	0	0	0	0	0
N-Dodecylcyclope	0	0	0	0	0	0	744.3995	0	0	0	0	0	0
1-Octadecene	0	0	0	0	0	0	851.7504	0	0	0	0	0	0
Oxygen	0	0	0	0	0	0	0	0	0	0	0	0	0
Nitrogen	0	0	0	0	0	0	0	0	0	0	0	0	0
Hydrogen	0	0	0	0	525	808.8831	1333.848	837.2614	837.2492	837.2492	0.3854	2.9638	2.9631
Carbon Monoxide	0	0	0	0	0	0	0	0	0	0	0	0	0
Carbon Dioxide	0	0	0	0	0	0	0	0	0	0	0	0	0
Methane	0	0	0	0	0	0	0	0	0	0	0	0	0
Acetylene	0	0	0	0	0	0	0	0	0	0	0	0	0
Ethane	119.1499	103.818	103.8174	103.8174	0	0	0	0	0	0	0	0	0
Propane	1321.446	1151.479	1151.492	1151.492	0	0	0	0	0	0	0	0	0
Water	0	0	0	0	0	0	0	0	0	0	0	0	0
Nitric Oxide	0	0	0	0	0	0	0	0	0	0	0	0	0
Methanol	0	0	0	0	0	0	0	0	0	0	0	0	0
Ethanol	0	0	0	0	0	0	0	0	0	0	0	0	0
N-Butane	1081.802	942.6346	942.5951	942.5951	0	0.0007	0.0011	0.0016	0.0016	0.0016	0	0.0009	0.0009
N-Pentane	0	0	0	0	0	0.0077	0.0077	0.0367	0.0367	0.0367	0	0.0288	0.0288
N-Hexane	0	0	0	0	0	0.7131	0.7129	8.6846	8.6846	8.6846	0.0004	7.949	7.9472
N-Decane	0	0	0	0	0	6.8844	6.8841	5223.863	5223.862	5223.862	0.0037	5216.761	5212.6299
N-Nonane	0	0	0	0	0	13.5991	13.5985	3616.893	3616.893	3616.893	0.0073	3602.866	3601.9707
N-Hexadecane	0	0	0	0	0	0.0043	0.0043	1800.304	1800.304	1800.304	0	1800.299	0
N-Heptane	0	0	0	0	0	112.7957	112.788	3711.11	3711.109	3711.109	0.0606	3594.763	3593.8164
N-Octane	0	0	0	0	0	67.4618	67.459	6283.304	6283.303	6283.303	0.0363	6213.718	6212.356
N-Undecane	0	0	0	0	0	1.6103	1.6102	3493.988	3493.988	3493.988	0.0009	3492.327	3383.8308
N-Dodecane	0	0	0	0	0	0.318	0.318	1966.003	1966.003	1966.003	0.0002	1965.674	104.4066
N-Tridecane	0	0	0	0	0	0.1318	0.1318	2316.469	2316.468	2316.468	0.0001	2316.332	0.1853
N-Tetradecane	0	0	0	0	0	0.0847	0.0847	4041.721	4041.72	4041.72	0	4041.632	0.0011
N-Pentadecane	0	0	0	0	0	0.0158	0.0158	2104.319	2104.318	2104.318	0	2104.302	0
N-Heptadecane	0	0	0	0	0	0.0007	0.0007	750.6843	750.684	750.684	0	750.6831	0
N-Octadecane	0	0	0	0	0	0.0003	0.0003	858.5552	858.5548	858.5548	0	858.5544	0
1,2-Propylene Gl	0	0	0	0	0	0	0	0	0	0	0	0	0

Name	S356	S357	S358	S359	S360	S361	S366	S367	S368	S370	S371	S372
Mass flow lb/h	13840.6387	22120.1348	22120.1348	22107.4336	13840.6289	35.1073	80000	89665.56	166277.6	6753.349	27394.41	34147.76
Temp F	551.4886	252.7315	150	150	364.364	150	**80**	2000	250	**25**	**25**	100
Pres psia	33	30	25	25	33	25	**14.7**	15.2	15.2	**65**	**65**	65
Vapor mass fraction	0	0.01101	0.007253	0	0	1	1	1	1	0	0	0
Enth MMBtu/h	-7.6751	-17.927	-19.272	-19.265	-9.5405	-0.02422	0.052962	-69.568	-124.7	-41.378	-167.85	-206.79
Flow rates in lb/h	13840.6387	22120.1348	22120.1348	22107.4336	13840.6289							
Ethylene	0	0	0	0	0	0	0	0	0	0	0	0
Propylene	0	0	0	0	0	0	0	0	0	0	0	0
1-Butene	0	0	0	0	0	0	0	0	0	0	0	0
1-Pentene	0	0	0	0	0	0	0	0	0	0	0	0
1-Hexene	0	0	0	0	0	0	0	0	0	0	0	0
1-Heptene	0	0	0	0	0	0	0	0	0	0	0	0
1-Octene	0	0	0	0	0	0	0	0	0	0	0	0
1-Nonene	0	0	0	0	0	0	0	0	0	0	0	0
1-Decene	0	0	0	0	0	0	0	0	0	0	0	0
1-Undecene	0	0	0	0	0	0	0	0	0	0	0	0
1-Dodecene	0	0	0	0	0	0	0	0	0	0	0	0
1-Tridecene	0	0	0	0	0	0	0	0	0	0	0	0
1-Tetradecene	0	0	0	0	0	0	0	0	0	0	0	0
1-Pentadecene	0	0	0	0	0	0	0	0	0	0	0	0
1-Hexadecene	0	0	0	0	0	0	0	0	0	0	0	0
N-Dodecylcyclope	0	0	0	0	0	0	0	0	0	0	0	0
1-Octadecene	0	0	0	0	0	0	0	0	0	0	0	0
Oxygen	0	0	0	0	0	0	18633.18	2201.889	17862.73	0	0	0
Nitrogen	0	0	0	0	0	0	61366.81	61358.09	119539	0	0	0
Hydrogen	0	2.9631	2.9631	0.5401	0	2.8816	0	0.0022	0.0022	0	0	0
Carbon Monoxide	0	0	0	0	0	0	0	0.0359	0.0359	0	0	0
Carbon Dioxide	0	0	0	0	0	0	0	15149.41	17919.2	0	0	0
Methane	0	0	0	0	0	0	0	0	0	0	0	0
Acetylene	0	0	0	0	0	0	0	0	0	0	0	0
Ethane	0	0	0	0	0	0	0	0	0	0	0	0
Propane	0	0	0	0	0	0	0	0	0	0	0	0
Water	0	0	0	0	0	0	0	10937.44	10937.47	5495.823	22293.31	27789.13
Nitric Oxide	0	0	0	0	0	0	0	18.6932	19.2366	0	0	0
Methanol	0	0	0	0	0	0	0	0	0	0	0	0
Ethanol	0	0	0	0	0	0	0	0	0	0	0	0
N-Butane	0	0.0009	0.0009	0.0008	0	0.0002	0	0	0	0	0	0
N-Pentane	0	0.0288	0.0288	0.0285	0	0.0021	0	0	0	0	0	0
N-Hexane	0	7.9472	7.9472	7.9175	0	0.2279	0	0	0	0	0	0
N-Decane	2.9554	5212.6211	5212.6211	5212.1592	2.9554	0	0	0	0	0	0	0
N-Nonane	0.0585	3601.9712	3601.9712	3601.1621	0.0585	0.001	0	0	0	0	0	0
N-Hexadecane	1799.9558	0	0	0	1799.9558	0	0	0.0001	0.0001	0	0	0
N-Heptane	0.0001	3593.8171	3593.8171	3588.5234	0.0001	28.9432	0	0	0	0	0	0
N-Octane	0.0031	6212.3579	6212.3579	6208.7944	0.0031	3.0512	0	0	0	0	0	0
N-Undecane	107.7313	3383.8347	3383.8347	3383.7168	107.731	0	0	0.0001	0.0001	0	0	0
N-Dodecane	1860.8507	104.4064	104.4064	104.405	1860.8419	0	0	0.0001	0.0001	0	0	0
N-Tridecane	2315.5862	0.1853	0.1853	0.1853	2315.5881	0	0	0.0001	0.0001	0	0	0
N-Tetradecane	4040.7832	0.0011	0.0011	0.0011	4040.7844	0	0	0.0001	0.0001	0	0	0
N-Pentadecane	2103.8362	0	0	0	2103.8335	0	0	0.0001	0.0001	0	0	0
N-Heptadecane	750.5091	0	0	0	750.5089	0	0	0	0	0	0	0
N-Octadecane	858.3699	0	0	0	858.3694	0	0	0	0	0	0	0
2-Propylene Gl	0	0	0	0	0	0	0	0	0	1257.526	5101.104	6358.63

Appendix B. Process Flow Diagrams (PFDs) and Material and Energy Balances for EtOH Pathway

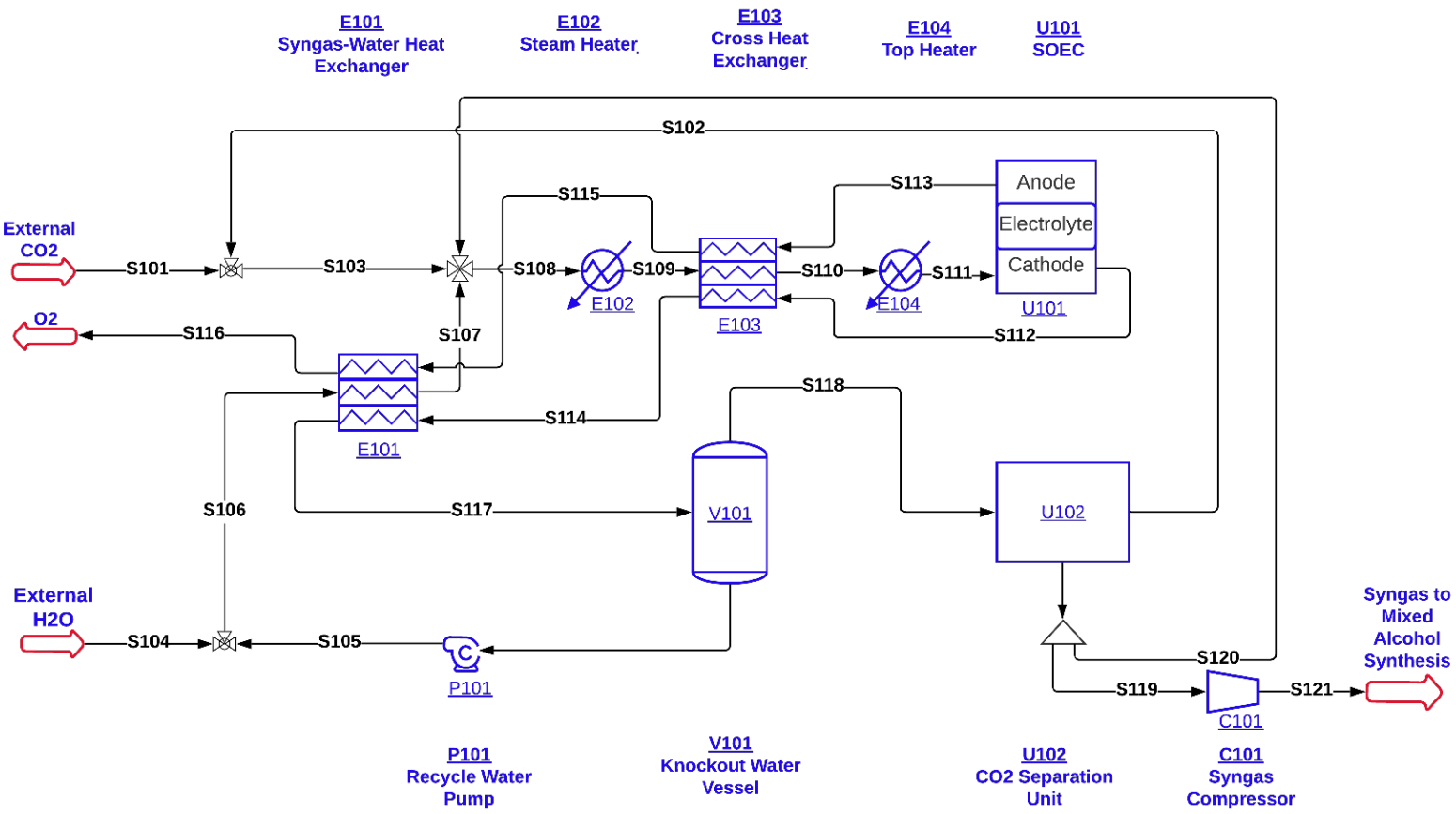

Fig. B1. Area 100: SOEC flowsheet Diagram

Name	S101	S102	S103	S104	S105	S107	S108	S109	S110	S111	S112
- - Overall - -											
Mass flow lb/h	253855.4	507509	761364	145165	52710.12	197875	1009468	1009469	1009469	1009469	811361
Temp F	**77**	120	106.483	**77**	120.108	362.7414	169.446	569.8857	1150	1472	1192.633
Pres psia	**15**	14.9	14.9	**15**	35	**15**	14.9	14.9	14.9	14.9	**14.9**
Vapor mass fraction	1	0.9892	0.9928	0	0	1	0.9999	1	1	1	1
Enth MMBtu/h	-974.47	-2007.9	-2982.4	-989.73	-357.07	-1116.1	-4204.3	-4105	-3907	-3788.4	-2524.4
Flow rates in lb/h											
Oxygen	0	0	0	0	0	0	0	0	0	0	0
Nitrogen	0	0	0	0	0	0	0	0	0	0	0
Argon	0	0	0	0	0	0	0	0	0	0	0
Carbon	0	0	0	0	0	0	0	0	0	0	0
Hydrogen	0	0	0	0	0.0184	0.0184	3377.226	5993.397	5993.397	5993.397	16886.06
Carbon Monoxide	0	0	0	0	0.2203	0.2203	39778.29	3426.007	3426.007	3426.007	198890.6
Carbon Dioxide	253855.4	476962	730817	0	12.6697	12.6697	731793	788911	788911	788911	481792
Methane	0	0	0	0	0	0	0	0	0	0	0
Acetylene	0	0	0	0	0	0	0	0	0	0	0
Ethylene	0	0	0	0	0	0	0	0	0	0	0
Ethane	0	0	0	0	0	0	0	0	0	0	0
Propane	0	0	0	0	0	0	0	0	0	0	0
Water	0	30547.28	30547.28	145165	52697.21	197862	234519	211138.4	211138.4	211138.4	113791.8

Table B1 Mainstreams for SOEC part

Name	S113	S114	S115	S116	S117	S118	S119	S120	S121
- - Overall - -									
Mass flow lb/h	198106.3	811361	198106.3	198106.3	811361	758651	200913.2	50228.3	176688
Temp F	**1472**	667.2922	700	140	120	120	120	120	140
Pres psia	**14.9**	14.9	14.9	14.9	14.9	**14.9**	14.9	14.9	3000
Vapor mass fraction	1	1	1	1	0.935	1	1	1	1
Enth MMBtu/h	67.227	-2683.6	28.39	2.7387	-2888.7	-2531.6	-423.43	-105.86	-288.78
Flow rates in lb/h									
Oxygen	198106.3	0	198106.3	198106.3	0	0	0	0	0
Nitrogen	0	0	0	0	0	0	0	0	0
Argon	0	0	0	0	0	0	0	0	0
Carbon	0	0	0	0	0	0	0	0	0
Hydrogen	0	16886.06	0	0	16886.06	16886.04	13508.83	3377.208	13508.62
Carbon Monoxide	0	198890.6	0	0	198890.6	198890.4	159112.3	39778.07	159110
Carbon Dioxide	0	481792	0	0	481792	481780	3854.244	963.5611	3853.19
Methane	0	0	0	0	0	0	0	0	0
Acetylene	0	0	0	0	0	0	0	0	0
Ethylene	0	0	0	0	0	0	0	0	0
Ethane	0	0	0	0	0	0	0	0	0
Propane	0	0	0	0	0	0	0	0	0
Water	0	113791.8	0	0	113791.8	61094.57	24437.83	6109.457	216.3225

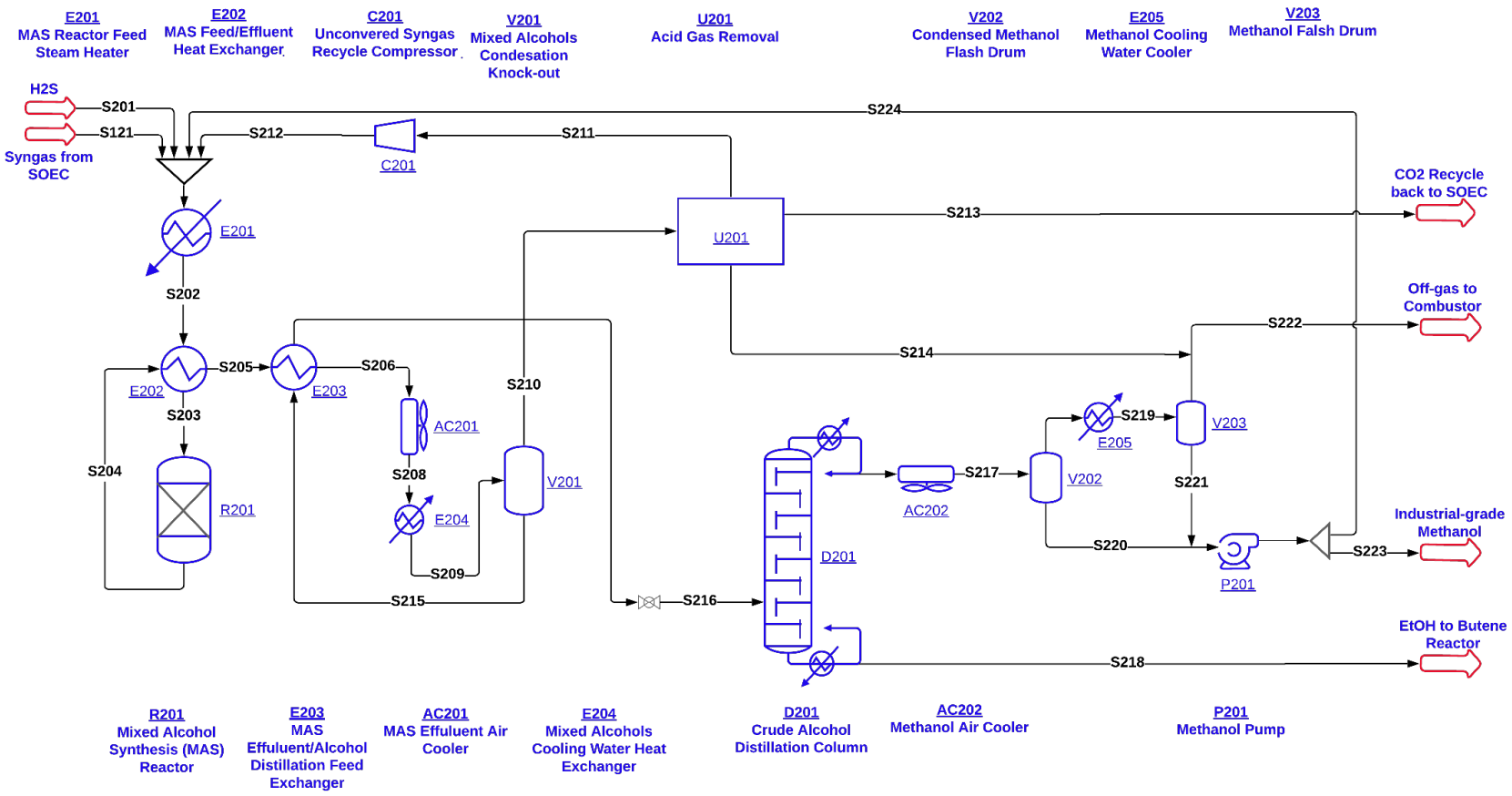

Fig. B2. Area 200: Mixed Alcohol Synthesis (MAS) Flowsheet Diagram

Table B2 Mainstreams for MAS part

Name	S121	S201	S202	S203	S204	S205	S206	S208	S209	S210	S211	S212
- - Overall - -												
Mass flow lb/h	176688	12	1129039	1129039	1129041	1129040	1129040	1129040	1129040	887487	791519	791519
Temp F	**140**	**110**	289	595	611	320.6197	157	140	110	110	110.2917	111.2961
Pres psia	**3000**	**3000**	3000	2995	**2988**	2984	2979	2974	2968	2968	2960.3	3000
Vapor mass fraction	1	0	0.957	1	1	0.9123	0.7933	0.7904	0.7861	1	1	1
Enth MMBtu/h	-288.78	-0.00529	-2629.9	-2457.1	-2709.2	-2881.9	-3005	-3015.1	-3032.2	-2267.3	-1949.1	-1948.1
Flow rates in lb/h												
Hydrogen	13508.62	0	57443.79	57443.79	44317.34	44315.57	44315.57	44315.57	44315.57	44299.68	43935.16	43935.16
Carbon Monoxide	159110	0	521064	521064	372437	372436.6	372436.6	372436.6	372436.6	372296.4	361954	361954
Carbon Dioxide	3853.19	0	309369.4	309369.4	379917	379916	379916	379916	379916	376101	305431.3	305431.3
Methane	0	0	78189.12	78189.12	89080.88	89081.51	89081.51	89081.51	89081.51	89028.63	78189	78189
Acetylene	0	0	0	0	0	0	0	0	0	0	0	0
Ethylene	0	0	0	0	0	0	0	0	0	0	0	0
Ethane	0	0	1883.831	1883.831	2588.189	2588.207	2588.207	2588.207	2588.207	2587.855	1883.831	1883.831
Propane	0	0	123.7868	123.7868	386.2697	386.2731	386.2731	386.2731	386.2731	299.3105	85.0367	85.0367
Water	216.3224	0	217.4042	217.4042	8857.781	8857.412	8857.412	8857.412	8857.412	53.2643	1.0661	1.0661
Sulphur	0	0	0	0	0	0	0	0	0	0	0	0
Carbonyl Sulfide	0	0	0	0	0	0	0	0	0	0	0	0
Hydrogen Sulfide	0	12	80.4396	80.4396	80.4396	80.4689	80.4689	80.4689	80.4689	40.0286	39.5944	39.5944
Methanol	0	0	160631.6	160631.6	172574.7	172572	172572	172572	172572	2394.54	0	0
Ethanol	0	0	25.3325	25.3325	53323.16	53323.24	53323.24	53323.24	53323.24	367.3881	0	0
N-Propanol	0	0	9.6585	9.6585	5471.874	5475.656	5475.656	5475.656	5475.656	19.0932	0	0
N-Butanol	0	0	0	0	7.2084	7.2084	7.2084	7.2084	7.2084	0.0021	0	0

Name	S213	S214	S215	S216	S217	S218	S219	S220	S221	S222	S223
- - Overall - -											
Mass flow lb/h	35636	60401.48	241552.5	241552.5	174348	67204.12	5055.461	169292.6	776.0128	64680.93	9240.644
Temp F	110	81.4233	110	250	140	237.3337	50	140	50	68.5412	131.7039
Pres psia	2960.3	20	2968	55	50	50	13	50	13	13	13
Vapor mass fraction	1	1	0	1	0.029	0	0.8465	0	0	1	0.002147
Enth MMBtu/h	-135.88	-182.77	-764.96	-641.94	-553.44	-200.99	-17.998	-535.89	-2.5002	-198.27	-29.295
Flow rates in lb/h											
Hydrogen	0	383.6359	15.8933	15.8933	15.8933	0	15.8716	0.0217	0	399.5074	0.0011
Carbon Monoxide	0	10349.86	140.1718	140.1718	140.1718	0	139.9862	0.1856	0.0006	10489.84	0.0099
Carbon Dioxide	35636	35081.4	3814.573	3814.573	3814.573	0	3725.142	89.4312	0.7547	38805.79	5.2262
Methane	0	10834.78	52.8858	52.8858	52.8859	0	52.7727	0.1132	0.0003	10887.55	0.006
Acetylene	0	0	0	0	0	0	0	0	0	0	0
Ethylene	0	0	0	0	0	0	0	0	0	0	0
Ethane	0	703.8967	0.3523	0.3523	0.3523	0	0.3522	0.0001	0.0004	704.2484	0.0004
Propane	0	214.2764	86.9626	86.9626	86.9626	0	46.1619	40.8007	0.163	260.2753	2.203
Water	0	52.1991	8804.149	8804.148	0.0166	8804.148	0	0.0166	0	52.1991	0.0009
Sulphur	0	0	0	0	0	0	0	0	0	0	0
Carbonyl Sulfide	0	0	0	0	0	0	0	0	0	0	0
Hydrogen Sulfide	0.0253	0.4093	40.4403	40.4403	40.4403	0	10.0713	30.369	0.1371	10.3434	1.6556
Methanol	0	2394.541	170177.5	170177.5	170159.7	17.254	1064.976	169094.7	774.845	2684.672	9229.579
Ethanol	0	367.3882	52955.86	52955.86	26.8996	52929.18	0.0949	26.8047	0.0817	367.4013	1.4219
N-Propanol	0	19.0932	5456.563	5456.563	10.2407	5446.334	0.032	10.2087	0.0298	19.0954	0.5402
N-Butanol	0	0.0021	7.2063	7.2063	0	7.2063	0	0	0	0.0021	0

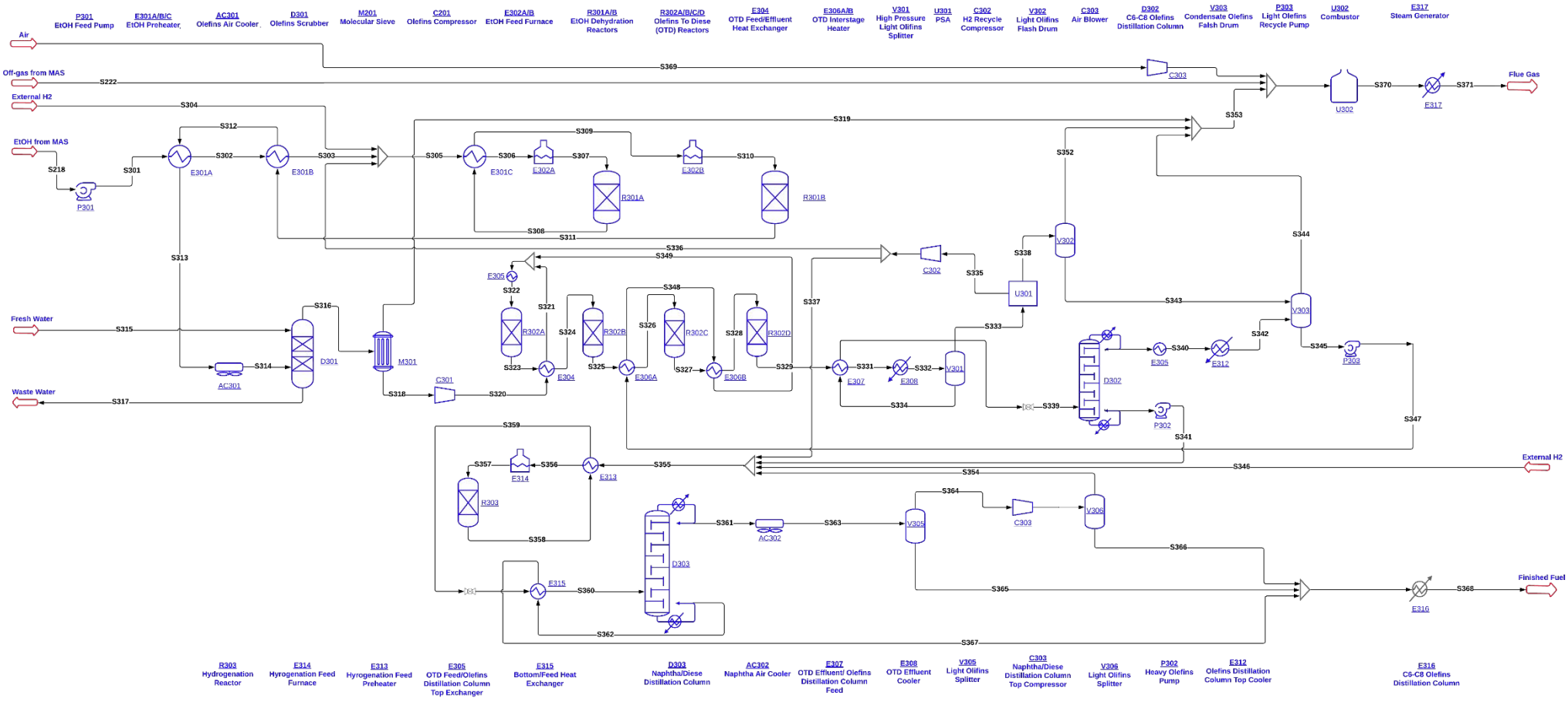

Fig. B3. Area 300: EtOH to Fuel Process Flowsheet Diagram

Table B3. Mainstreams for EtOH to Fuel

Name	S218	S301	S302	S303	S304	S305	S306	S307	S308	S309	S310	S311	S312	S313
Mass flow lb/h	67196.29	67201	67201	67204.12	6.4	70982	70982	70982	70981.7	70976.88	70976.88	70976.59	70976.59	70976.59
Temp F	**237.3323**	200.4997	257	306.4041	**80**	226.7524	483.566	617	785.7575	246.7524	617	695.2728	277	270.542
Pres psia	**50**	150	**147**	**147**	**200**	147	147	147	**147**	147	142	142	142	142
Vapor mass fraction	0	0	0	0.2402	1	0.4557	1	1	0.7341	0.7953	0.7353	0.5718	0.896	0.851
Enth MMBtu/h	-200.96	-203.04	-199.82	-190.79	-0.00083	-188.7	-161.34	-154.84	-154.84	-182.19	-167.68	-167.68	-176.72	-179.94
Flow rates in lb/h														
Oxygen	0	0	0	0	0	0	0	0	0	0	0	0	0	0
Nitrogen	0	0	0	0	0	0	0	0	0	0	0	0	0	0
Hydrogen	0	0	0	0	6.4	3772.294	3772.294	3772.294	3809.171	3809.119	3809.12	3845.996	3845.996	3845.996
Carbon Monoxide	0	0	0	0	0	0	0	0	0	0	0	0	0	0
Carbon Dioxide	0	0	0	0	0	0	0	0	0.0253	0.0253	0.0253	0.0506	0.0506	0.0506
Ethylene	0	0	0	0	0	0	0	0	805.7936	805.7924	805.7923	1611.585	1611.585	1611.585
Propane	0	0	0	0	0	0	0	0	44.0512	44.0511	44.0511	88.1023	88.1023	88.1023
Water	8800.259	8804.513	8804.513	8804.148	0	8809.012	8809.012	8809.012	18740.61	18740.21	18740.21	30305.04	30305.04	30305.04
Hydrogen Sulfide	0	0	0	0	0	0	0	0	0	0	0	0	0	0
Sulfur Dioxide	0	0	0	0	0	0	0	0	0	0	0	0	0	0
Methanol	17.3235	17.8295	17.8295	17.254	0	17.5749	17.5749	17.5749	17.5749	17.1609	17.1609	17.1609	17.1609	17.1609
Ethanol	52928.88	52928.93	52928.93	52929.18	0	52929.5	52929.5	52929.5	26464.75	26464.71	26464.71	0.001	0.001	0.001
N-Propanol	5442.621	5442.559	5442.559	5446.334	0	5446.371	5446.371	5446.371	5446.371	5442.478	5442.478	0	0	0
N-Butanol	7.2062	7.2063	7.2063	7.2063	0	7.2063	7.2063	7.2063	7.2063	7.2063	7.2063	0	0	0
Propylene	0	0	0	0	0	0	0	0	322.3416	322.3411	322.3411	4455.643	4455.643	4455.643
1-Butene	0	0	0	0	0	0	0	0	14181.71	14181.69	14181.69	28368.84	28368.84	28368.84
Diethyl Ether	0	0	0	0	0	0	0	0	214.6489	214.6486	214.6486	429.2973	429.2973	429.2973
Acetaldehyde	0	0	0	0	0	0	0	0	805.6116	805.6105	805.6105	1611.221	1611.221	1611.221
Acetic Acid	0	0	0	0	0	0	0	0	59.4055	59.4054	59.4054	118.8109	118.8109	118.8109
I-Butane	0	0	0	0	0	0	0	0	32.6213	32.6213	32.6213	65.2426	65.2426	65.2426
I-Pentane	0	0	0	0	0	0	0	0	29.8005	29.8005	29.8005	59.601	59.601	59.601
1-Hexene	0	0	0	0	0	0	0	0	0	0	0	0	0	0
1-Heptene	0	0	0	0	0	0	0	0	0	0	0	0	0	0
1-Octene	0	0	0	0	0	0	0	0	0	0	0	0	0	0
1-Nonene	0	0	0	0	0	0	0	0	0	0	0	0	0	0
1-Decene	0	0	0	0	0	0	0	0	0	0	0	0	0	0
1-Dodecene	0	0	0	0	0	0	0	0	0	0	0	0	0	0
1-Hexadecene	0	0	0	0	0	0	0	0	0	0	0	0	0	0
N-Nonane	0	0	0	0	0	0	0	0	0	0	0	0	0	0
N-Decane	0	0	0	0	0	0	0	0	0	0	0	0	0	0
N-Dodecane	0	0	0	0	0	0	0	0	0	0	0	0	0	0
N-Hexane	0	0	0	0	0	0	0	0	0	0	0	0	0	0
N-Octane	0	0	0	0	0	0	0	0	0	0	0	0	0	0

Name	S314	S315	S316	S317	S318	S319	S320	S321	S322	S323	S324	S325	S326	S327
Mass flow lb/h	70976.5	1000	43695.8	28280.8	38512.1	5183.62	38512.1	38512.1	74042.5	74042.5	74055.4	74055.4	74053.5	74053.4
Temp F	140	**80**	181.664	344.344	120	181.664	304.941	496.658	437	516.271	401.337	458.818	437	482.389
Pres psia	132	**125**	125	125	125	125	340	340	340	**330**	327	**317**	317	299
Vapor mass fraction	0.5807	0	1	0	1	0	1	1	1	1	1	1	1	1
Enth MMBtu/h	-203.98	-6.815	-17.637	-184.8	1.9074	-24.61	6.4436	12.527	5.077	5.077	-0.82625	-0.82625	-1.9868	-1.9868
Flow rates in lb/h														
Oxygen	0	0	0	0	0	0	0	0	0	0	0	0	0	0
Nitrogen	0	0	0	0	0	0	0	0	0	0	0	0	0	0
Hydrogen	3845.99	0	3845.99	0	3845.99	0	3845.99	3845.99	3846.10	3848.26	3848.51	3848.51	3848.06	3848.06
Carbon Monoxide	0	0	0	0	0	0	0	0	0.0016	14.9765	14.9152	14.9152	14.9152	14.9152
Carbon Dioxide	0.0506	0	0.0506	0	0.0506	0	0.0506	0.0506	0.0509	0.0509	0.0506	0.0506	0.0506	0.0506
Ethylene	1611.58	0	1611.58	0	1611.58	0	1611.58	1611.58	1611.74	1128.22	1128.15	789.704	789.704	473.822
Propane	88.1023	0	88.1023	0	88.1023	0	88.1023	88.1023	145.188	145.188	88.0931	88.0931	88.0931	88.0931
Water	30305.0	1000	3130.50	28174.5	0	3130.50	0	0	0	0	0	0	0	0
Hydrogen Sulfide	0	0	0	0	0	0	0	0	0	0	0	0	0	0
Sulfur Dioxide	0	0	0	0	0	0	0	0	0	0	0	0	0	0
Methanol	17.1609	0	17.1305	0.0303	17.1305	0	17.1305	17.1305	17.1305	0	0	0	0	0
Ethanol	0.001	0	0.001	0	0.001	0	0.001	0.001	0.001	0.001	0	0	0	0
N-Propanol	0	0	0	0	0	0	0	0	0	0	0	0	0	0
N-Butanol	0	0	0	0	0	0	0	0	0	0	0	0	0	0
Propylene	4455.64	0	4455.64	0	4455.64	0	4455.64	4455.64	5220.16	3654.11	3709.85	2967.88	2967.82	1780.69
1-Butene	28368.8	0	28368.8	0	28368.8	0	28368.8	28368.8	31849.9	22778.4	22850.1	16333.5	16333.3	9800
Diethyl Ether	429.297	0	429.297	0	0	429.297	0	0	0	0	0	0	0	0
Acetaldehyde	1611.22	0	1611.22	0	0	1611.22	0	0	0	0	0	0	0	0
Acetic Acid	118.810	0	12.606	106.204	0	12.606	0	0	0	0	0	0	0	0
I-Butane	65.2426	0	65.2425	0	65.2425	0	65.2425	65.2425	121.043	121.043	65.2358	65.2358	65.2358	65.2358
I-Pentane	59.601	0	59.5816	0.0194	59.5816	0	59.5816	59.5816	117.723	117.723	59.5754	59.5754	59.5754	59.5754
1-Hexene	0	0	0	0	0	0	0	0	9959.80	11525.8	11553.9	9985.08	9985	9985
1-Heptene	0	0	0	0	0	0	0	0	0	0	0	0	0	0
1-Octene	0	0	0	0	0	0	0	0	16402.6	25957.6	25986.4	32841.5	32840.5	32840.5
1-Nonene	0	0	0	0	0	0	0	0	4649.23	4649.23	4648.73	4648.73	4648.69	5835.80
1-Decene	0	0	0	0	0	0	0	0	84.9618	84.9618	84.9565	84.9565	84.947	400.826
1-Dodecene	0	0	0	0	0	0	0	0	16.8114	16.8114	16.8108	2327.56	2327.54	8860.84
1-Hexadecene	0	0	0	0	0	0	0	0	0.029	0.029	0.029	0.029	0.029	0.029
N-Nonane	0	0	0	0	0	0	0	0	0	0	0	0	0	0
N-Decane	0	0	0	0	0	0	0	0	0	0	0	0	0	0
N-Dodecane	0	0	0	0	0	0	0	0	0	0	0	0	0	0
N-Hexane	0	0	0	0	0	0	0	0	0	0	0	0	0	0
N-Octane	0	0	0	0	0	0	0	0	0	0	0	0	0	0

Name	S328	S329	S331	S332	S333	S334	S335	S336	S337	S338	S339	S340	S341	S342
Mass flow	74053.47	74053.45	74053.45	74053.45	7550.393	66503	3770.893	3765.893	5	3779.499	66503	32918.93	33584.12	32918.93
Temp F	437	519.8234	267.9878	104	104	104	152.9678	268.7492	268.7492	140	510	395.8014	713.7718	110
Pres psia	296	296	290	290	290	290	50	340	**340**	**290**	220	220	300	**220**
Vapor mass	1	0.9405	0.2805	0.102	1	0	1	1	1	0.5048	0.3093	0.2495	0	1.15E-05
Enth	-4.388	-4.388	-23.36	-33.202	-0.12488	-33.077	0.45295	2.1247	0.002821	-0.26095	-14.108	-7.1421	-3.2138	-13.431
Flow rates in														
Oxygen	0	0	0	0	0	0	0	0	0	0	0	0	0	0
Nitrogen	0	0	0	0	0	0	0	0	0	0	0	0	0	0
Hydrogen	3848.065	3848.065	3848.065	3848.065	3847.85	0.2147	3770.893	3765.893	5	76.957	0.2147	0.2147	0	0.2147
Carbon	14.9152	14.9152	14.9152	14.9152	14.9143	0.0009	0	0	0	14.9143	0.0009	0.0009	0	0.0009
Carbon	0.0506	0.0506	0.0506	0.0506	0.0505	0.0001	0	0	0	0.0505	0.0001	0.0001	0	0.0001
Ethylene	473.8228	189.5291	189.5291	189.5291	189.4731	0.056	0	0	0	189.4731	0.056	0.056	0	0.056
Propane	88.0931	88.0931	88.0931	88.0931	58.0595	30.0337	0	0	0	58.0595	30.0337	30.0337	0	30.0337
Water	0	0	0	0	0	0	0	0	0	0	0	0	0	0
Hydrogen	0	0	0	0	0	0	0	0	0	0	0	0	0	0
Sulfur	0	0	0	0	0	0	0	0	0	0	0	0	0	0
Methanol	0	0	0	0	0	0	0	0	0	0	0	0	0	0
Ethanol	0	0	0	0	0	0	0	0	0	0	0	0	0	0
N-Propanol	0	0	0	0	0	0	0	0	0	0	0	0	0	0
N-Butanol	0	0	0	0	0	0	0	0	0	0	0	0	0	0
Propylene	1780.694	1246.486	1246.486	1246.486	858.5609	387.9247	0	0	0	858.5609	387.9247	387.9247	0	387.9247
1-Butene	9800	3920	3920	3920	1622.892	2297.109	0	0	0	1622.892	2297.109	2297.109	0	2297.109
Diethyl Ether	0	0	0	0	0	0	0	0	0	0	0	0	0	0
Acetaldehyde	0	0	0	0	0	0	0	0	0	0	0	0	0	0
Acetic Acid	0	0	0	0	0	0	0	0	0	0	0	0	0	0
I-Butane	65.2358	65.2358	65.2358	65.2358	29.9027	35.3331	0	0	0	29.9027	35.3331	35.3331	0	35.3331
I-Pentane	59.5754	59.5754	59.5754	59.5754	12.543	47.0324	0	0	0	12.543	47.0324	47.0323	0	47.0323
1-Hexene	9985	9985	9985	9985	739.5894	9245.411	0	0	0	739.5894	9245.411	9245.411	0	9245.411
1-Heptene	0	0	0	0	0	0	0	0	0	0	0	0	0	0
1-Octene	32840.5	16420.25	16420.25	16420.25	153.2289	16267.03	0	0	0	153.2289	16267.03	16250.76	16.2671	16250.76
1-Nonene	5835.809	6370.013	6370.013	6370.013	20.4835	6349.529	0	0	0	20.4835	6349.529	4530.661	1818.864	4530.661
1-Decene	400.8265	685.1182	685.1182	685.1182	0.7437	684.3744	0	0	0	0.7437	684.3744	79.6565	604.7184	79.6565
1-Dodecene	8860.842	14740.81	14740.81	14740.81	2.0729	14738.74	0	0	0	2.0729	14738.74	14.7386	14724	14.7386
1-	0.029	16420.3	16420.3	16420.3	0.0284	16420.27	0	0	0	0.0284	16420.27	0.0005	16420.28	0.0005
N-Nonane	0	0	0	0	0	0	0	0	0	0	0	0	0	0
N-Decane	0	0	0	0	0	0	0	0	0	0	0	0	0	0
N-Dodecane	0	0	0	0	0	0	0	0	0	0	0	0	0	0
N-Hexane	0	0	0	0	0	0	0	0	0	0	0	0	0	0
N-Octane	0	0	0	0	0	0	0	0	0	0	0	0	0	0

Name	S343	S344	S345	S346	S347	S348	S349	S352	S353	S354	S355	S356	S357	S358
Mass flow lb/h	2510.63	0.537	35530.3	226.536	35530.3	35530.3	35530.3	1268.87	6453.04	684.928	34507	34507	34507	34507.2
Temp F	104	109.558	109.558	**140**	110.557	169.519	282.805	104	134.849	110	633.145	594.856	700	572
Pres psia	290	220	220	**340**	340	340	340	290	125	**300**	300	300	300	**300**
Vapor mass fraction	0	1	0	1	0	0	0.00348	1	0.328	1	0.7728	0.56	1	0.359
Enth MMBtu/h	-0.56106	1.40E-05	-14.042	0.02721	-14.023	-12.862	-10.461	0.14863	-24.461	-0.05091	-3.237	-4.76	-1.1288	-12.529
Flow rates in lb/h														
Oxygen	0	0	0	0	0	0	0	0	0	0	0	0	0	0
Nitrogen	0	0	0	0	0	0	0	0	0	0	0	0	0	0
Hydrogen	0.0108	0.1143	0.1112	226.536	0.1112	0.1112	0.1112	76.9452	77.0595	611.789	843.456	843.456	843.456	629.074
Carbon Monoxide	0.0022	0.0015	0.0016	0	0.0016	0.0016	0.0016	14.9121	14.9137	0.0004	0.0004	0.0004	0.0004	0.0004
Carbon Dioxide	0.0002	0	0.0003	0	0.0003	0.0003	0.0003	0.0503	0.0503	0.0001	0.0001	0.0001	0.0001	0.0001
Ethylene	0.1406	0.0325	0.1641	0	0.1641	0.1641	0.1641	189.332	189.365	0.0004	0.0004	0.0004	0.0004	0.0004
Propane	27.061	0.0084	57.0857	0	57.0857	57.0857	57.0857	30.999	31.0074	11.5601	12.298	12.298	12.298	12.298
Water	0	0	0	0	0	0	0	0	3130.50	0	0	0	0	0
Hydrogen Sulfide	0	0	0	0	0	0	0	0	0	0	0	0	0	0
Sulfur Dioxide	0	0	0	0	0	0	0	0	0	0	0	0	0	0
Methanol	0	0	0	0	0	0	0	0	0	0	0	0	0	0
Ethanol	0	0	0	0	0	0	0	0	0	0.0001	0.0001	0.0001	0.0001	0.0001
N-Propanol	0	0	0	0	0	0	0	0	0	0	0	0	0	0
N-Butanol	0	0	0	0	0	0	0	0	0	0	0	0	0	0
Propylene	376.727	0.1275	764.516	0	764.516	764.516	764.516	481.839	481.966	0.7374	0.7799	0.7799	0.7799	0.7799
1-Butene	1184.17	0.1809	3481.07	0	3481.07	3481.07	3481.07	438.738	438.919	1.6659	1.845	1.845	1.845	1.845
Diethyl Ether	0	0	0	0	0	0	0	0	429.297	0	0	0	0	0
Acetaldehyde	0	0	0	0	0	0	0	0	1611.22	0	0	0	0	0
Acetic Acid	0	0	0	0	0	0	0	0	12.606	0	0	0	0	0
I-Butane	20.4721	0.0035	55.8013	0	55.8013	55.8013	55.8013	9.431	9.4345	12.0897	13.3196	13.3196	13.3196	13.3196
I-Pentane	11.1113	0.0011	58.1423	0	58.1423	58.1423	58.1423	1.432	1.4331	13.8632	17.2701	17.2701	17.2701	17.2701
1-Hexene	714.921	0.0558	9959.80	0	9959.80	9959.80	9959.80	24.65	24.7058	0	0.4626	0.4626	0.4626	0
1-Heptene	0	0	0	0	0	0	0	0	0	0	0	0	0	0
1-Octene	152.700	0.0105	16402.6	0	16402.6	16402.6	16402.6	0.5248	0.5353	0	16.7461	16.7461	16.7461	0
1-Nonene	20.4606	0.001	4649.23	0	4649.23	4649.23	4649.23	0.0225	0.0235	0	1818.94	1818.94	1818.94	0
1-Decene	0.7435	0	84.9618	0	84.9618	84.9618	84.9618	0.0003	0.0003	0	604.718	604.718	604.718	0
1-Dodecene	2.0729	0	16.8114	0	16.8114	16.8114	16.8114	0.0001	0.0001	0	14724	14724	14724	0
1-Hexadecene	0.0284	0	0.029	0	0.029	0.029	0.029	0	0	0	16420.2	16420.2	16420.2	16420.2
N-Nonane	0	0	0	0	0	0	0	0	0	30.5669	30.2616	30.2616	30.2616	1878.25
N-Decane	0	0	0	0	0	0	0	0	0	0.0991	0.0978	0.0978	0.0978	613.507
N-Dodecane	0	0	0	0	0	0	0	0	0	0	0	0	0	14900.5
N-Hexane	0	0	0	0	0	0	0	0	0	0.5646	0.5638	0.5638	0.5638	1.0374
N-Octane	0	0	0	0	0	0	0	0	0	1.9911	1.9778	1.9778	1.9778	19.0247

Name	S359	S360	S361	S362	S363	S364	S365	S366	S367	S368	S369	S370	S371
Mass flow lb/h	34403.23	34403.23	1979.951	32422.07	1979.951	788.8887	1191.062	80.295	32422.07	33693.43	380000	451153	451153
Temp F	613.1457	704.2728	251.2582	724.2728	140	140	140	110	616.556	116.1947	**80**	2600	550
Pres psia	300	200	200	200	200	200	200	300	200	200	**15**	13	13
Vapor mass	0.5198	1	1	0	0.3984	1	0	0	0	0	1	1	1
Enth MMBtu/h	-10.949	-7.4111	-0.61624	-8.7336	-1.1296	-0.07366	-1.056	-0.0726	-12.272	-24.957	0.26475	-276.11	-563.11
Flow rates in lb/h													
Oxygen	0	0	0	0	0	0	0	0	0	0	88507.57	18640.34	18640.34
Nitrogen	0	0	0	0	0	0	0	0	0	0	291492.4	291492.4	291492.4
Hydrogen	630.7136	630.7136	630.7136	0	630.7136	630.7109	0.0026	0.0003	0	0.0029	0	0.4957	0.4957
Carbon Monoxide	0.0004	0.0004	0.0004	0	0.0004	0.0004	0	0	0	0	0	24.5262	24.5262
Carbon Dioxide	0.0001	0.0001	0.0001	0	0.0001	0.0001	0	0	0	0	0	100369.6	100369.6
Ethylene	0.0004	0.0004	0.0004	0	0.0004	0.0004	0	0	0	0	0	0	0
Propane	12.298	12.298	12.298	0	12.298	11.9677	0.3303	0.0485	0	0.3788	0	0.0001	0.0001
Water	0	0	0	0	0	0	0	0	0	0	0	40606.43	40606.43
Hydrogen Sulfide	0	0	0	0	0	0	0	0	0	0	0	0.0001	0.0001
Sulfur Dioxide	0	0	0	0	0	0	0	0	0	0	0	19.4416	19.4416
Methanol	0	0	0	0	0	0	0	0	0	0	0	0.0001	0.0001
Ethanol	0.0001	0.0001	0.0001	0	0.0001	0.0001	0	0	0	0	0	0.0001	0.0001
N-Propanol	0	0	0	0	0	0	0	0	0	0	0	0.0001	0.0001
N-Butanol	0	0	0	0	0	0	0	0	0	0	0	0.0001	0.0001
Propylene	0.7799	0.7799	0.7799	0	0.7799	0.7628	0.0171	0.0025	0	0.0196	0	0.0001	0.0001
1-Butene	1.845	1.845	1.845	0	1.845	1.735	0.11	0.017	0	0.127	0	0.0001	0.0001
Diethyl Ether	0	0	0	0	0	0	0	0	0	0	0	0.0001	0.0001
Acetaldehyde	0	0	0	0	0	0	0	0	0	0	0	0.0001	0.0001
Acetic Acid	0	0	0	0	0	0	0	0	0	0	0	0.0001	0.0001
I-Butane	13.3196	13.3196	13.3196	0	13.3196	12.5797	0.7399	0.1127	0	0.8526	0	0.0001	0.0001
I-Pentane	17.2701	17.2701	17.2701	0	17.2701	14.7169	2.5531	0.4123	0	2.9654	0	0.0001	0.0001
1-Hexene	0	0	0	0	0	0	0	0	0	0	0	0.0001	0.0001
1-Heptene	0	0	0	0	0	0	0	0	0	0	0	0	0
1-Octene	0	0	0	0	0	0	0	0	0	0	0	0.0002	0.0002
1-Nonene	0	0	0	0	0	0	0	0	0	0	0	0.0002	0.0002
1-Decene	0	0	0	0	0	0	0	0	0	0	0	0.0002	0.0002
1-Dodecene	0	0	0	0	0	0	0	0	0	0	0	0	0
1-Hexadecene	16419.43	16419.42	0	16418.54	0	0	0	0	16418.54	16418.54	0	0	0
N-Nonane	1778.249	1778.249	1259.903	518.2914	1259.903	111.0578	1148.845	77.1603	518.2914	1744.296	0	0.0002	0.0002
N-Decane	608.8787	608.8788	23.5481	585.3329	23.5481	0.8443	22.7039	0.7199	585.3329	608.7567	0	0.0002	0.0002
N-Dodecane	14900.38	14900.38	0.3039	14899.81	0.3039	0.0016	0.3023	0.0015	14899.81	14900.12	0	0	0
N-Hexane	1.0374	1.0374	1.0374	0	1.0374	0.6492	0.3882	0.0652	0	0.4533	0	0.0001	0.0001
N-Octane	19.0266	19.0266	18.9314	0.0951	18.9314	3.8619	15.0695	1.7549	0.0951	16.9196	0	0.0002	0.0002